MASTERARBEIT | MASTER'S THESIS

Titel | Title

Investigation of the suspected methyltransferases from ORF80 and 82 of ϕCh1, a virus of the haloalkaliphilic archaeon N. magadii

verfasst von | submitted by

Benjamin Koltschik BSc

angestrebter akademischer Grad | in partial fulfilment of the requirements for the degree of

Master of Science (MSc)

Wien | Vienna, 2026

Studienkennzahl lt. Studienblatt | Degree programme code as it appears on the student record sheet:	UA 066 830
Studienrichtung lt. Studienblatt | Degree programme as it appears on the student record sheet:	Masterstudium Molecular Microbiology, Microbial Ecology and Immunobiology
Betreut von | Supervisor:	ao. Univ.-Prof. i.R. Dipl.-Biol. Dr. Angela Witte

Abstract

ϕCh1 is a temperate head-tail virus, using *N. magadii* as it's only known host. The host *N. magadii*, native to the soda lake Magadi, lives under extreme conditions of high pH and salinity and adapted to this environment, making this virus host pair somewhat unique and therefore an interesting subject of study.

Many aspects of the interactions of ϕCh1 and *N. magadii* are currently unknown or not completely elucidated, which is also true for the function of the open reading frames 80 and 82. Previous studies, performing sequence analysis and comparison, indicate that both ORFs are likely to be DNA-methyl-transferases, particularly ORF80 seems to be a m5C-mtase and ORF82 a m4C-mtase. Another ORF, ORF94 was confirmed to be a methyltransferase, which plays a major role in the regulation of the viral lifecycle.

Like ORF94 was studied before, so the functions of ORF80 and ORF82 in ϕCh1 were analysed in this thesis. To achieve this, first, deletion mutants of lysogenicly infected strains of *N. magadii*, L11, were created by replacing one or both ORFs with a novobiocin resistance cassette. These deletion mutants were then complemented by transforming them with a plasmid, carrying the deleted ORFs. Additionally, overexpression variants of L11 were created by transforming regular L11 with the complementation plasmids. All of these constructs were then compared in regard to their growth behaviour, viral-titers, and production patterns of certain proteins of ϕCh1.

Zusammenfassung

ϕCh1 ist ein temperenter Kopf-Schwanz-Virus, welcher *N. magadii* als einzigen bekannten Wirt verwendet. Der Wirt *N. magadii*, der im Sodasee Magadi beheimatet ist, lebt dort unter extremen Bedingungen, mit hohem pH-Wert und Salzgehalt und hat sich an diese Umgebung angepasst, was dieses Virus-Wirtspaar einzigartig und daher zu einem interessanten Studienobjekt macht.

Viele Aspekte der Wechselwirkungen von ϕCh1 und *N. magadii* sind derzeit unbekannt oder nicht vollständig geklärt, so auch die Funktion der Open Reading Frames 80 und 82. Frühere Studien, die eine Sequenzanalyse und Vergleich durchführten, deuten darauf hin, dass es sich bei beiden ORFs wahrscheinlich um DNA-Methyltransferasen handelt, genauer bei ORF80 um eine m5C-mtase und bei ORF82 um eine m4C-mtase. Bei einem weiteren ORF, ORF94, wurde bereits bestätigt, dass es sich um eine Methyltransferase handelt, die eine wichtige Rolle bei der Regulation des viralen Lebenszyklus spielt.

So wie ORF94 untersucht wurde, wurden nun auch in dieser Arbeit die Funktionen von ORF80 und ORF82 in ϕCh1 analysiert. Um dies zu erreichen, wurden erst Deletionsmutanten des lysogen infizierten Stammes von *N. magadii*, L11, erzeugt, indem jeweils einer oder beide ORFs durch eine Novobiocin-Resistenzkassette ersetzt wurden. Diese Deletionsmutanten wurden dann komplementiert, indem sie mit einem Plasmid transformiert wurden, welches die deletierten ORFs trug. Zusätzlich wurden Überexpressionsvarianten von L11 durch Transformation von regulärem L11 mit den Komplementationsplasmiden. erzeugt. Alle diese Konstrukte wurden dann hinsichtlich ihres Wachstumsverhaltens, ihres Virustiters und ihrer Produktionsmuster bestimmter Proteine von ϕCh1 verglichen.

Inhalt

Introduction

Natrialba magadii, host of ϕCh1

At the end of the 1970s novel technologies changed the approach of exploring the microbial world radically. With the help of 16s rRNA phylogenetic analysis which recently had become available, archaea were discovered as a new domain of life (Woese and Fox, 1977). At first, this new domain was thought to mainly be comprised of extremophiles, predominantly thriving in extreme conditions. Interestingly, since

then genetic and biochemical methods have shown that, archaea are also present in a variety of mesophilic environments. Despite some archaea preferring extreme conditions like low and high Temperatures (Psychrophiles & Thermophiles), acidic and alkaline conditions (Acidophiles & Alkaliphiles) as well as high salt concentrations (Halophiles) (Rothschild and Mancinelli 2001; Pikuta *et al.,* 2007), countless others were detected in mesophilic environments like various aquatic (Lloyd *et al*., 2013; Karner *et al.,* 2001) and terrestrial environments (DeLong 1998) and even as part of human microbiomes (Lurie-Weinberger and Gophna 2015).

Although environmental genetic screening approaches to better understand the phylogeny of the microbial world certainly uncovered previously unknown archaea in environments, which are difficult to sample with traditional approaches, Soliman and Trüper discovered haloalkaliphilic archaea (Soliman and Trüper, 1982) by more traditional culturing approaches. These poly-extremophiles not only require high salt concentrations (3.5-5M) to thrive, but also an extremely high pH (8-11). These conditions were found to be fulfilled by so called Soda Lakes, which exhibit highly alkaline and hypersaline conditions, named so for their high concentrations of usually sodium carbonates. For example, Wadi el Natrun in Egypt or lake Magadi in Kenya.

Compounding on Soliman's and Trüper's work, Tindall *et al.,* reported the isolation of *Natrialba magadii* from the lake Magadi in Kenya in 1984, another haloalkaliphilic archaeon. *Natrialba magadii* belonging to the phylum *Euryarchaeota* is a rod-shaped, flagella-containing, haloalkaliphilic archaeon. Based on its phenotypic properties originally classified as member of the genus *Natronobacterium*, it was later discovered to better fit into the genus *Natrialba* (Kamekura *et al*., 1997), with the help of 16s rRNA phylogenetic data. As poly-extremophile *N. magadii*, best proliferates in extreme alkalic (pH 8.5-11) and highly saline (4-5M) conditions. Additionally, the haloalkaliphile needs high levels of carbonate minerals and low Mg^{2+}-concentration as well as temperatures of 37-42°C to optimally grow (Kamekura *et al.,* 1997). The chemoorganotrophic *N. magadii* utilizes amino acids and peptides as carbon source (Tindall, Ross and Grant, 1984).

To survive in the extreme conditions *N. magadii* finds itself in, multiple adaptations, typical for extremophiles living in these environments, are present in *N. magadii*. To prevail in highly saline environments *N. magadii*, like other halophiles, compensates the otherwise resulting osmotic pressure by storing large amounts of inorganic ions in the cytoplasm, which in case of *N. magadii* is mostly KCl (Lanyi *et al.*, 1979; Madern *et al.*, 2000). Although salt concentrations in the cytoplasm are highly elevated, the internal pH of alkaliphiles is close to neutral, which eases the maintenance of protein function, even in environments with a high pH (Cook *et al.*, 1996; Guffanti & Hicks, 1991; Sturr *et al.*, 1994). To achieve this physiology, in many organisms, transporter systems are utilized for the regulation of the concentration of different ions in the cytoplasm and producing a negatively charged cell envelope for aerobic respiration, for example Na+/H+-antiporters (Hunte *et al.*, 2005; Oren, 1999; Tenchov *et al.*, 2006).

Additionally, proteins of haloarchaea are adapted to the high internal salt concentrations to enable their solubility under these, compared to mesophilic organisms, extreme conditions. These adaptations usually consist of low isoelectric points and a high share of hydrophobic and acidic amino acids in their proteins (Lanyi, 1974; Mevarech *et al.*, 2000; Oren, 2002).

N. magadii, like many other extremophiles, is polyploid, meaning one cell possesses multiple copies of the cell's chromosome (Comai, 2005). Although more energy intensive, polyploidy offers several advantages, which are especially crucial in extreme environments. Firstly, since multiple copies of every gene exist, their diversification, which can lead to a fitness advantage, is more likely, while disadvantageous mutation can be compensated by the remaining copies of the still functioning genes (Breuert *et al.*, 2006). The increased amount of DNA, which contains large amounts of phosphorus, can also be utilized as storage system for the same.

More than a decade after the first identification of *N. magadii*, the virus ϕCh1 was discovered to use the archaeon as its host, existing as a provirus within *N. magadii* (Witte et al., 1997). Simultaneously Witte *et al* reported two strains of *N. magadii*, L11 and L13 (**Figure 1**) (Witte et al., 1997). L11 strains are wild type strains carrying the

provirus and possesses immunity to superinfection by the ϕCh1 virus. Polyploid *N. magadii* L13 is cured of the provirus due to continuous passaging (Witte et al., 1997).

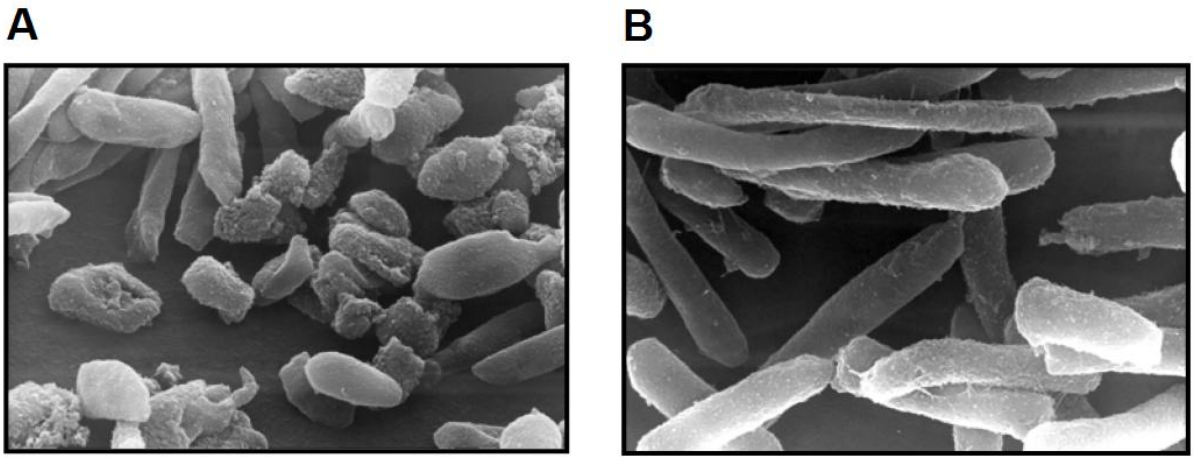

***Figure 1: Morphology of N. magadii L11 and N. magadii L13 strain**. (A) Electron micrograph showing lysed cells of lysogenic strain N. magadii L11. (B) Electron micrograph of non-lysogenic strain N. magadii L13. (Adapted from Iro, 2007)*

Manipulation of *Natrialba magadii*

Due to *N. magadii's* special physiology, adequate working practices have to be adapted while working with it. Especially the high concentration of salt within its cytoplasm can pose a significant challenge and forces an adaption of standard laboratory practices, like when working with its proteins (Holmes *et al.*, 1997). Also, the relatively long generation time of up to 9 h can be a major inconvenience. Especially for transformations, a completely new protocol had to be developed, since chemical methods cannot be applied due to the already high salt concentration and high pH, which also prevents the application of electroporation, since the conductivity would be too great. Instead, bacitracin and Proteinase K are used to generate competent spheroblasts, which are *N. magadii* without S-Layer (Mayrhofer-Iro *et al.*, 2013).

Next to competent cells also functioning vectors are needed, of which two exist for *N. magadii*, pNB102 and pRo-5. First pNB102, a plasmid with the ColE1 origin of replication (ori), which confers ampicillin and mevinolin resistances, was originally constructed from pNB101, which was itself isolate from Natronobacterium sp. strain AS7091 (see **Figure 2**; Zhou *et al.*, 2004). Second pRo-5, containing the operon ORF53/ORF54 of ΦCh1 (*repH*) as ori, confers ampicillin (via beta lactamase genes)

and novobiocin resistance (via a mutated version of the *gyrB* gene, which normally would get inhibited by novobiocin), which was constructed from pKS_{II}^{+} (see **Figure 2**; Mayrhofer-Iro *et al.*, 2013).

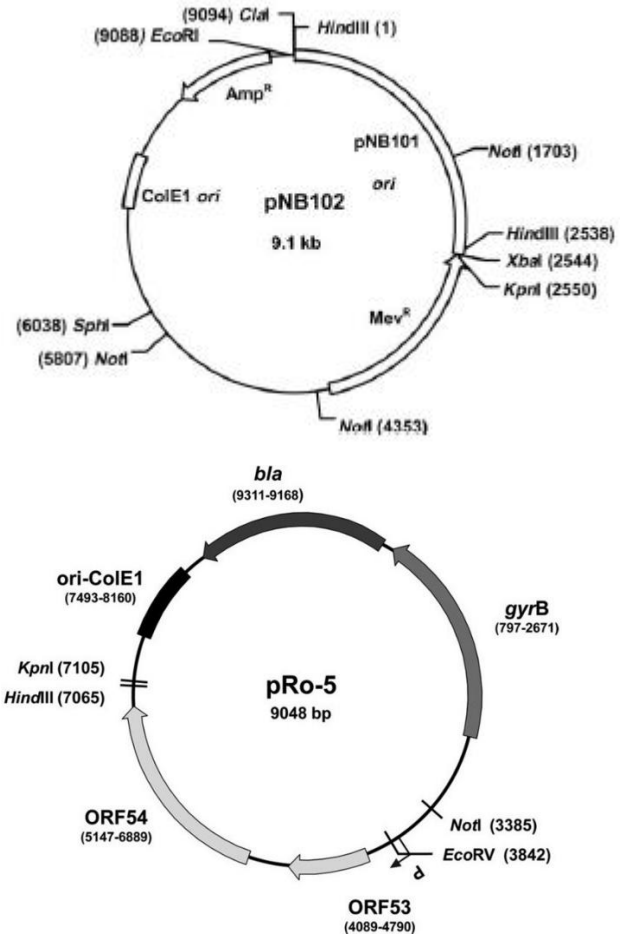

Figure 2: Plasmid-map of the vectors pNB102 (left) and pRo-5 (right). *Restriction sites indicated, genetic elements depicted as arrows in transcriptional direction (Mayerhofer-Iro et al., 2013; Zhou et al., 2004)*

With this method and the use of shuttle vectors for *N. magadii*, the genetic manipulation of this organism is possible.

Characterisation of virus ϕCh1

ϕCh1 is a head and tail virus, part of the family *Myoviridae* and possesses double stranded DNA (dsDNA). Isolation of the virus was first reported by Witte *et al*. in 1997, after spontaneous lysis of *N. magadii*, a haloalkalophilic archaeon and only known host of ϕCh1, growing under extreme salinity (4-5M) and alkalinity (pH 8.5-11), where to ϕCh1 is adapted to (Witte *et al.*, 1997). In moderate conditions, however, ϕCh1 is inactivated. The virus can exist as particle or chromosomally integrated into the

genome of *N. magadii* strain L11 as provirus. As temperate virus, ϕCh1 is capable of existing in 2 different life cycles, a lysogenic and lytic one. The lytic cycle occurs between the late logarithmic and stationary growth phase of its host *N. magadii*, leading to the production and release of virus particles through cell lysis, which are around 200 nm long and 20 nm wide at the tail with a icosahedral head of about 70 nm diameter (**Figure 3**). The tail of the virus is capable of contraction to reveal an internal shaft. Additionally, a collar-like structure is present at the end of the phage's tail which seem to be responsible for adsorption to the host.

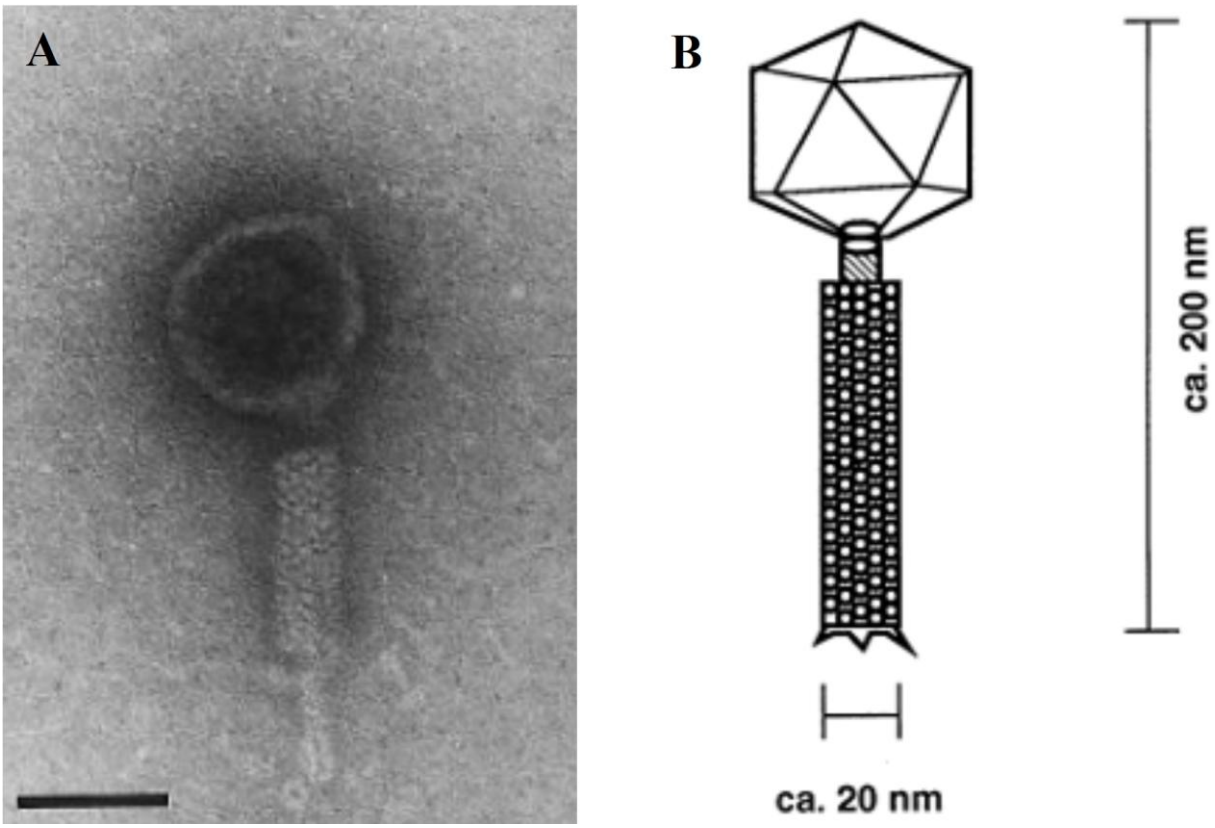

***Figure 3: Morphology of the ϕCh1 virus**. (A) Electron micrograph of ϕCh1 exhibiting head-tail morphology. The black bar represents 50nm. (B) Schematic representation with estimated dimension of the mature ϕCh1 particles. (Adapted from Witte et al., 1997)*

The genome of ϕCh1 has been shown to consist of 58498 bp dsDNA with a GC-content of 61.9 % and several RNA species within the virus particle (Klein *et al*. 2000). Additionally, the viral genome contains 98 open-reading-frames (ORFs) (**Figure 4**) All ORFs except ORF3, ORF41, ORF79 and ORF83 possess the ATG as start-codon, whereas the other four use GTG as start-codon. Furthermore, the genome can be divided into 3 transcriptional regions. In the left area of the genome, genes are mostly responsible for providing information for structural proteins and proteins involved in

virion morphogenesis. The genes of the central region are mostly responsible for replication, plasmid stabilization and regulation of gene expression. The functions of the genes of the right region, that are known, mostly revolve around methylation and restriction, although the function of most is unknown. The functional annotations of ORFs of ϕCh1 are mostly inferred due to their sequence similarities with previously identified genes. Although some ORFs are assigned with certain probable functions, like ORF80 and 82 as Methyltransferases (mtase) (Klein *et al.*, 2002), some ORFs lack any meaningful sequence similarities, which indicates that these ORFs code for functional and structural novel proteins.

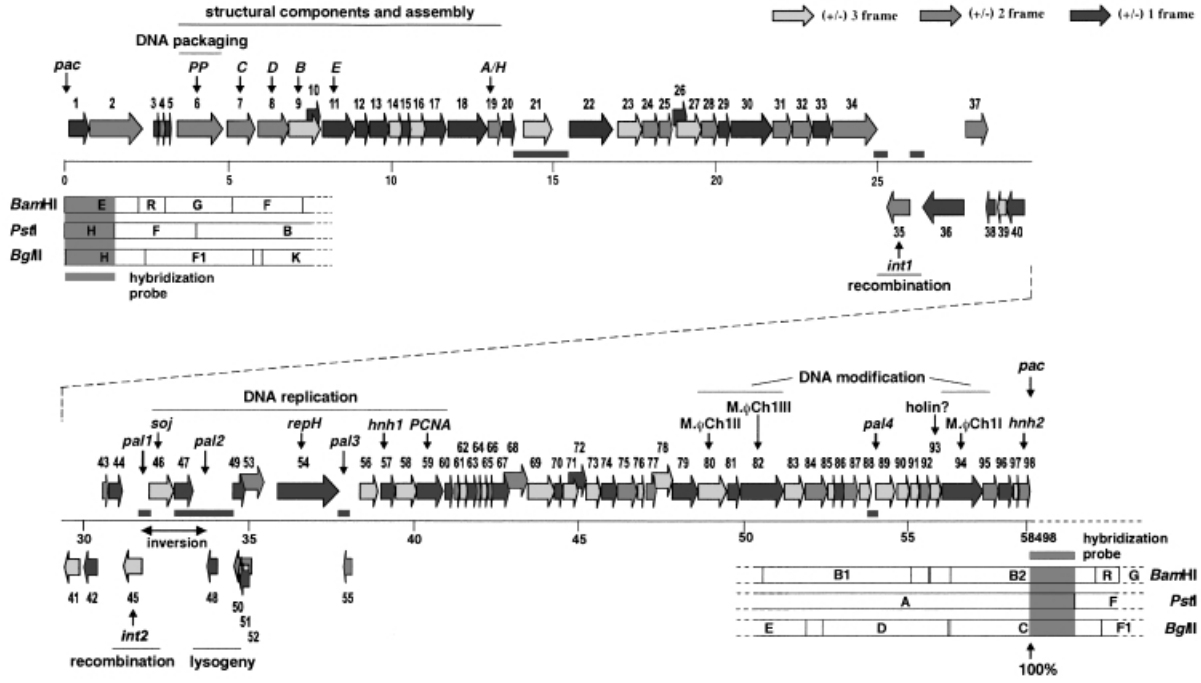

Figure 4: Genome map of phage ϕCh1. *Schematic of the 58498 bp long genome of ϕCh1, all 98 ORFs with verified and predicted function(s) are indicated. ORFs are depicted in 3 colours representing different reading frames, dark grey: 1st frame, mid grey: 2nd framed and light grey: 3rd frame. Up-Stream or Down-Stream Orientation is indicated by the direction of the arrows. (Adapted from Klein et al., 2002)*

ϕCh1 is able to switch from the lysogenic to the lytic phase by inducing virion production in the host. Maintaining either state or transitioning from one to the other, dependent on a variety of factors such as environmental conditions host physiology as well as host and virus genetics, requires a complex regulatory mechanism, controlling the activity of the virus genome. Part of this regulatory machinery are also methyltransferases (Baranyi *et al.*, 2000), which ORF80, ORF82 and ORF94 are suspected to be (Klein *et al.*, 2002).

DNA-Methyltransferases

DNA-Methyltransferases are enzymes which specifically methylate certain functional groups of nucleotide bases. All known DNA-Methyltransferases use S-Adenosyl methionine (AdoMet) to methylate either the nucleotide base adenine or cytosine and are mostly active as monomeric units. Since the methylated DNA is dissimilar enough to not be recognized by DNA-processing enzymes, many Mtases in prokaryotes are part of restriction/modification (R/M) systems, which function to protect DNA from indigenous restriction systems. Methylation of DNA furthermore has important roles in regulation transcription, cell cycle control and DNA replication (Wilson, 1991).

These important enzymes show some generally shared structural similarities. Structurally mtases can be divided into 3 functional domains, the AdoMet-binding domain, the target recognition domain which recognizes a specific DNA-Sequence and the catalytic domain which facilitates the methylation. The three domains consist of 10 conserved motifs, which can be arranged in different sequences to achieve enzymatic activity (Bheemanaik, 2006).

For classification according to their different substrates for methylation, mtase can be divided into 2 groups. For Adenine the exocyclic nitrogen of the nucleotide base can be methylated by so called m6A-mtases, or alternatively dam (DNA adenine methyltransferases). DNA-Cytosine methylases so called dcm methylate in two different ways. m4C-mtases methylate the exocyclic nitrogen of the cytosine, while m5C-mtases methylate the 5th cyclic carbon of the nucleotide base (Bheemanaik, 2006).

DNA-Methyltransferases of ϕCh1

Three ORFs encoding methyltransferases are known in ϕCh1. Firstly ORF80, containing the gene *dcm5*, encodes a potentially active m5C-mtase, named M.*Nma*ϕCh1II, which is also present in ϕH a related halophilic virus. Secondly ORF82 containing the gene *yhdJ*, which encodes for a potentially active m4C-mtase named M.*Nma*ϕCh1III (Dyall-Smith *et al*. 2018). The last ORF, ORF94, that contains M.*Nma*ϕCh1I, which has been shown to be a dam-like (DNA adenine

methyltransferases) or m6A-mtases, since it was able to complement a dam deficient *E. coli* strain despite the low salinity of the cytoplasm of *E. coli*. *ycdA* is the gene coding for M.*Nma*ϕCh1I (Baranyi *et al*., 2000).

M.*Nma*ϕCh1I is 419 amino acids long, 46.6 kDa heavy and possesses an isoelectric point of 4.17. Baranyi *et al*. showed in 2000 that synthesis of the enzyme mainly happens shortly before the release of virus particles during the lytic cycle of ϕCh1. This was achieved by comparing the share of methylation of the genome during different stages of the life cycle of ϕCh1. Additionally, restriction analysis revealed, that the genomes of ϕCh1 are partially adeno-methylated (Witte *et al*., 1997).

Although the M.*Nma*ϕCh1I has been experimentally shown to be a dam like methylase, for the other two methylases, M.*Nma*ϕCh1II and M.*Nma*ϕCh1III with corresponding ORFs 80 and 82, only sequence similarities are known, neither their actual activity nor the time of expression during the production of the virus.

Since Methylases are often involved in the regulation of expression (Wilson, 1991), and ORF94 was shown to be involved in the regulation of lysis and protein production, by deletion of ORF94 (Sommerkamp, 2022 and Eliaçık, 2024), it was chosen to investigate other similar ORFs in the same way. To this end mutants of ϕCh1 with deleted ORFs80 and 82 were created, to evaluate differences in the phenotype of the host infected by these mutants, compared to host infected by the wild-type virus.

Aim of study

Beforehand studies confirmed the methylation of the virus genome (Witte *et al*., 1997). Furthermore, the resulting search for Mtases in the genome of ϕCh1 yielded 3 different candidates, (ORF80, ORF82 and ORF94) via sequence similarity, of which one (ORF94) was confirmed to be a methylase and to be involved in the regulation of lysis and protein production (Sommerkamp, 2022 and Eliaçık, 2024). The experiments showing ORF94 to be a Mtase, where able to confirm its function by creating a deletion mutant by utilizing the plasmid pKS_{II}^{+} to replace the gene via homologous recombination with a novobiocin resistance cassette. By analyzing this mutant in different experiments, its function as a Mtase was revealed, and differences in growth virus titer and protein expression confirmed, showing ORF94 to

be involved in the regulatory processes of ϕCh1. To confirm the deletion of this mutant PCR of the gene and southern blots were utilized. Additionally, the expression of protein E, gp34 and Mtases in general was analyzed via western blot. To confirm the phenotypic changes hailed from the absence of ORF94, a mutant was complemented and analyzed in comparison and showed a successful reversion to the behaviour of the wild type strain L11.

Since ORF80 and ORF82 are only confirmed to be Methyltransferase via sequence similarity, the aim of this study is to perform the previously described experiments to show the function of ORF80 and ORF82 of the virus ϕCh1 residing in *Natrialba magadii*.

Materials and Methods

Materials

Strains

Escherichia coli

Table 1: Used strains of E. coli

Strain	Genotype	Source
XL1-Blue	*end*A1, *gyr*A96(nal^{R}), *thi*-1, *rec*A1, relA1, *lac*, *gln*V44, F'[::Tn10(tetR), proAB^{+} lacI^{q} Δ(lacZ)M15] *hsd*R17(r_K^- m_K^+)	Stratagene
BL-21 (DE3)	F$^-$ *omp*T *hsdS$_B$* (r_B^-, m_B^-) *gal dcm* (DE3)	Stratagene
Rosetta (DE3)	F$^-$ ompT hsdS$_B$(r_B^- m_B^-) gal dcm (DE3) pRARE (Cam^{R})	Stratagene

Lemo (DE3)	*fhuA2 [lon] ompT gal (λ DE3) [dcm] ΔhsdS/* pLemo(Cam^{R}) *λ DE3 = λ sBamHIo ΔEcoRI-B int::(lacI::PlacUV5::T7 gene1) i21 Δnin5* pLemo = pACYC184-*PrhaBAD-lysY*	New England BioLabs

Natrialba magadii

Table 2: Used strains of N. magadii

Strain	Genotype	Source
N. magadii L11	Wild type strain carrying provirus ϕCh1	Witte *et al.*, 1997
N. magadii L13	Derivate from L11 and cured of ϕCh1	Witte *et al.*, 1997
N. magadii L11-ΔORF80	*N. magadii* L11 with deletion of ORF80 by replacement with gyrB-via homologous recombination	This study
N. magadii L11-ΔORF82	*N. magadii* L11 with deletion of ORF82 by replacement with gyrB-via homologous recombination	This study
N. magadii L11-ΔORF80/ORF82	*N. magadii* L11 with deletion of ORF80 and ORF82 by replacement with gyrB-via homologous recombination	This study

N. magadii L11-ΔORF80 (pNB102)	*N. magadii* L11 with deletion of ORF80 and vector plasmid pNB102	This study
N. magadii L11-ΔORF82 (pNB102)	*N. magadii* L11 with deletion of ORF82 and vector plasmid pNB102	This study
N. magadii L11-ΔORF80-ORF82 (pNB102)	*N. magadii* L11 with deletion of ORF80 and ORF82 and vector plasmid pNB102	This study
N. magadii L11-ΔORF80 (pNB102-ORF80)	*N. magadii* L11 with deletion of ORF80 and vector plasmid pNB102 carrying ORF80	This study
N. magadii L11-ΔORF82 (pNB102-ORF82)	*N. magadii* L11 with deletion of ORF82 and vector plasmid pNB102 carrying ORF82	This study
N. magadii L11-ΔORF80-ORF82 (pNB102-ORF80-ORF82)	*N. magadii* L11 with deletion of ORF80 and ORF82 and vector plasmid pNB102 carrying ORF80 and ORF82	This study
N. magadii L11 (pNB102-ORF80)	*N. magadii* L11 with vector plasmid pNB102 carrying ORF80	This study
N. magadii L11 (pNB102-ORF82)	*N. magadii* L11 with vector plasmid pNB102 carrying ORF82	This study

N. magadii L11 (pNB102-ORF80-ORF82)	*N. magadii* L11 with vector plasmid pNB102 carrying ORF80 and ORF82	This study

Growth media

Lysogeny Broth (LB) medium

Peptone	10 g
Yeast extract	5 g
NaCl	5 g
pH adjusted to	7.0
ad dd H_2O	1 l

For LB media plates, before autoclaving add 10 g/l agar.

NVM+ rich medium

Yeast extract	11.7 g
Casein hydrolysate	8.8 g
Tri-Na citrate	0.8 g
NaCl	235 g
KCl	2.35 g
pH adjusted to	9-9.5
ad ddH_2O	935 ml

For plates, add 8 g/l agar before autoclaving. For soft agar, add 4 g/l agar before autoclaving. For complementation add this after autoclaving:

1 M $MgSO_4$	1 ml
20 mM $FeSO_4$	1 ml
Trace elements	1 ml

0.57 M Na_2CO_3	65 ml

1000X Trace Elements

$ZnSO_4.7H_2O$	0.1 g
$CoCl_2.6H_2O$	0.2 g
$CuCl_2.6H_2O$	10 mg
H_3BO_3	0.3 g
$MnCl_3.4H_2O$	30 mg
$Na_2MoO_4.H_2O$	30 mg
$NiCl_2.6H_2O$	20 mg

For sterilization filtered with 0.2 µm pore size.

Antibiotics and additives

Table 3: Additives for growth media

Antibiotic/additive	Stock concentration	Final concentration	Preperation
Ampicilin	20 mg/ml	100 µg/ml	Dissolve in dd.H_2O, sterile filter and store at 4°C
Tetracyclin	10 mg/ml	10 µg/ml	Dissolve in 50% Vol. dd.H_2O 50% Vol. 96 % Ethanol. Store at - 20°C (light sensitive)
Bactitracin	7 mg/ml	70 µg/ml	Dissolve in dd.H_2O sterile filter and store at

			4°C (light sensitive)
Mevinolin	10 mg/ml	7.5 µg/ml	Dissolved in 96% EtOH, store at - 20°C (light sensitive)
Novobiocin	3 mg/ml	3 µg/ml	Dissolve in dd.H_2O, sterile filter and store at - 20°C
IPTG	1 M	1 mM	Dissolve in dd.H_2O, sterile filter and store at - 20°C

Primers

Primers were ordered from Eurofins Genomics AT and/or Microsynth AG.

Table 4: Primer list

Number	Name	Sequence	T_M [°C]
123	ORF89-3	TGC TGG TAC CTC AGT CAT CGC CCT GC	61.3
476	34-Kpn	CAGCAGGGTACCCGGCGTTCGAGGTCA	62.2
548	Nov-9	GATGTCGGTCATCGCGG	65.4
706	79-BgI	GAT AAG ATC TAT GGT CGA AGT GAC GAA CC	61.4
734	79-KpnI	GAC GGG TAC CTC AAG CAT CGG TCG AGT CA	64.6
737	79-5	GAC CGG GAC TGG CTG T	61.1

829	Nov-12	GCCGGTGAGTACTTAACGC	61.1
1096	84-K	GAATGGTACCTCAGTCATCGTCTGTTGGGAGT	64.8
1097	84-B	GATCGGATCCATGACCGTCTTCGAGGACG	64.1
1196	DORF94-1	ATCCCCCGGGCTGCAGGAATTCGATATGACGCC CCCGCGATATTCGCGGA	82.2
1199	DORF94-4	GGTCGACGGTATCGATAAGCTTGATATCAGTCGTC GACGTCGCCGTCGGA	81
1221	NB-34up	ACGGCCGGTTTAAAGCTTCTTCTAGATCGGGTGG GATCCCGACGCGATTT	79.4
1273	D94-3_2	TCGTTCCAGTCGACACCCGGGGATCGCGAAGGA GGCGGCCGAGGACGGCG	86.4
1292	80-3-en	GAGTTCTGCAAGAACCTCCTCG	65.2
1293	82-5-en	GTTCACGAACGACGACCC	63.1
1294	82-3-en	GCCGTCGACGTCATATCGTT	65.9
1295	ORF80-5	GCCGCTGCAGATGCTTGAGAGCAGTCAGTTC	60
1296	ORF82-5	GCCGCTGCAGATGATCTCCGAATGGACCG	63.3
1297	pNB-ORF80	CCATGCCACTCTTCACACGCGGTACTCAGTCATC GCCCTGCCCTCCTTCT	75.9
1298	pNB-ORF82	CCATGCCACTCTTCACACGCGGTACCATCGAGGT CGGTGATACCCCGTGA	75.8
1306	ORF82-3	GCATGGTACCTCACGGGGTATCACCGAC	63.3

1308	ORF82-5-BglII	GCCGAGATCTATGATCTCCGAATGGACCG	63.6
1309	82-1-probe	GACCGAAAACCCGTACTTCG	64.3
1310	82-2-probe	GTCTCGACGAGCTCCCACTC	65.3
1311	ORF80-5-BglII	GCCGAGATCTATGCTTGAGAGCAGTCAGTTC	60
1325	ORF82-5-sc	GTCGCGGTCGAGGC	49.4
1326	ORF82-3-sc	GTCGACGCGCTTGCCG	56.2
1334	GA_ORF80-pRSET-A1	TGACGATAAGGATCGATGGGGATCCATGCTTGAGAGCAGTCAGTTCCTTG	67
1335	GA_ORF80-pRSET-A2	ATCAAGCTTCGAATTCCATGGTACCTCAGTCATCGCCCTGCCCTCCTTCT	75.9
1336	GA_ORF82-pRSET-A1	TGACGATAAGGATCGATGGGGATCCATGATCTCCGAATGGACCGGCGACA	77.2
1337	GA_ORF82-pRSET-A2	ATCAAGCTTCGAATTCCATGGTACCTCACGGGGTATCACCGACCTCGATG	75.8
1369	pRo-5-ORF80	CCTCACTAAAGGGAACAAAAGCTGGTCAGTCATCGCCCTGCCCTCCTTCT	75.9

Plasmids

Table 5: Used Plasmids

Name	Features	Source

pNB102	*bla*, ColE1 ori, *hmg* (Mev$_R$), ϕCh1 derived origin of replication	Zhou *et al.*, 2004
pNB102-ORF80	ORF80 cloned under control of the promoter of ORF34 in pNB102	This study
pNB102-ORF82	ORF82 cloned under control of the promoter of ORF34 in pNB102	This study
pNB102-ORF80-ORF82	ORF80 and ORF82 cloned under control of the promoter of ORF34 in pNB102	This study

DNA purification kits

All kits were used per manufacturer's protocol.

Name	Manufacturer	Use
Promega WizardR SV Gel and PCR Clean-Up System	Promega	Purification of PCR products and gel-eluted DNA fragments
WizardR Plus SV Minipreps DNA Purification System	Promega	Isolation of Plasmid DNA in *E. coli*

Enzymes

All enzymes and kits were used per manufacturer's protocol, with buffers recommended accordingly.

Table 6: List of used Enzymes

Enzymes	Manufacturer	Use
Restriction enzymes: *Kpn*I, *HindIII*, *Sau*3AI, *Dpn*I, *Mbo*I and *Eco*RI, *Bgl*II, *Bam*HI, *Sma*I, *Hind*III	Thermo Scientific and New England Biolabs	DNA restriction
GoTaq DNA Polymerase/Mastermix	Promega	Analytic PCR (lacks 3' – 5' proofreading activity)
Phusion Hifi Master Mix	Thermo Scientific	Fragment amplification for cloning (has 3' – 5' proofreading activity)
T4 DNA ligase	Promega	Ligate DNA fragments
Proteinase K	Qiagen	Digest S- layer in *Archaea*
Lysozyme from chicken egg white	Sigma	Hydrolysis polysaccharide backbone of peptidoglycans in the cell wall
FastAP Thermosensitive Alkaline Phosphatase	Thermo Scientific	To remove of 3' and 5' phosphate groups after restriction, that is, dephosphorylation

DNA and protein ladders

Used per manufactures instructions.

Table 7: Used size indicators ladders for gel electrophoresis

DNA/Protein Ladder	Manufacturer	Size range
GeneRuler 1kb DNA Ladder	Thermo Scientific	250-10000 bp
PageRuler™ Prestained Protein Ladder	Thermo Scientific	10-170 kDa

Antibodies

Table 8: Used Antibodies in western blots

Primary Antibody	Target	Dilution	Source
α-E (from rabbit)	Major capsid protein E of ΦCh1	1:2500	Klein *et al.*, 2000
α-Mtase	Mtase (ORF94) of ϕCh1	1:500	Baranyi *et al.*, 1999
α-gp34	Tail fibre protein of (ORF34) ϕCh1	1:1500	Klein *et al.*, 2012
Secondary antibody	Target	Dilution	Source
α-rabbit IgG, horseradish peroxidase linked (donkey)	rabbit IgG	1:5000	GE Healthcare

Solutions, buffers, and reagents

Agarose gel electrophoresis

50x TAE		50x Super Buffer		5x DNA Loading Dye	
Tris/HCl pH 8.2	2 M	Tris	2 M	Tris/HCl pH 8.2	50 mM
Acetic acid	1 M	Acetic acid	1 M	Sucrose	25 %
EDTA	0.1 M	EDTA pH 8.2	0.1 M	SDS	0.1 %
				Bromophenol blue	0.05 %
				Xylene cyanol	0.05 %

Sodium Dodecyl Sulphate–Polyacrylamide Gel Electrophoresis (SDS-PAGE)

2x Laemmli Buffer		1M Sodium phosphate buffer (1L)	
Tris/HCl pH 6.8	120 mM	1M Na_2HPO_4	463 ml

Glycerol	20%	1M $NaH2PO_4$	537 ml
β-mercaptoethanol	10%		
Bromophenol blue	0.02%		
SDS	4%		

10x SDS PAGE running buffer		30% Acrylamide	
Glycine	1.92 M	Acrylamide	29%
Tris	0.25 M	N,N'-methylenebisacrylamide	1%
SDS	1%		

Separating gel buffer		Stacking gel buffer	
Tris/HCl pH 8.8	1.5 M	Tris/HCl pH 8.8	0.5 M
SDS	0.4%	SDS	0.4%

Coomassie staining solution		De-staining solution	
Methanol	25%	Glacial acetic acid	10%
Acetic acid	10%	Methanol	10%
Coomassie Brilliant Blue R250	0.15%	dd.H_2O	80%

Western Blot

Transblot buffer		10x TBS	
Tris	48 mM	Tris/HCl pH 8.8	0.25 M
Glycine	39 mM	NaCl	1.37 M
SDS	0.037%	KCl	27 mM
Methanol	20%		

Coumaric Acid		Luminol	
Coumaric Acid	1.48%	Luminol	8.86%

DMSO	Solvent	DMSO	Solvent

ECL (200 ml)		Blocking solution	
Coumaric acid	250 µl	Skimmed milk powder	5%
Luminol	500 µl	1x TBS	Solvent
1.5M Tris/HCl pH 8.5	13.3 ml		

Southern Blot

20x SSC		50x Denhardt's solution (100 ml)	
NaCl	3 M	Ficoll 400	1 g
Trisodium Citrate 2 H_2O	300 mM	Polyvinylpyrolidone	1 g
Adjust pH with HCl to	7	BSA	1 g

Hybridization buffer	
20x SSC	25 ml
50x Denhardt´s Solution	10 ml
10 % BSA	5 ml
1 M Na_2HPO_4	5 ml
20 % SDS	500 µl
0,5 M EDTA	200 µl
ddH_2O	55 ml

Chemiluminescent Nucleic Acid Detection Module Kit from Thermo Scientific™

Generation of E. coli competent cells

MOPS I	MOPS II

MOPS	100 mM
$CaCl_2$	10 mM
RbCl	10 mM
Adjust pH with KOH	7.0

MOPS	100 mM
$CaCl_2$	70 mM
RbCl	10 mM
Adjust pH with KOH	6.5

MOPS IIa

MOPS	100 mM
CaCl2	70 mM
RbCl	10 mM
Glycerol	15%
Adjust pH with KOH	6.5

Generation of N. magadii competent cells and transformation

Buffered high-salt spheroplast solutions:

Buffered high salt spheroblast solution	
KCl	27 mM
NaCl	2 M
Tris/HCl pH9.5	50 mM
Sucrose*	15%
*Add after autoclaving	

Unbuffered high salt spheroblast solution (USS)	
KCl	27 mM
NaCl	2 M
Sucrose*	15%

60% PEG 600

PEG 600	60%
USS	40%

Isolation of Virus particles

1.1 CsCl		1.3 CsCl	
CsCl	0.6 M	CsCl	3.7 M
NaCl	2 M	NaCl	2 M
Tris/HCl pH9.5	50 mM	Tris/HCl pH9.5	50 mM

1.5 CsCl		High-Salt alkaline solution	
CsCl	4 M	NaCl	4 M
NaCl	2 M	Tris/HCl pH9.5	50 mM
Tris/HCl pH9.5	50 mM		

Gibson Assembly

5X ISO buffer		2X Gibson Assembly Master Mix	
DL-Dithiothreitol	50 mM	5X ISO buffer	320 µl
dATP	1 mM	Phusion polymerase	20 µl
dCTP	1 mM	T5 Exonuclease	1.5 µl
dGTP	1 mM	Taq DNA ligase	160 µl
dTTP	1 mM		
NAD	5 mM		
PEG 6000	25%		
Tris/HCl pH 7.5	500 mM		

2X Gibson Assembly Master Mix	
5x ISO reaction buffer	100 µl
10U/µl T5 Exonuclease (NEB M0363S)	0.2 µl
2 U/µl Phusion polymerase (NEB M0530S)	6.25 µl
40 U/µl Taq DNA ligase (NEB M0208S)	50 µl
Nuclease-free water	218.55 µl

5X ISO buffer	
PEG-8000 (25%w/v)	2.5 g
1 M Tris-HCl, pH 7.5 (500 mM)	5 ml
1 M MgCl2 (50 mM)	500 µl
DL-Dithiothreitol (50 mM)	77 mg
100 mM dATP (1mM)	100 µl
100 mM dATP (1mM)	100 µl
100 mM dATP (1mM)	100 µl
100 mM dATP (1mM)	100 µl
NAD (5 mM)	33.2 mg
Nuclease-free water	Ad 10 ml

Methods

Molecular cloning

Agarose gel electrophoresis

0.8% agarose-super buffer-gels and 1.6% agarose-TAE-gels were used for the size based separation of DNA for the purpose of purification or visualization and analysis (Wood 1983). For purification and analysis of DNA-fragments with bigger size differences the super buffer setup was used, for more accurate separations and visualization of size differences TAE-gels were used.

Polymerised Chain Reaction (PCR)

PCR was used to amplify desired DNA-fragments for analysis or for creating desired inserts for plasmid constructs (Weier and Gray, 1988). For uses which require an accurate DNA sequence, such as fragments for cloning, Phusion™ High-Fidelity DNA Polymerase was used. For reactions only needing to produce PCR products of accurate length, like analysis via gel electrophoresis, GoTaq® DNA Polymerase was used.

DNA template for PCR

For reaction with purified DNA as template around 20-100 ng were used. If culture was directly used for PCR, 1 µL was used if taken fom *E. coli* cultures. If the *N. magadii* culture was used for PCR, it was prepared by centrifuging 20 µL of culture and resuspending the cell pellet in sterile deionized water.

Primers

Unless indicated otherwise primers of a concentration of 100 ng/µL were used for PCR. Annealing temperatures were obtained with the online calculation program "*Tm Calculator* of New England Biolabs (NEB)".

PCR program

Analytical PCR

GoTaq® DNA Polymerase was used for analytical PCRs (no 3'-5'-exonuclease activity).

Table 9: Reaction mix for analytical PCR

Compound	Volume [µl]
Template	1
Forward Primer	1.5
Revers Primer	1.5
2x GoTaq Green Master Mix	12.5
dd. H_2O	8.5

Table 10: Temperature program for analytical PCRs

	Time	Temperature [°C]	Repeats
Initial Denaturation	3 min	95	1
Denaturation	15 s	95	25
Annealing	7 s	*	
Extension	**	72	
Final Extension	3xExtension	72	1

*Dependent on annealing temperature calculated for used primer

**Dependent on size of PCR product (Amplification rate of GoTaq 1kb/min)

Preparative PCR

For amplification of accurate sequences Phusion™ High-Fidelity DNA Polymerase Master mix was used (3'-5'-exonuclease activity).

Table 11: Reaction mix for preperative PCR

Compound	Volume [µL]
Template	1
Forward Primer	2.5
Revers Primer	2.5
2x High-Fidelity Green Master Mix	25
dd. H_2O	19

Table 12: Temperature program for preperative PCRs

	Time	Temperature [°C]	Repeats
Initial Denaturation	3 min	98	1
Denaturation	15 s	98	35
Annealing	7 s	*	
Extension	**	72	
Final Extension	3xExtension	72	1

*Dependent on annealing temperature calculated for used primer

**Dependent on size of PCR product (Amplification rate of Phusion HIFI Polymerase 1kb/15 s)

DNA purification

Purification of plasmid DNA

Wizard®Plus SV Minipreps DNA Purification System was used for plasmid isolation.

Purification of PCR fragments

Gel electrophoresis with Super buffer was used for separation of DNA-fragments together with purification from the gel via the Wizard®SV Gel and PCR Clean-Up System.

Gibson assembly

This technique was employed to construct some of the plasmids used. For this, plasmids and, per PCR obtained, inserts were purified by the respective purification kit, like described above. To ensure successful assembly a molar excess of fragment(s) was used (1:5) (Gibson et al., 2009). One reaction had a volume of 20 µl total with 10 µl Gibson-Master-Mix and the remaining volume used to add the purified DNA. The reactions were incubated at 50°C for 15 min-1 h and afterwards either frozen for later use or directly used for transformation into *E. coli*.

Ligation with T4-DNA-Ligase

This technique was employed to construct some of the plasmids used. For this, plasmids and, per PCR obtained, inserts were purified by the respective purification kit, like described above. To ensure successful assembly a molar excess of fragment(s) was used (1:5). One reaction had a volume of 15 µl total with 1.5 µl T4-buffer, 1 µl T4-DNA-ligase and the remaining Volume used to add the purified DNA. The reactions were incubated at 16°C or room temperature for 15 min-24 h and afterwards frozen for later use or directly used for transformation into *E. coli*.

Transformation

E. coli

E. coli cells, harvested during the exponential growth phase and made competent via RbCl, were used to transform plasmids into them (Froger and Hall, 2019), either directly after preparation or after being stored on -80°C.

N. magadii

For inducing competency in *N. magadii*, cells were treated with proteinase K to remove the S-Layer, afterwards transformation was performed via a protocol based on polyethylene glycol 600 (PEG 600) (Mayrhofer-Iro et al., 2013). 3-15 µg of DNA were used, and after plating on NVM CAA plates the same were incubated in sealed plastic

bags on 42°C until colonies were clearly visible, which usually occurred after 2-4 weeks.

Screening of transformants

E. coli

After transformation single colonies were picked and inoculated in 500 µL LB-media with appropriate selective antibiotics and incubated overnight, at 37°C, shaking at 165 rpm in an Eppendorf tube. If growth occurred, this culture was then tested by PCR (see Analytical PCR, DNA template for PCR) and gel electrophoresis (see Agarose gel electrophoresis).

N. magadii

After transformation single colonies were picked and inoculated in 500 µL NVM CAA-media with appropriate selective antibiotics and incubated 1-5 days, at 37°C shaking, at 165 rpm in an Eppendorf tube. If growth occurred, this culture was then tested by PCR (see Analytical PCR, DNA template for PCR) and gel electrophoresis (see Agarose gel electrophoresis).

Southern Blot

First, the DNA which was to be analysed, was digested via a restriction enzyme appropriate for the desired analysis. In parallel unedited ϕCh1 genome was treated the same way as a control (see Table 13). Afterwards a Southern blot of the, via agarose gel separated, restriction was performed, using the appropriate probe, produced by performing a PCR of ϕCh1 with the adequate primers (see Table 13).

Table 13: Testing scheme for Southern blot

Binding site	ϕCh1 Genotype	Probe used (primers for synthesis)	Restriction enzyme
ORF80-5’	Δ80	79-Bgl/79-Kpn	*Bam*HI
ORF80-3’	Δ80	82-5-en/80-3-en	*Sma*I
ORF80-5’	Δ80/82	79-Bgl/79-Kpn	*Bam*HI
ORF82-3’	Δ80/82	84-B/84-K	*Bam*HI

Blotting of DNA

To separate DNA for southern blots, TAE-agarose gels were used. To facilitate blotting, the gel had to undergo several incubation steps first. Initially the gel was incubated for 30 min with0.25 N HCl, afterwards for 30 min with 0,4 N NaOH/ 0,6 M NaCl and finally for 30 min with 1,5 M NaCl/ 0,5 M Tris-HCl pH 7.5. Blotting itself was done by capillary action overnight onto an Amersham Hybond™ nylon membrane (GE Healthcare), with 10x SSC as transfer buffer. After blotting the membrane was incubated for 1 min in 0.4 N NaOH and afterwards for 1 min in 0.2 M Tris-HCl pH 7.5. To finalize the blot the DNA was fixed to the nitrocellulose membrane via UV-crosslinking.

Production Probes

Probes were obtained by production via PCR. To allow detection after hybridization with the blotted DNA, biotinylated nucleotides were added to the PCR reaction to be incorporated into the probes (see Table 14 and Table 15).

Table 14: PCR reaction Mix for the production of probes

Compound	Volume [µl]
ϕCh1-DNA (Template)	1
Forward Primer	10
Revers Primer	10
2x GoTaq Green Master Mix	50
dd. H_2O	28
Biotinylated dUTP	1

Table 15: Temperature program for probe production

	Time	Temperature [°C]	Repeats
Initial Denaturation	3 min	95	1
Denaturation	15 s	95	35
Annealing	7 s	*	
Extension	**	72	

Final Extension	3xExtension	72	1

*Dependent on annealing temperature calculated for used primer

**Dependent on the probe (see Table 16)

Table 16: Probes used for detection

Probe	Annealing Temperature [°C]	Probe produced with Primers		Amplification time
1	58	79-BgI	79-KpnI	1 min and 30 s
2	60	82-5-en	80-3-en	1 min and 30 s
3	60	84-B	84-K	1 min

After production, the probes were purified via Promega WizardR SV Gel and PCR Clean-Up System. Before hybridization, all used probes were denatured by heating to 95°C for 5 min.

Detection

First, the membrane harbouring the DNA was blocked by incubation in Hybridization solution with 10 mg/ml herring sperm for 3 h at 65°C. Afterwards the appropriate probe was added, and the incubation at 65°C continued overnight.

Table for probes and detection (see Table 13)

After overnight incubation the membrane was washed 2x for 5 min with 2 x SSC/ 0.1 % SDS at room temperature. Additionally, 2 wash steps with 0.1 x SSC/ 0.1 % SDS at 65 °C for 15 min were performed.

For detection itself, the Chemiluminescent Nucleic Acid Detection Module was used according to the manual.

Growth experiments

All growth experiments were conducted by inoculating the respective strain to an OD of 0.1, from a starter culture, in the indicated medium and grown at 37°C under agitation, to ensure aerobic conditions. The starter cultures were grown at 42°C and otherwise under the same conditions as previously mentioned.

Protein methods

Crude protein extracts

For analysis via western blot, crude protein extracts were prepared by spinning down of 1.5 ml of *N. magadii* culture and resuspending the cell pellet in (OD_{600} x 75) ml of 5 mM sodium phosphate buffer and the same amount of 2x Laemmli buffer. After resuspension the mixture was incubated at between 24-48 h at 37°C.

SDS-PAGE

12% SDS-PAGE was used for separating the proteins of the extracts (Laemmli, 1970). Since *N. magadii* contains high amounts of NaCl to counteract the osmotic pressure of its highly saline environment, which influences conductivity, the voltage used for separation was limited to 40 V.

Western blot

Western blots were used for qualitative analysis of proteins. Via SDS-PAGE, separated proteins (see SDS-PAGE) were then blotted like described in Harlow and Lane 1988. After three final washing steps, the membrane was analyzed by adding 3 ml ECL and 3 µl H_2O_2 (Haan and Behrmann, 2007). For the detection the ChemiDoc XRS+ imager was used with an exposure time of 180 seconds.

Acetone powder

All used antibodies were polyclonal. To reduce unspecific bands acetone powder, derived from *N. magadii* L13, was used (Sabic, 2019).

ϕCh1

Plaque assay

To assess the number of virus particles, plaque assays were performed by plating a serial dilution (10^{-2} to 10^{-8}), prepared in NVM CH, in soft agar mixed with *N. magadii* L13. The plates were then incubated in sealed plastic bags at 37°C for 7-14 days.

Isolation and concentration of ϕCh1 virus particles

CsCl-gradient centrifugation was used to isolate ϕCh1-particles released from lysogenic strains (L11) of *N. magadii* (Witte et al., 1997). Equipment used consisted of Beckman model L-70 and SW40-Ti swinging bucket rotor.

Dialysis of Virus particles

To remove Cs-Ions, after centrifugation the obtained solution of phage particles was dialysed against high-salt alkaline solution (see Isolation of Virus particles), for 1 h and afterwards with new solution a second time overnight, at room temperature.

Extraction of ϕCh1 viral DNA

To obtain virus-DNA, dialysed virus particles were used in a phenol-chloroform extraction, followed by isopropanol precipitation (Witte et al., 1997). The DNA was taken up in sterile dH_2O and used, or after freezing stored at - 20°C and used after rethawing.

Cloning strategies

Construction Methods

Ligation with T4-Ligase

Insert and Vector were restricted with 2 Restriction enzymes, to ensure orientation of the insert in a desired direction. Ratios of insert to vector of 3:1 to 5:1 were used and if less than 11.5 µl of insert were used, the remaining volume was replaced with water. Otherwise, the reaction was composed like in Table 17.

Table 17: Reaction mixture for ligation with T4-DNA-Ligase

Compound	Volume [µl]
Insert	11.5
Vector	1
T4-DNA-Ligase-buffer	1.5
T4-DNA-Ligase	1

Ligation via Gibson Assembly

For assembling a plasmid construct via Gibbson assembly 10 µl of DNA containing insert(s) and vector were mixed with 10 µl of Gibbson-Assembly-Mastermix. The molar ratio of inserts to vector was (3-5):1. The Gibbson-Assembly-Mastermix was composed according to Gibson Assembly in the Materials section.

pQE-30-ORF80

Vector	pQE30
Restriction of vector with	*Bam*HI, *Kpn*I
Insert	ORF80
Template Insert	ϕCh1-DNA
Primer for Insert	ORF80-5-*Bgl*II / ORF89-3
Restriction of Insert	*Bgl*II, KpnI
Ligation Method	T4-DNA-Ligase
Host organism	*E. coli* strains XL-1-Blue, Lemo, BL-21, Rosetta

pRSET-A-ORF80 (1)

Vector	pRSET-A
Restriction of vector with	*Bam*HI, *Kpn*I
Insert	ORF80
Template Insert	ϕCh1-DNA
Primer for Insert	ORF80-5-*Bgl*II / ORF89-3
Restriction of Insert	*Bgl*II, *Kpn*I
Ligation Method	T4-DNA-Ligase
Host organism	*E. coli* strains XL-1-Blue, Lemo, BL-21, Rosetta

pRSET-A-ORF80

pRSET-A with *Kpn*I / *Bam*HI

GA_ORF80-pRSETA1 / GA_ORF80-pRSETA2

GA

Vector	pRSET-A
Restriction of vector with	*Bam*HI, *Kpn*I
Insert	ORF80
Template Insert	ϕCh1-DNA
Primer for Insert	GA_ORF80-pRSETA1 / GA_ORF80-pRSETA2
Ligation Method	GA
Host organism	*E. coli* strains XL-1-Blue, Lemo, BL-21, Rosetta

pRSET-A-ORF80/82

pRSET-A with *Kpn*I / *Bam*HI

GA_ORF80-pRSETA1 / GA_ORF82-pRSETA2

GA

Vector	pRSET-A
Restriction of vector with	*Bam*HI, *Kpn*I
Insert	ORF80/82
Template Insert	ϕCh1-DNA
Primer for Insert	GA_ORF80-pRSETA1 / GA_ORF82-pRSETA2
Ligation Method	GA
Host organism	*E. coli* strains XL-1-Blue, Lemo, BL-21, Rosetta

pRSET-A-ORF82

pRSET-A with *Kpn*I / *Bam*HI

GA_ORF82-pRSETA1 / GA_ORF82-pRSETA2

GA

Vector	pRSET-A
Restriction of vector with	*Bam*HI, *Kpn*I
Insert	ORF82
Template Insert	ϕCh1-DNA
Primer for Insert	GA_ORF82-pRSETA1 / GA_ORF82-pRSETA2
Ligation Method	GA
Host organism	*E. coli* strains XL-1-Blue, Lemo, BL-21, Rosetta

pKS-34up-ORF80

pKS-34up with *Kpn*I and *Pst*I

ORF80-5 / ORF89-3 with *Kpn*I and *Pst*I

Lig T4

Vector	pKS-34up
Restriction of vector with	*Kpn*I, *Pst*I
Insert	ORF80
Template Insert	ϕCh1-DNA
Primer for Insert	ORF80-5 / ORF89-3
Ligation Method	T4-Ligase
Host organism	*E. coli* strain XL-1-Blue

pKS-34up-ORF80/82

pKS-34up with *Kpn*I and *Pst*I

ORF80-5 / ORF82-3 with *Kpn*I and *Pst*I

Lig T4

Vector	pKS-34up
Restriction of vector with	*Kpn*I, Pst*I*
Insert	ORF80/82
Template Insert	ϕCh1-DNA
Primer for Insert	ORF80-5 / ORF82-3 (T_A=56°C)
Restriction of Insert	*Kpn*I and *Pst*I
Ligation Method	T4-Ligase
Host organism	*E. coli* strain XL-1-Blue

pKS-34up-ORF82

pKS-34up with *Kpn*I and *Pst*I

ORF82-5 / ORF82-3 with *Kpn*I and *Pst*I

Lig T4

Vector	pKS-34up
Restriction of vector with	*Kpn*I, *Pst*I
Insert	ORF80/82
Template Insert	ϕCh1-DNA
Primer for Insert	ORF82-5 / ORF82-3
Restriction of Insert	*Kpn*I and *Pst*I
Ligation Method	T4-Ligase
Host organism	*E. coli* strain XL-1-Blue

pNB102-34up-ORF80 (Complementation plasmid)

pNB102 with *Xba*I and *Kpn*I

NB-34up / pNB-ORF80 form pKS-34up-ORF80

GA

Vector	pNB102
Restriction of vector with	*Xba*I and *Kpn*I
Insert	ORF80
Template Insert	pKS-34up-ORF80
Primer for Insert	NB-34up / pNB-ORF80
Restriction of Insert	-
Ligation Method	GA
Host organism	*N. magadii* L13

pNB102-34up-ORF80/82 (Complementation plasmid)

pNB102 with *Xba*I and *Kpn*I

NB-34up / pNB-ORF82 form pKS-34up-ORF80/82 68°C

GA

Vector	pNB102
Restriction of vector with	*Xba*I and *Kpn*I
Insert	ORF80/82
Template Insert	pKS-34up-ORF80/82
Primer for Insert	NB-34up / pNB-ORF80/82
Restriction of Insert	-
Ligation Method	GA
Host organism	*N. magadii* L13

pNB102-34up-ORF82 (Complementation plasmid)

pNB102 with *Xba*I and *Kpn*I

NB-34up / pNB-ORF82 form pKS-34up-ORF82

GA

Vector	pNB102
Restriction of vector with	*Xba*I and *Kpn*I
Insert	ORF82
Template Insert	pKS-34up-ORF82
Primer for Insert	NB-34up / pNB-ORF82
Restriction of Insert	-
Ligation Method	GA
Host organism	*N. magadii* L13

Screening strategies for Constructs and deletion mutants

Table 18: Employed screening strategies via PCR

Construct/Organism (screened section)	Primer 1	Primer 2	T_A [°C]
pKS-34up-ORF80/82 (Outside insertions)	NB-34up	pNB-ORF82	68
?	ORF82-5-Bg/II	ORF82-3	63.3
pRSET-A-ORF80	ORF82-5-sc	ORF82-3-sc	62
pQE-ORF80	ORF82-5-sc	ORF82-3-sc	62
pNB102-34up-ORF80/82	ORF82-3	ORF82-5-BgIII	63.3
pNB102-34up-ORF80/82	NB-34up	pNB-ORF82	68
L11/ϕCh1-ΔORF80 (ORF80 5'*)	ORF80-5	34-Kpn	56

Probe1	79-Bgl	79-Kpn	58
Probe2	85-5-en	82-3-en	60
Probe3	82-1-probe	82-2-probe	60
L11/ϕCh1-ΔORF80 (Insertion 5'-end)	79-5	Nov-12	56.1
L11/ϕCh1-ΔORF80 (ORF80 5'*)	79-5	80-3-en	60
L11/ϕCh1-ΔORF80 (ORF80 5'*)	ORF80-5	34-Kpn	56
L11/ϕCh1-ΔORF80/ORF82 (5'-end)	79-5	Nov-12	56.1
L11/ϕCh1-ΔORF80/ORF82 (3'-end)	Nov-9	82-3-en	60.4
L11/ϕCh1-ΔORF80/ORF82 (80/82*)	79-5	84-K	56.1
L11/ϕCh1-ΔORF80/ORF82 (3'-end)	Nov-9	84-K	60.4
L11/ϕCh1-ΔORF80/ORF82 (Insertion 5'-end)	79-5	Nov-12	56.1
L11/ϕCh1-ΔORF80/ORF82 (ORF80/82*)	79-5	82-3-en	60
L11/ϕCh1-ΔORF80/ORF82 (ORF80&82*)	ORF80-5	ORF82-3	56
L11/ϕCh1-ΔORF82 (Δ82)	ORF82-5	ORF82-3	59
L11/ϕCh1-ΔORF82 (5'-end)	ORF82-5	Nov-12	59
L11/ϕCh1-ΔORF82 (5'-end Insertion)	82-5-en	Nov-12	56.1
L11/ϕCh1-ΔORF82 (ORF82*)	82-5-en	82-3-en	60
L11/ϕCh1-ΔORF82 (Δ82 5'-end)	ORF80-5	Nov-12	56.1

*Screening for respective ORFin deletion mutants to ensure deletion in all copies of the genome/Verifying insertion of only a single copy of insert.

Sequencing

Certain constructs were sequenced to ensure sequence similarity of the insert to the source. For this the following sequencing-primers were used. Sequencing was performed by the company Microsynth AG.

Table 19:Used Sequencing Primers

Standard-Primer	Sequence
T7*	TAATACGACTCACTATAGGG
QE-for*	GTATCACGAGGCCCTTTCG

*Provide by Microsynth AG via their standard primer list

Table 20:Pimer use for sequencing plasmid products

Plasmid to be sequenced	Used Sequencing Primer
pRSET-A	T7
pQE-30	QE-for

Results and Discussion

Results

Creation of deletion mutants ΔORF 80, ΔORF 82 and ΔORF 80/ORF 82

As a first step to analyse the function of the ORFs 80 and 82, three deletion mutants were created, 2 deleting one of the ORFs and one with both deleted. In these mutants the targeted regions were replaced by novobiocin resistance cassettes (gyrB) via homologous recombination. This was achieved by transforming the *N. magadii* L11 strain with a pKS_{II}^{+}-Plasmid containing the resistance cassette with the respective adjacent genetic code of the region to be replaced with the cassette, pKS_{II}^{+}-ΔORF80, pKS_{II}^{+}-ΔORF82 and pKS_{II}^{+}-ΔORF80/82 respectively. This enabled the homologous recombination replacing the genetic code between the target sequences, with the novobiocin resistance cassette. Since the pKS_{II}^{+}-Plasmid only possesses an Origin of Replication (ori) capable of operating in mesophilic conditions, but not in halophilic ones, *N. magadii* successfully transformed with it, rapidly loose it afterwards, creating the required deletion strains without superfluous plasmids.

Construction and isolation of the plasmids for the deletion of ORF 80, ORF 82 and both simultaneously

All deletion plasmids were constructed via Gibbson assembly and subsequently transformed into *E. coli* strain XL-1-Blue for replication. After isolation of a sufficient amount of plasmid-DNA of the respective construct, *N. magadii* L11 was transformed with it. To ensure the successful integration of the novobiocin resistance cassette, the resulting colonies were screened via PCR for the 5' and 3' end of the cassette (see **Figure 5**, **Figure 6** and **Figure 7**) as well as the length of the entire cassette (see **Figure 8**), in the case of the single deletions, to ensure that the resistance cassette was only integrated once. The entire length of the double deletion was not examined since the size difference between the cassette, and the original sequence was too small for a clear difference to be seen by agarose-gel electrophoresis.

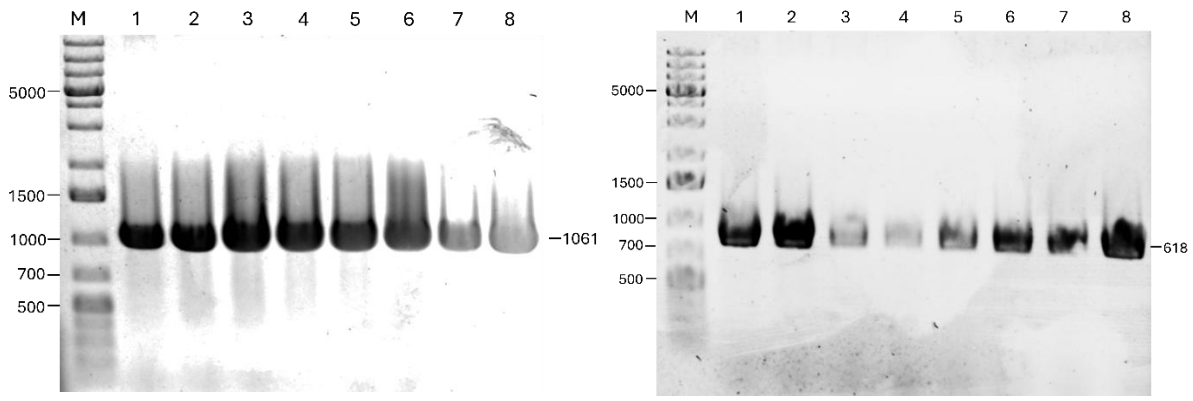

***Figure 5: Screening of L11-ΔORF80 for 5' and 3' end of the deletion**: M: GeneRuler 1 kb Plus DNA Ladder, 1-8: clones tested, Left Side: Screening for 5' end of cassette, Primers used 79-5 and Nov-12, expected size 618bp; Left Side Screening for 5' end of cassette, Primers used Nov-9 and 80-3-en, expected size 1061bp*

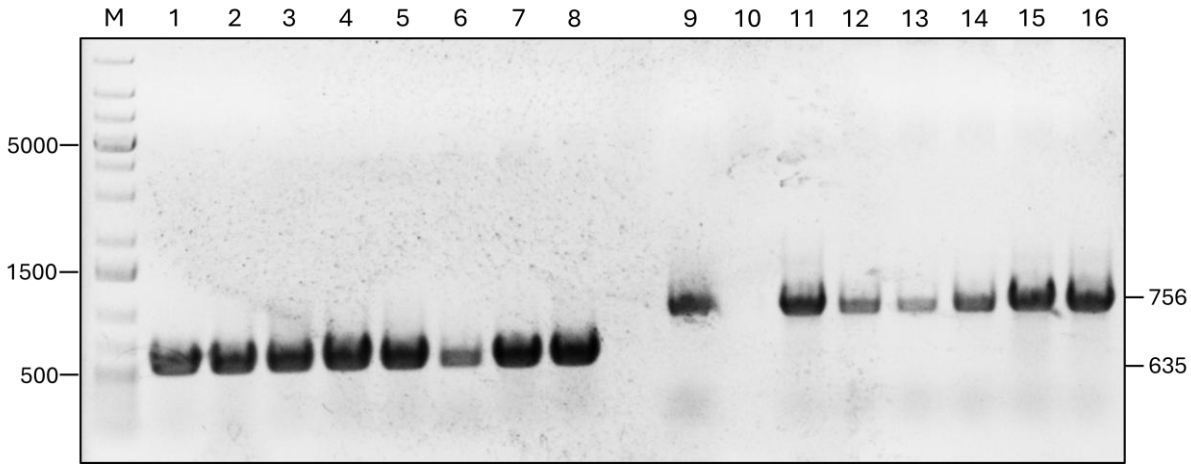

Figure 6: Screening of L11-ΔORF82 for 5' and 3' end of the deletion*: M: GeneRuler 1 kb Plus DNA Ladder, 1-8: clones tested for the 5' end of the resistance cassette and the adjacent sequence of ϕCh1, Primers used 82-5-en and Nov-12, expected size 635bp; 9-16: clones tested for the 3' end of the resistance cassette and the adjacent sequence of ϕCh1, Primers used Nov-9 and 82-3-en, expected size 756bp*

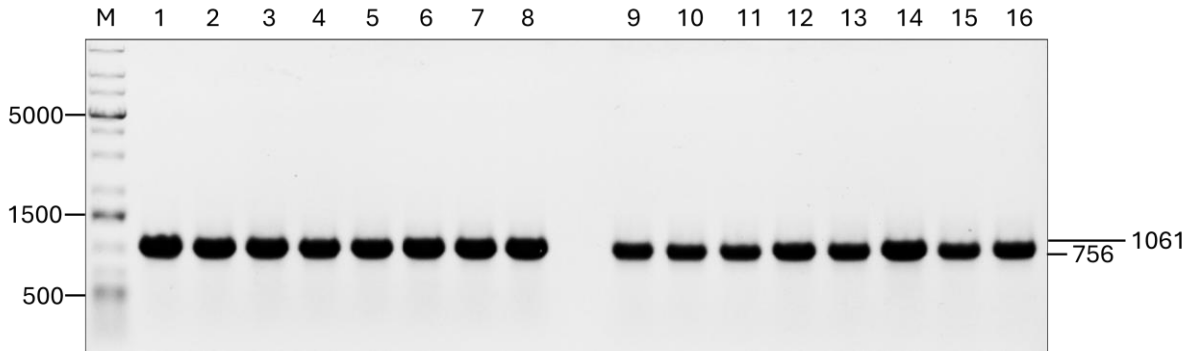

Figure 7: Screening of L11-ΔORF80/ORF82 for 5' and 3' end of the deletion*: M: GeneRuler 1 kb Plus DNA Ladder, 1-8: clones tested for the 5' end of the resistance cassette and the adjacent sequence of ϕCh1, Primers used 79-5 and Nov-12, expected size 1061bp; 9-16: 1-8: clones tested for the 3' end of the resistance cassette and the adjacent sequence of ϕCh1, Primers used Nov-9 and 82-3-en, expected size 756bp*

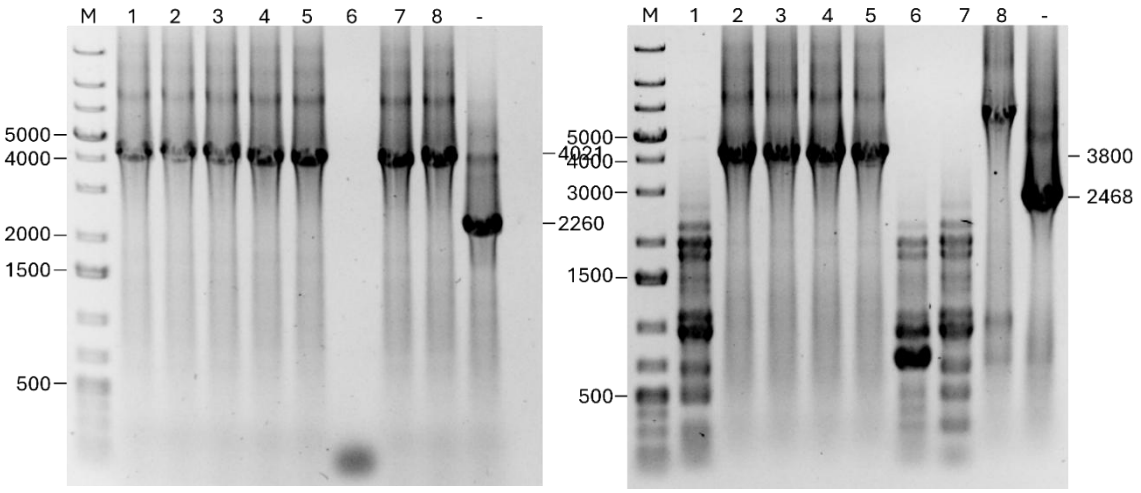

Figure 8: Screening of the single deletion mutants for the entire length of the resistance cassette*: M: GeneRuler 1 kb Plus DNA Ladder, 1-8: tested clones of the single deletions, -: l11 used as negative control; Left Side: Test PCR for the resistance cassette of L11-ΔORF80, Primers: 79-5 and 80-3-en, expected size: resistance cassette of L11-ΔORF80: 4021 and 2260bp for L11; Right Side: Test PCR for the resistance cassette of L11-ΔORF82, Primers: 82-5-en and 82-3-en, expected size: resistance cassette of L11-ΔORF82: 3800 and 2468bp for L11*

Infection of N. magadii L13 for homozygous mutants

After the successful integration of resistance cassette into *N. magadii* L11, only a heterozygous deletion was achieved, due to the multiple copies of the genomes present in *N. magadii*. To create homozygous deletion mutants, first the heterozygous deletion strains of L11 were grown until lysis and the subsequently released virus particles isolated from the supernatant by centrifugation. The so acquired virus particles were used to infected completely cured *N. magadii* L13. Since a superinfection with multiple different virus particles is not possible the resulting L11 strains of *N. magadii* were al homozygous. The infected *N. magadii* were incubated at 37°C without agitation and, after 3 times of washing with NVM+-medium, plated on NVM+-plates with novobiocin.

The resulting homozygous L11 colonies were screened via PCR for the presence of the novobiocin resistance cassette at the desired insertion point to ensure homozygosis.

Conformation of homozygosis by Southern Blot

To ensure the successful creation of a homozygous deletion mutant, the chosen mutants were also verified via Southern Blot. For this the genome of isolated virus particles of ϕCh1 and the deletion mutants were separately digested with *Sma*I and *Bam*HI. Since the size of the resulting fragments differs from the wild type, due to some of the restriction sites being located in the regions replaced by homologous recombination with resistance cassettes, the resulting restriction pattern also differs from the wild type *N. magadii* L11 strain. This was shown by hybridization of the blotted agarose gel electrophoresis pattern of the restriction of the genome of the mutants and wild type with biotinylated DNA-probes, confirming the successful homozygous integration of the novobiocin resistance cassette, resulting in the deletion of the respective ORFs. The probes used were designed to verify 5’ and 3’ ends of the respective genomes of the deletion mutants producing signals at a certain fragment size differing between mutants and wild type (see **Figure 9** and **Figure 10**)

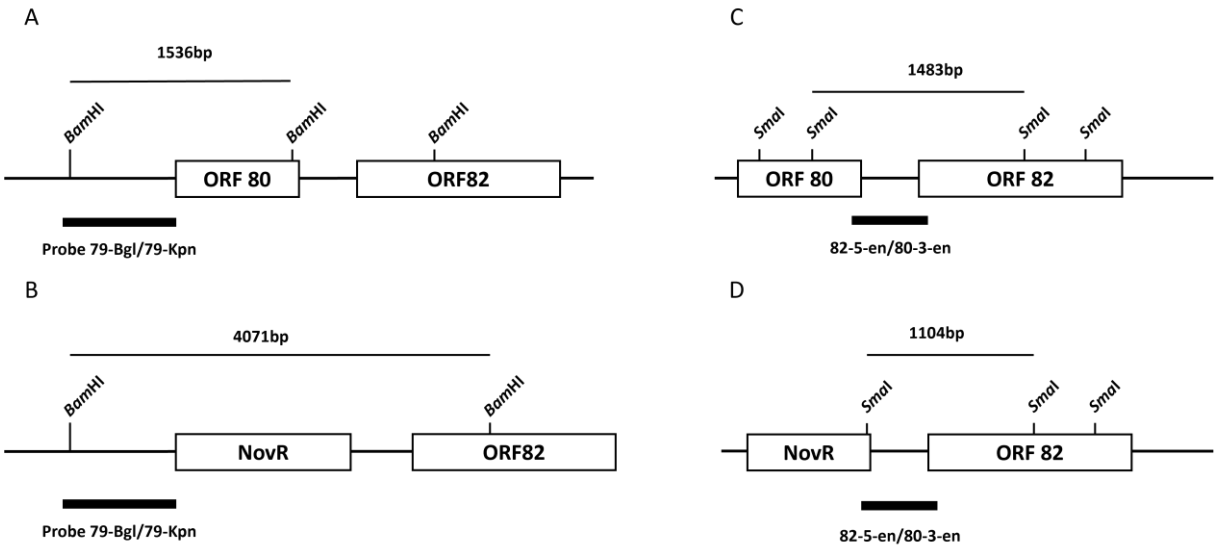

Figure 9: Schematic depiction of the Southern blot hybridization pattern and predicted band lengths for determining the successful deletion of ORF 80: *A and B show the southern blot strategy for ORF 80 by binding a biotinylated probe upstream, C and D show the southern blot strategy for ORF 80 by binding a biotinylated probe downstream; A: Expected hybridization of Probe 79-Bgl/79-Kpn with ϕCh1-DNA digested by* BamHI *with a resulting signal at a size of 1536 bp; B: Expected hybridization of Probe 79-Bgl/79-Kpn with ϕCh1-ΔORF80-DNA digested by* BamHI *with a resulting signal at a size of 4071 bp; C: Expected hybridization of Probe 82-5en/80-3-en with ϕCh1-DNA digested by* SmaI *with a resulting signal at a size of 1483 bp; D: Expected hybridization of Probe 82-5en/80-3-en with ϕCh1-ΔORF80-DNA digested by* SmaI *with a resulting signal at a size of 1104 bp*

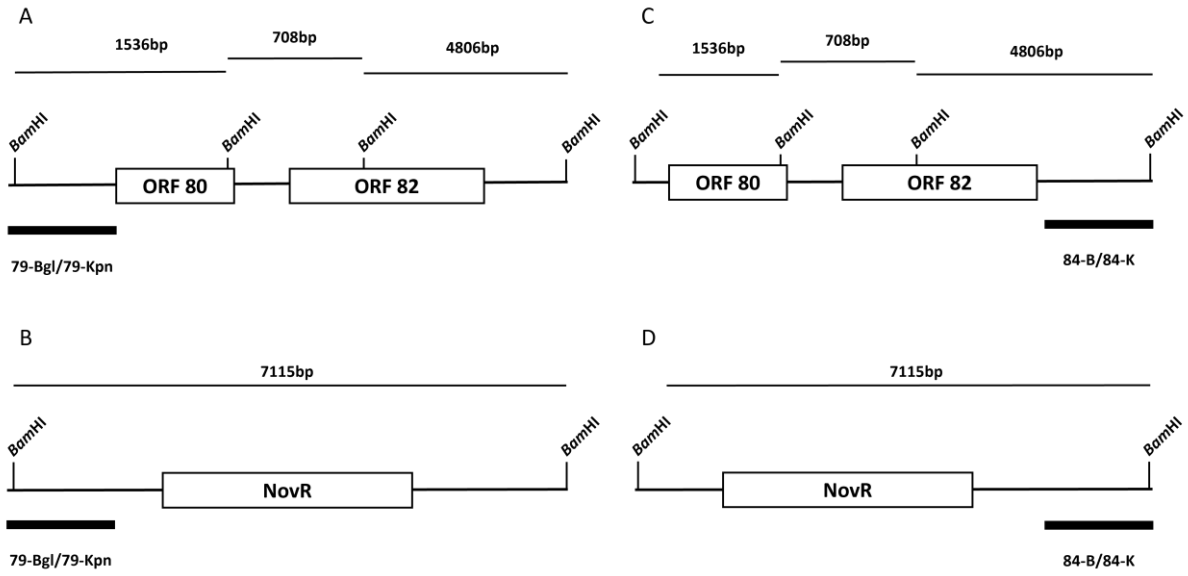

Figure 10: Schematic depiction of the Southern blot hybridization pattern and predicted band lengths for determining the successful deletion of ORF 80 and ORF 82*: A and B show the southern blot strategy for ORF 80 and 82 by binding a biotinylated probe upstream, C and D show the southern blot strategy for ORF 80 and ORF82 by binding a biotinylated probe downstream; A: Expected hybridization of Probe 79-Bgl/79-Kpn with ϕCh1-DNA digested by BamHI with a resulting signal at a size of 1536 bp; B: Expected hybridization of Probe 79-Bgl/79-Kpn with ϕCh1-ΔORF80-82-DNA digested by BamHI with a resulting signal at a size of 7115 bp; C: Expected hybridization of Probe 84-B/84-K with ϕCh1-DNA digested by* SmaI *with a resulting signal at a size of 4806 bp; D: Expected hybridization of Probe 84-B/84-K with ϕCh1-ΔORF80-82-DNA digested by* SmaI *with a resulting signal at a size of 7115 bp*

After isolation of the virus-DNA, like described in “Isolation and concentration of ϕCh1 virus particles”, “Dialysis of Virus particles” and “Extraction of ϕCh1 viral DNA”, the obtained DNA of the mutants was digested with the required restriction enzymes to obtain signals verifying the successful deletions. For verification the respective 5’ and 3’ ends of the mutants were analysed like described in the chapter “Southern Blot” of the Methods section.

The restricted DNA was separated by electrophoresis using a 0.8 % TAE-agarose-gel (see Agarose gel electrophoresis). Afterwards the gel was blotted to a nylon membrane by capillary blot (see Blotting of DNA) and hybridized with the respective biotinylated DNA-Probes, delivering the hybridization pattern shown in (see Production Probes and Detection).

As shown in **Figure 11** and **Figure 12**, the resulting signals of the southern blots match the expected pattern for successfully created deletion mutants, for ORF80 and ORF80 and 82 simultaneously, with only single insertions of novobiocin resistance cassettes.

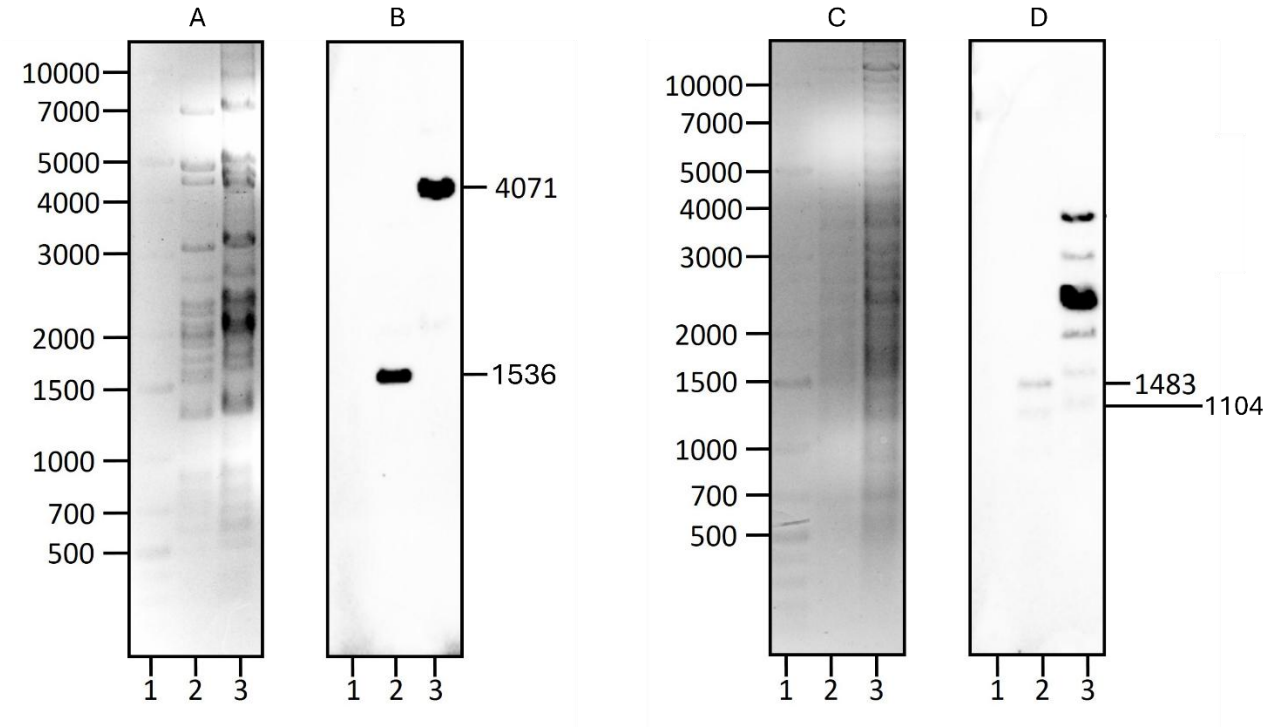

Figure 11: Southern blot of ΔORF80-ϕCh1: *Southern blots of the genome of ΔORF80-ϕCh1 to confirm the successful deletion of ORF 80; lanes 1: DNA-Ladder, lanes 2: digest of wild type ϕCh1, lanes 3: digest of ΔORF80-ϕCh1; A: Restriction pattern if digested with* Bam*HI, B: Detection pattern of blot of A hybridized with probe 79-Bgl/79-Kpn (detected fragments labelled with size according to DNA-ladder) for conformation of the deletion via*

5'-end of ORF 80, C: Restriction pattern if digested with SmaI*, D: Detection pattern of blot of C hybridized with probe 82-5-en/80-3-en (detected fragments labelled with size according to DNA-ladder) for conformation of the deletion via 3'-end of ORF80*

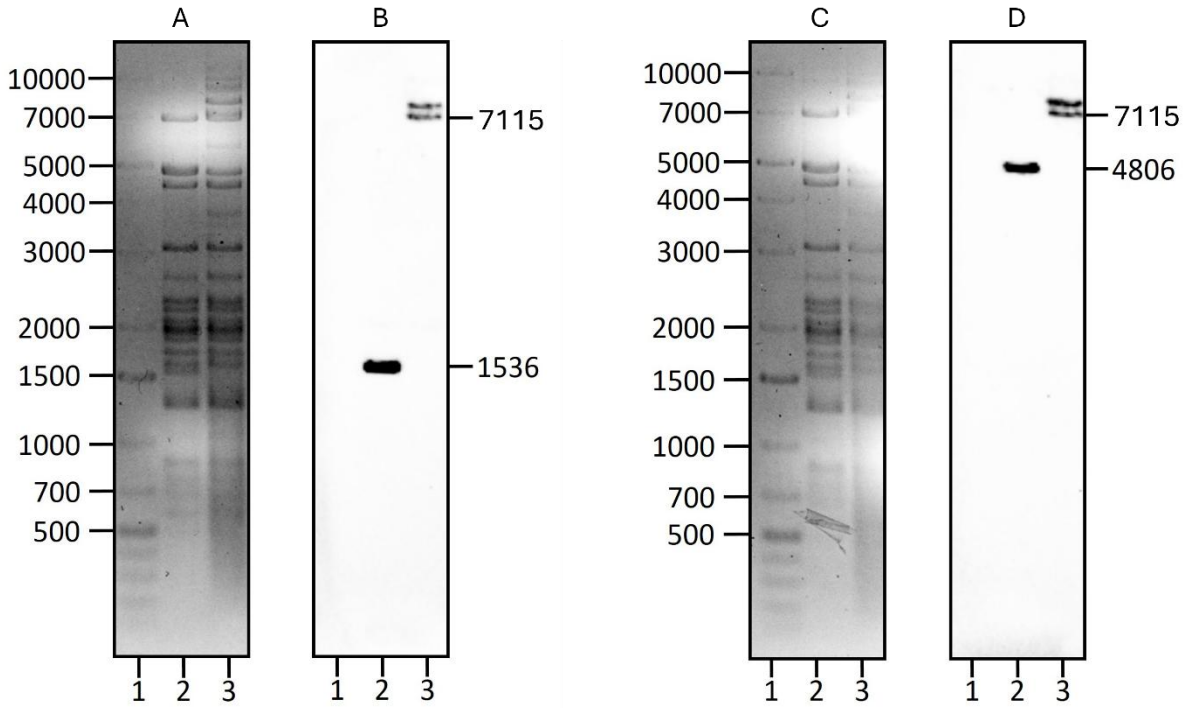

Figure 12: Southern blot of ΔORF80-82-ϕCh1*: Southern blots of the genome of ΔORF80-82-ϕCh1 to confirm the successful deletion of ORF 80 and 82; lanes 1: DNA-Ladder, lanes 2: digest of wild type ϕCh1, lanes 3: digest of ΔORF80-82-ϕCh1; A: Restriction pattern if digested with* Bam*HI, B: Detection pattern of blot of A hybridized with probe 79-BgI/79-Kpn (detected fragments labelled with size according to DNA-ladder) for conformation of the deletion via 5'-end of ORF 80, C: Restriction pattern if digested with* Bam*HI, D: Detection pattern of blot of C hybridized with probe 84-B/84-K (detected fragments labelled with size according to DNA-ladder) for conformation of the deletion via 3'-end of ORF82*

Complementation of *N. magadii* L11-ΔORF80, ΔORF82 and ΔORF80/82

To ensure that all seen effects on the phenotype of the deletion mutants hailed purely from the removal of the respective genes, the deletion mutants were complemented again to a full genome and their phenotype analysed. The deletions mutants were complemented with pNB102-plasmids carrying the respectively deleted ORFs 80, 82 or 80 and 82. After transformation of competent mutant cells with the respective complementation plasmids, the regenerated cells were plated on NVM+-plates containing mevinolin ensuring the retention of the complementation plasmids.

Creation of *N. magadii* L11 overexpressing ORF80, ORF82 or both

To gain further insights in the effects of the methyltransferase genes, the ORFs 80 and 82 were overexpressed separately and together in *N. magadii* to observe effects on the phenotype regarding growth, virus titer and expression behaviour of certain proteins. To perform the overexpression *N. magadii* L11 was transformed with pNB102-plasmids carrying the respective ORFs. After transformation of the plasmids in L11 and regeneration of the transformed cells, they were plated on NVM+-plates containing mevinolin for which pNB102 carries a resistance gene. The resulting colonies were screened via PCR to confirm successful transformation.

Impact of genotypic alterations of ϕCh1 on the phenotype of *N. magadii* as a host of ϕCh1

Growth behaviour of N. magadii L11 strains over time

One phenotypic property chosen to be compared was the growth rate and lysis behaviour of the different *N. magadii* L11 strains. To achieve this the growth rate of the different mutant strains and the wild type *N. magadii* L11 strain or a *N. magadii* L11 strain with an empty plasmid, were compared. For this, the strains were grown for 7 days, in aerobic conditions, in NVM-CAA-medium. To measure culture growth, every 24 h, beginning 24 h after inoculation, the absorption of light of 600 nm wavelength was measured (OD_{600}).

Growth behaviour of the deletion mutants

First the growth behaviour of the deletion strains was compared to each other and the wild type *N. magadii* L11 strain. As visible in **Figure 13** the growth behaviour of all deletion strains is different to each other and the *N. magadii* L11 strain.

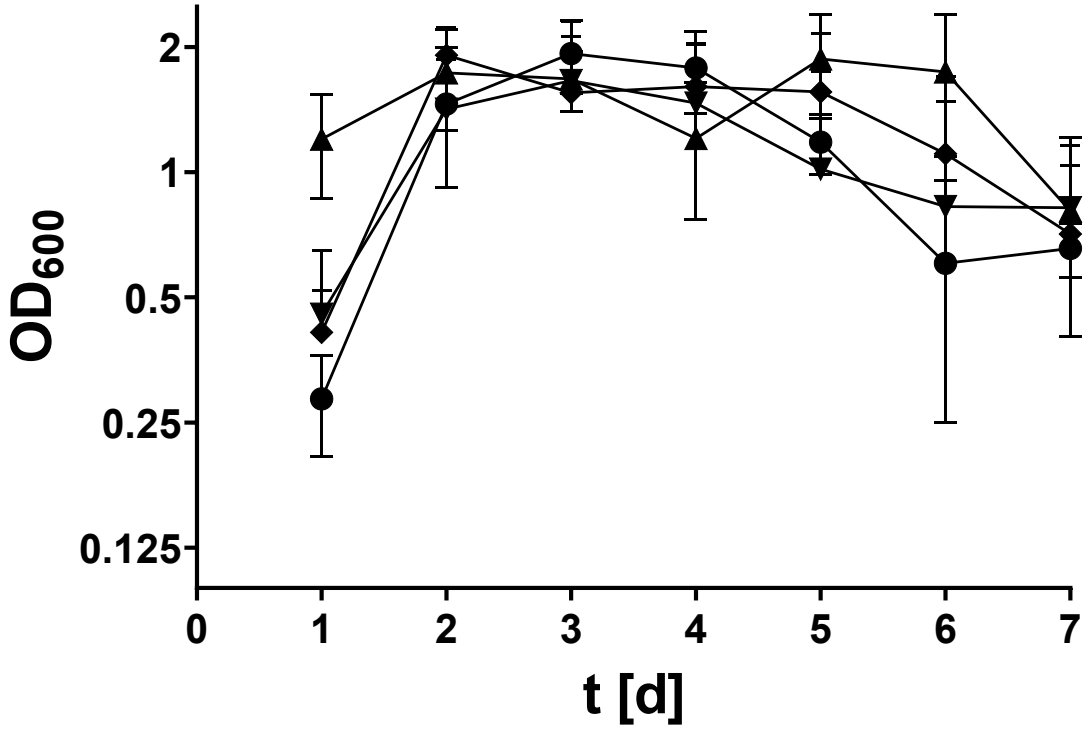

Figure 13: Growth kinetics of all deletion mutants*: optical density measured with light of 600 nm wavelength every 24 h, starting 1 day after inoculation; grown in NVM CAA; Error bars (±1SD) indicated.*
Filled Circle: N. magadii L11.
Triangle pointed upwards: N. magadii L11/ϕCh1-ΔORF80.
Triangle pointed downwards: N. magadii L11-ΔORF82.
Rhombus: N. magadii L11-ΔORF80-82.

Firstly, the difference between *N. magadii* L11 and *N. magadii* L11-ΔORF80 as shown in **Figure 14**. *N. magadii* L11 grows rapidly from a low OD of 0.28 till day 2 reaching a peak at day 3 through somewhat slower growth, with an OD of nearly 2. The OD of L11 then continues to fall until a minimum at day 6 of about 0.6, rising again on day 7 slightly to 0.65. The *N. magadii* L11-ΔORF80-strain already had grown significantly to an OD of 1.2 growing to the first maximum of 1.7 on day 2, only to dip back to an OD of 1.2 on day 4, before rising on day 5 again to a maximum of about 1.9. The OD slightly lowered at day 6 and plummeted again on day 7 to an OD of approximately 0.8. So, the growth trend of the deletion stain seems very different than that of *N. magadii* L11, since the deletion stains shows two growth maxima instead of one, but ending up on a similar OD at the end of measurement.

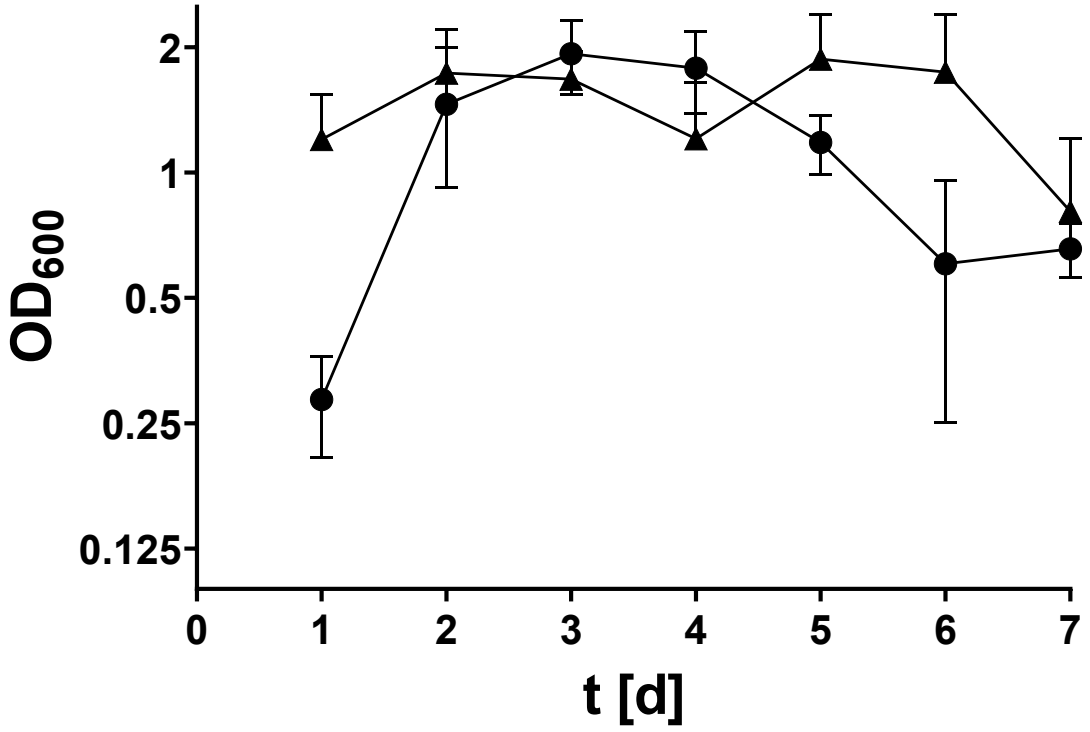

Figure 14: Growth kinetics of deletion mutant for ORF80: *optical density measured at 600 nm wavelength every 24 h, starting 1 day after inoculation; grown in NVM CAA; Error bars (±1SD) indicated; Filled Circle: N. magadii L11; Triangle: N. magadii L11-ΔORF80.*

The growth behaviour of the deletion mutant without ORF82 was more like *N. magadii* L11 (see **Figure 15**). The first measurement at day 1 slightly higher than *N. magadii* L11 at an OD of 0.46. On the second day the OD values of *N. magadii* L11 and *N. magadii* L11-ΔORF82 were nearly the same between the ODs of 1.4 to 1.45. Afterwards the general growth pattern was the same although the amplitude of the growth curve was smaller, with a maximum on day 3 of 1.6 and minimum of 0.82 at day 6. Overall, the growth behaviour seems very similar to *N. magadii* L11, even more so if the variation and range of the single growth cultures is accounted for, as depicted with error bars in **Figure 15**.

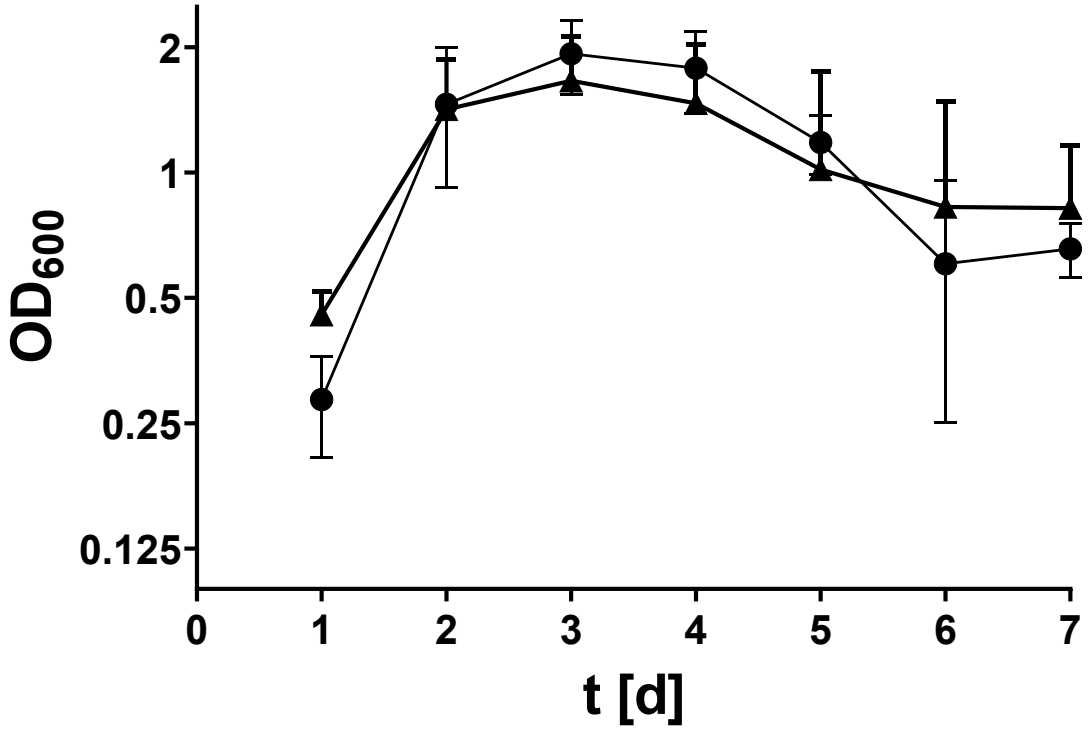

Figure 15: Growth kinetics of deletion mutant for ORF82*: optical density measured at 600 nm wavelength every 24 h, starting 1 day after inoculation; grown in NVM CAA; Error bars (±1SD) indicated; Circle: N. magadii L11; Triangle: N. magadii L11-ΔORF82.*

The deletion mutant missing both ORF80 and ORF82 (see **Figure 16**) showed an OD_{600} of 0.41 at the first measurement point day 1 and the global maximum already at day 2 with an OD_{600} of 1.91. Day 3 shows a local minimum of 1.55, with a small growth phase afterwards reaching an OD of 1.6 on day 4. Day 5-7 show a linear decline to an OD of 0.7. The growth trend of the double deletion mutant seems to be a combination of the trends of the single deletion mutants. Showing a similar growth to, both in absolute cell density and growth rate, *N. magadii* L11 at the beginning, like *N. magadii* L11-ΔORF82, until day 2. Afterwards the intermediate stalling of the cultures and the second growth phase, like in the *N. magadii* L11-ΔORF80-strain, are visible.

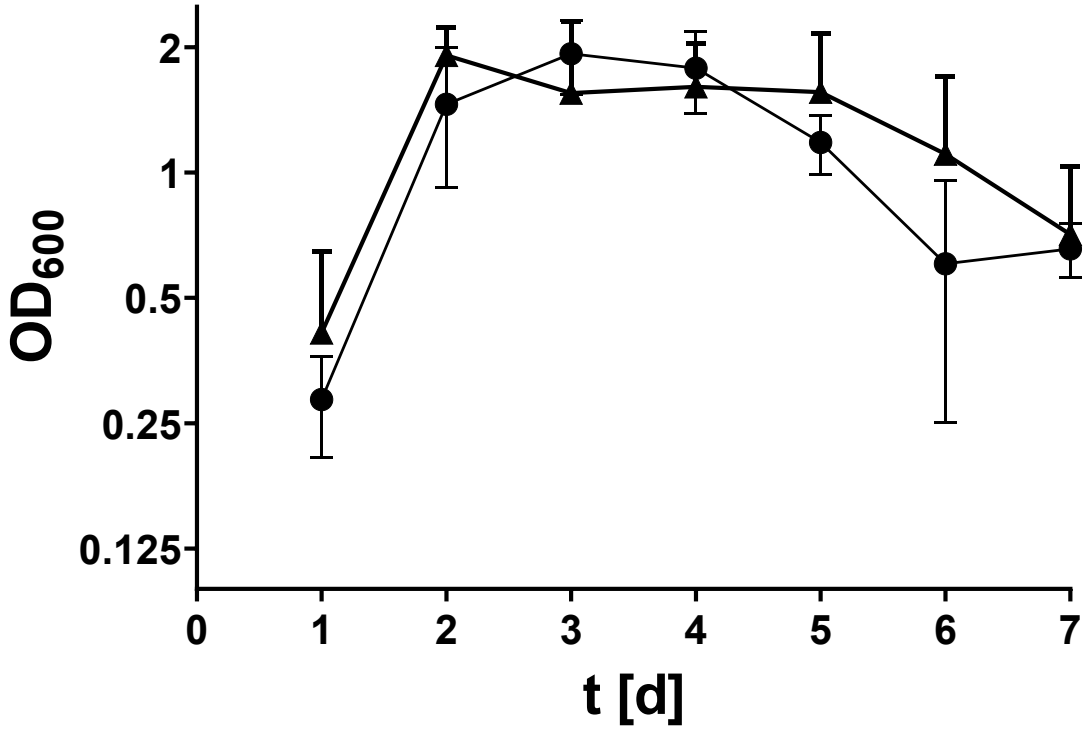

Figure 16: Growth kinetics of deletion mutant for ORF80 and ORF82 combined: *optical density measured at 600 nm wavelength every 24 h, starting 1 day after inoculation; grown in NVM CAA; Error bars (±1SD) indicated; Filled Circle: N. magadii L11; Triangle: N. magadii L11-ΔORF80-82.*

Growth behaviour of the overexpression strains

To better understand the influence of the 2 ORFs on the growth behaviour of *N. magadii* L11, overexpression strains were created (see Complementation of *N. magadii* L11-ΔORF80, ΔORF82 and ΔORF80/82) and their growth behaviours were compared to *N. magadii* L11 and each other.

As shown in **Figure 17**, the growth trends of the overexpression strains are very similar, with a relatively low range of deviation between the cultures of same strain. The most deviation between the overexpression strains was measured on day 1, with an OD of 0.39 for *N. magadii* L11 (pNB102-ORF80), 0.45 for *N. magadii* L11 (pNB102-ORF82) and 0.57 for *N. magadii* L11 (pNB102-ORF80-82). A peak was reached at day 2 with OD values between 1.56 and 1.59. Until now the overexpression strains showed very similar behaviour compared to *N. magadii* L11. Afterwards the overexpression strains only slight deviation from these values till day 7 as seen in

Figure 17. The growth of the overexpression strains divers from *N. magadii* L11 in this, which, as previously described, peaks in growth at day 3, declines from there until day 6 and recovers slightly on day 7.

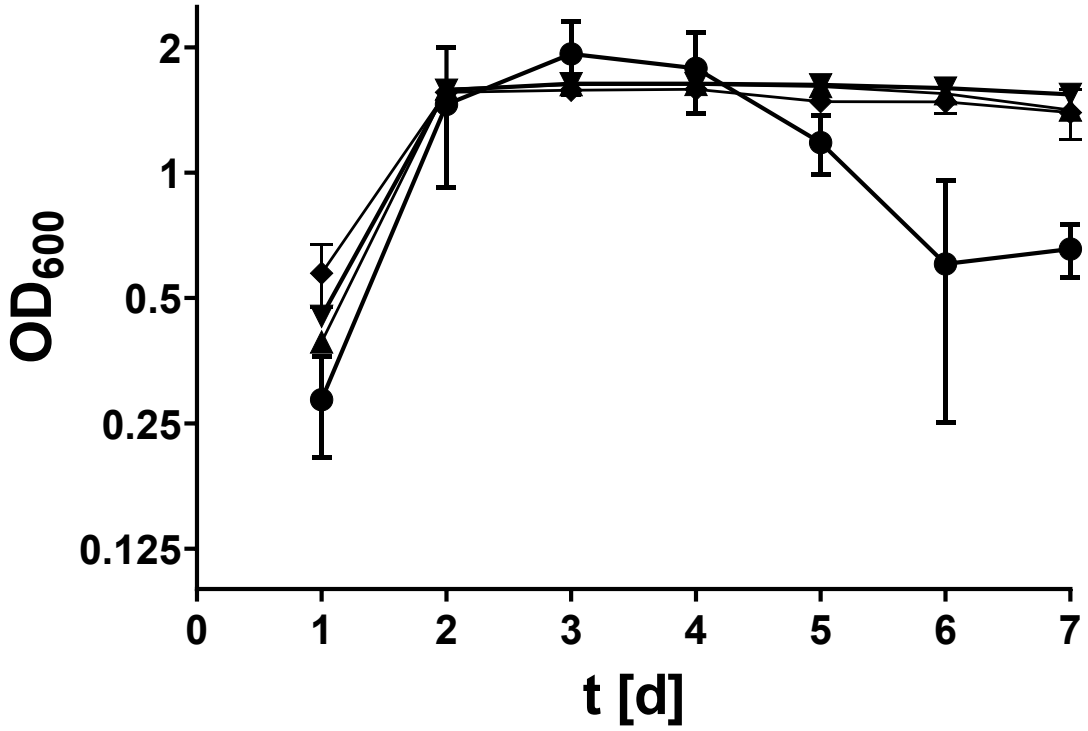

***Figure 17: Growth kinetics of overexpression strains**: Optical density measured with light of 600 nm wavelength every 24 h, starting 1 day after inoculation; grown in NVM CAA; Error bars (±1SD) indicated.*

Circle: N. magadii L11.
Triangle pointed upwards: N. magadii L11 (pNB102-ORF80).
Triangle pointed downwards: N. magadii L11 (pNB102-ORF82).
Rhombus: N. magadii L11 (pNB102-ORF80-82).

This behaviour shows that if either ORFs or both ORF80 and ORF82 are overexpressed in *N. magadii* L11 the lysis of *N. magadii,* or at least the reduction of the optical density is prevented, hinting at an involvement in the regulation of the life cycle of *N. magadii* and/or the production of ϕCh1-virus-particles. Additionally, since all constructs showed the same OD, comparison of the protein expression later was especially easy.

Growth behaviour of the complementation strains

To assess if all effects of seen on deletion and overexpression strains are caused solely by the absence or presence of the respective ORFs, complementation strains were analysed and compared to the other constructs.

To compare the growth behaviour of the complementation strains an *N. magadii* L11 strain with an empty plasmid carrying no ORF for complementation was used. *N. magadii* L11 (pNB102) showed generally the same growth trend as *N. magadii* L11, but with a slightly lower OD. The only exception to this similarity is the logarithmic decline of OD without recovery from day 4 onward, as seen in **Figure 18**. Both differences can be tentatively explained by a higher energy demand, caused by the presence and replication of the plasmid pNB102, which becomes even more challenging during the lysis phase.

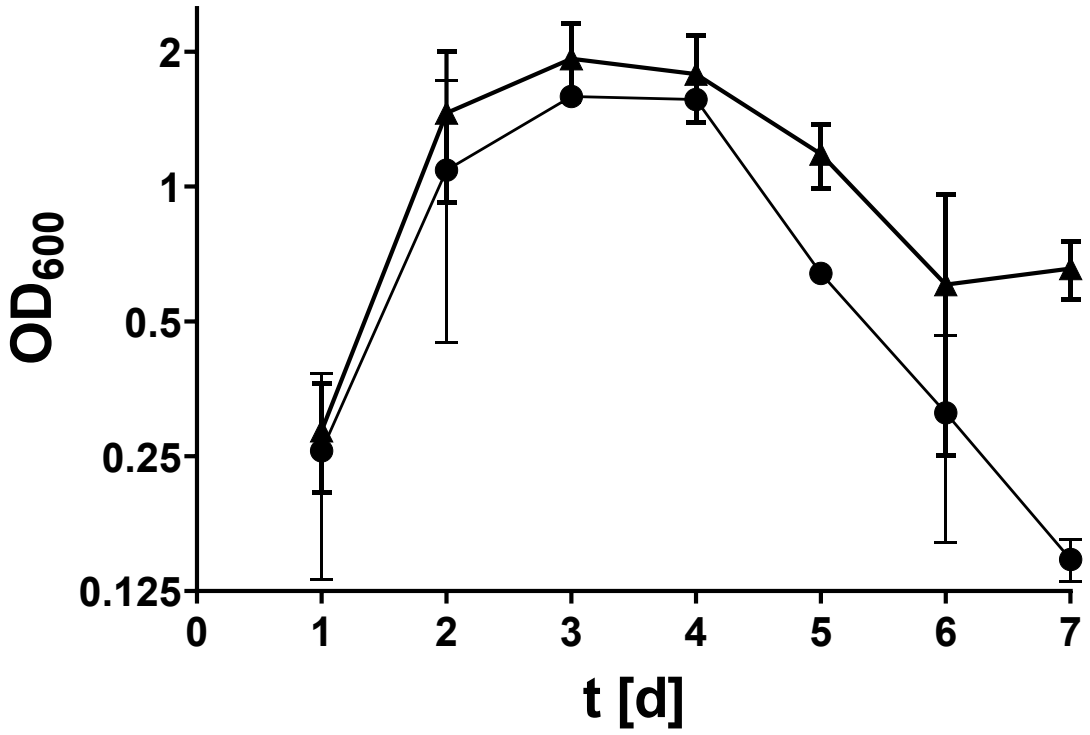

Figure 18: Comparison of the growth kinetics of L11 and L11 with the carrier plasmid pNB102*: Optical density measured with light of 600 nm wavelength every 24 h, starting 1 day after inoculation; grown in NVM CAA; Error bars (±1SD) indicated. Circle: N. magadii L11 (pNB102). Triangle pointed upwards: N. magadii L11.*

The general growth trend of all complementation strains seems rather like the one of *N. magadii* L11 (pNB102) (see **Figure 19**). All grow at roughly the same rate until day

2 and peak and/or plateau till day 4, after which a rapid decline sets in which seems to stabilize on day 7. The ORF80 complementation strain shows the strongest decline of all constructs in rate as well as in OD at day 7. The ORF82 complementation strain and the double complementation show nearly the same OD-values during the peak/plateau-phase but differ during lysis. While the ORF82-complement kept the OD higher on day 5 it declined even lower on day 6 and recovered to a lower OD at day 7 compared to the double complement.

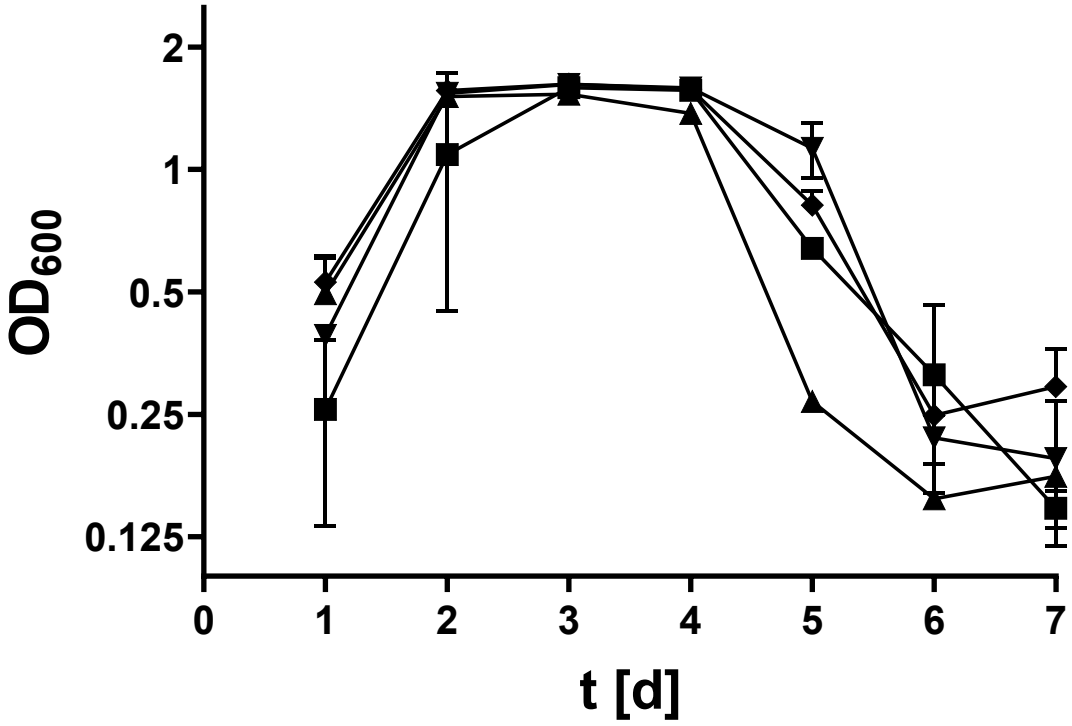

***Figure 19: Growth kinetics of all complemented mutants**: Optical density measured at 600 nm every 24 h, starting 1 day after inoculation; grown in NVM CAA; Error bars (±1SD) indicated.*

Square: N. magadii L11 (pNB102).
Triangle pointed upwards: N. magadii L11-ΔORF80 (pNB102-ORF80).
Triangle pointed downwards: N. magadii L11-ΔORF82 (pNB102-ORF82).
Rhombus: N. magadii L11-ΔORF80-82 (pNB102-ORF80-82).

N. magadii L11 (pNB102-ORF80) and *N. magadii* L11-ΔORF80 (pNB102) (see **Figure 20**) were growing exponentially till day 2, peaking/plateauing from day 2 to 4, rapidly declining during day 5 and 6, to than stagnate on day 7. The growth pattern is relatively like that of *N. magadii* L11 (pNB102) and differs only by the rate of decline during day 5 to 7. The growth difference of *N. magadii* L11-ΔORF80 (pNB102) cultures to each other is somewhat greater though.

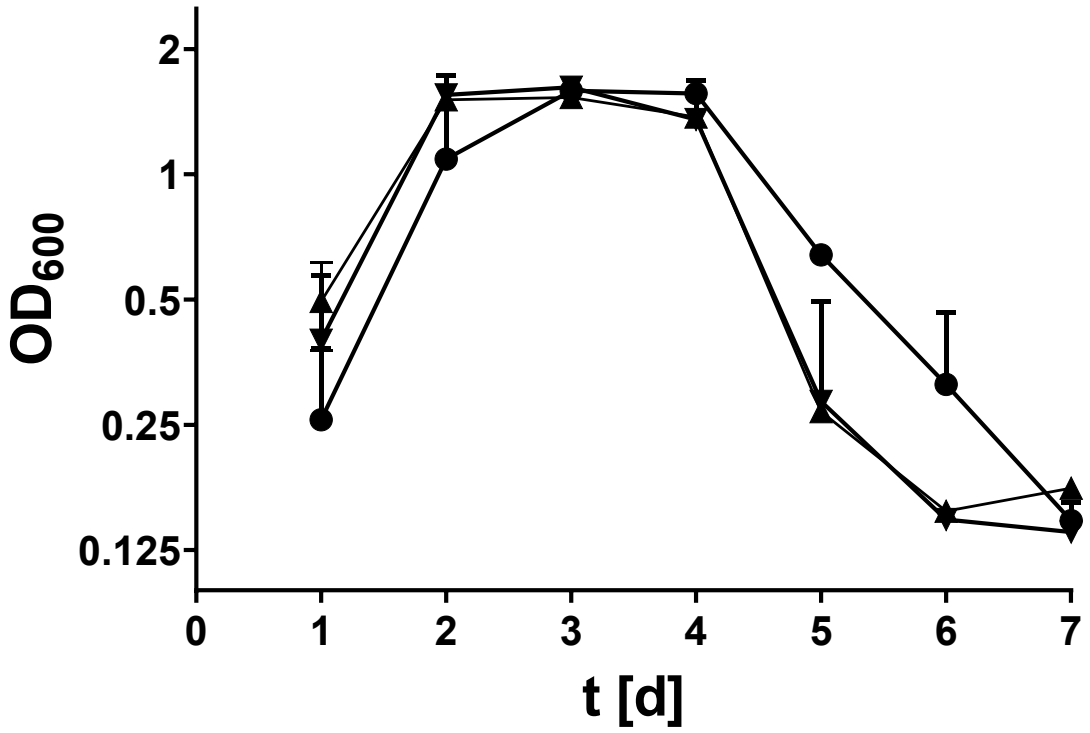

Figure 20: Growth kinetics of deletion and complementation of ORF80*: Optical density measured at 600 nm every 24 h, starting 1 day after inoculation; grown in NVM CAA; Error bars (±1SD) indicated.*

Circle: N. magadii L11 (pNB102).
Triangle pointed upwards: N. magadii L11-ΔORF80 (pNB102-ORF80).
Triangle pointed downwards: N. magadii L11-ΔORF80 (pNB102).

The deletion mutant for ORF82 (*N. magadii* L11-ΔORF82) containing the empty plasmid and the complementation construct (pNB102-ORF82) show similar behaviour during the first 4 days only differing through the absolute values (see **Figure 21**). At day 5 the deletion construct showed the sharpest decline in OD followed by the control *N. magadii* L11 (pNB102), with the complementation construct retaining the most OD. At the day 6 the OD of *N. magadii* L11-ΔORF82 (pNB102) and *N. magadii* L11-ΔORF82 (pNB102-ORF82) started to show similar behaviour again, stagnating till day 7, with the complementation construct showing a slightly higher OD and control *N. magadii* L11 (pNB102) showing the lowest OD.

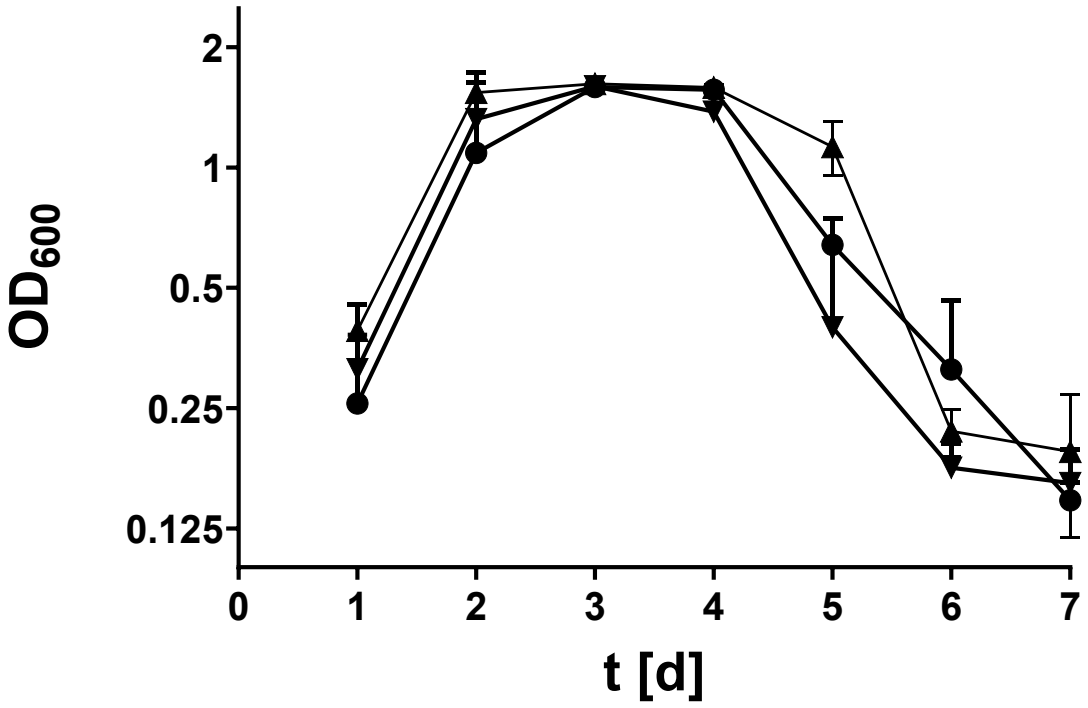

***Figure 21: Growth kinetics of deletion and complementation of ORF82**: Optical density measured at 600 nm every 24 h, starting 1 day after inoculation; grown in NVM CAA; Error bars (±1SD) indicated.*

Circle: N. magadii L11 (pNB102).
Triangle pointed upwards: N. magadii L11-ΔORF82 (pNB102-ORF82).
Triangle pointed downwards: N. magadii L11-ΔORF82 (pNB102).

For the double deletion *N. magadii* L11-DORF80_82 with the pNB102, and the complementation construct for the double deletion the growth behaviour was even more similar to *N. magadii* L11 (pNB102) (see **Figure 22**), only diverging on day 7 when the OD began to stagnate for *N. magadii* L11-ΔORF80-ORF82 (pNB102) and *N. magadii* L11-ΔORF80-ORF82 (pNB102-ORF80-ORF82), but not for *N. magadii* L11 (pNB102). The only other difference is higher OD of the complementation construct on day 1.

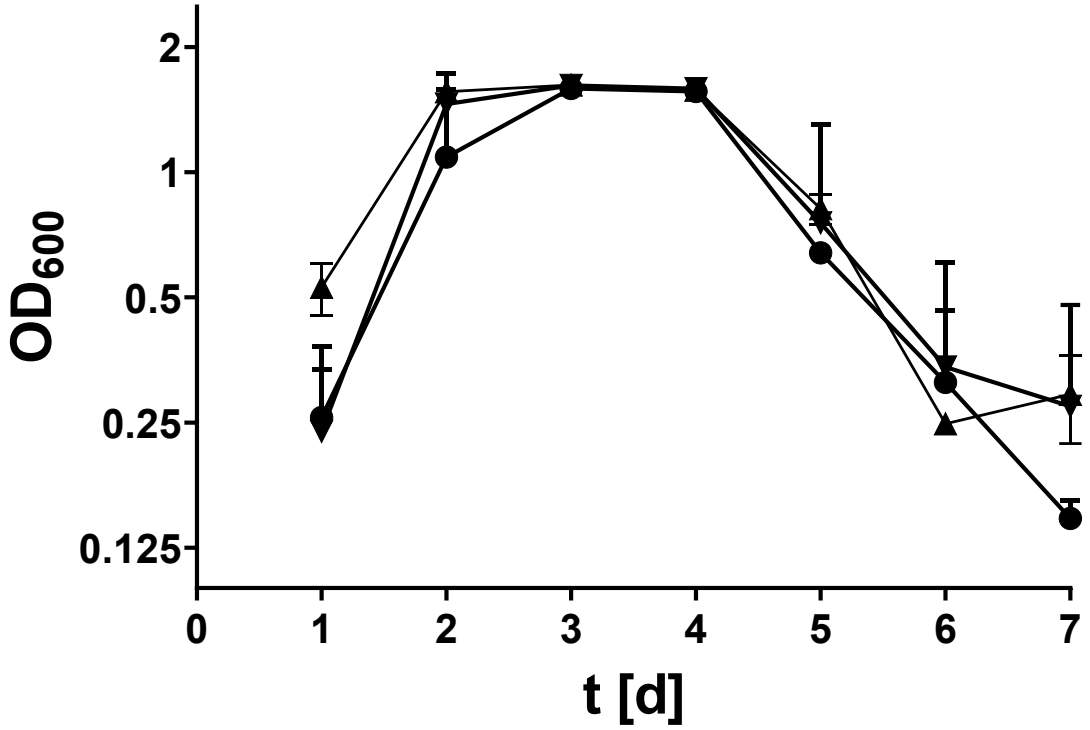

Figure 22: Growth kinetics of deletion and complementation of ORF80 and ORF82*: Optical density measured at 600 nm wavelength every 24 h, starting 1 day after inoculation; grown in NVM CAA; Error bars (±1SD) indicated.*

Circle: N. magadii L11 (pNB102).
Triangle pointed upwards: N. magadii L11-ΔORF80-82 (pNB102-ORF80-ORF82).
Triangle pointed downwards: N. magadii L11-ΔORF80-82 (pNB102).

Since all complementation constructs appeared nearly identical in growth to regular *N. magadii* L11 and differ in behaviour from both the deletion and overexpression constructs, judging only by the OD measurements the complementation seemed to be successful.

Virustiter of *N.magadii* L11 ΔORF80, ΔORF82 and ΔORF80/ORF82

Another metric that was compared to assess differences in the phenotype of the different *N. magadii* L11 strains was the virus titer. For this samples were taken every 24 h during the growth experiment, starting 24 h after inoculation, and a plaque assay performed like described in the methods section (see Plaque assay).

Virustiter of the deletion mutants

First the titers of the deletion mutants were compared to each other and the titer of the unedited *N. magadii* L11 strain. As visible in **Figure 23** *N. magadii* L11 and all the deletion strains start with a very similar viral load increasing till day 3. L11 from here on only shows relatively small fluctuations between $1.3*10^7$ and $3*10^7$ pfu/ml.

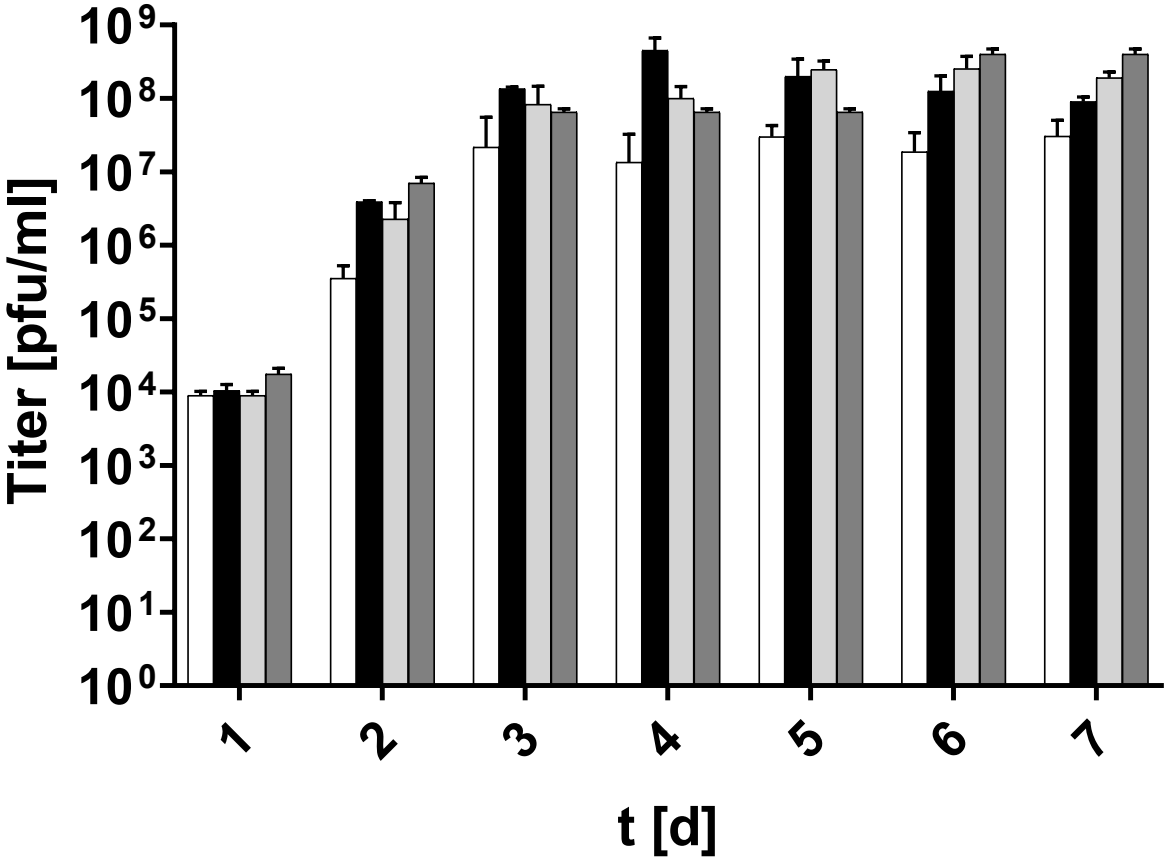

***Figure 23: Virus-Titer of Deletion experiments**: Virus-titer determined in supernatants of cultures by infecting the cured N. magadii L13 strain. Samples were taken every 24 h, starting one day after inoculation; Error bars (±1SD) indicated.*

White: supernatants form culture N. magadii L11.
Black: supernatants form culture N. magadii-ΔORF80.
Light Grey: supernatants form culture N. magadii-ΔORF82.
Grey: supernatants form culture N. magadii-ΔORF80-82.

Virustiter of the overexpression mutants

To assess the influence of the ORF80 and ORF82 on the viral titer the overexpression constructs titer was compared to them self's and to *N. magadii* L11/ϕCh1 (see **Figure 24**). *N. magadii* L11 (pNB102-ORF80) started with a nearly 10-times higher viral load on day 1 compared to *N. magadii* L11 and strongly grows on day 2 to a nearly $6*10^6$

pfu/ml but only increases the viral load to $9*10^6$ on day3. Afterwards the titer droped to a level between $1*10^6$ on day 4 steadily increasing to level of $2.75*10^6$ pfu/ml on day 7, which was consistently the lowest titer of all overexpression constructs and lower than *N. magadii* L11 from day 4 onward. *N. magadii* L11 (pNB102-ORF82) started with a slightly higher titer (125000 pfu/ml) than *N. magadii* L11 (pNB102-ORF80) but grew slower till day 4 to a titer of $3.75*10^6$. On day 5 the titer declined slightly to about the same as the titer of pNB102-ORF80/ϕCh1. The titer of *N. magadii* (pNB102-ORF82) rose to $1.02*10^8$ on day 6 only to decrease again on day 7 to a value of $2.32*10^7$. *N. magadii* L11 (pNB102-ORF80-82) started with the highest titer of $1.25*10^6$ slowly increasing till day 5 to $9.8*10^6$ pfu/ml. On day 6 pNB102-ORF80-82/ϕCh1's titer increased to maximum of $1.025*10^8$ and slightly decreased on day 7 to $4.5*10^7$. All deletion strains showed a higher titer in the beginning, compared to *N. magadii* L11, but showed a slower increase of titer, till being overtaken by *N. magadii* L11 on day 3. Afterwards the titer of *N. magadii* L11 stayed approximately constant till day 7, while the titer of *N. magadii* L11 (pNB102-ORF80) only stablized after it dropped on day 4, while the titer of both *N. magadii* L11 pNB102-ORF82)and *N. magadii* L11 (pNB102-ORF80-82) increased relatively strongly on day 6 over taking *N. magadii* L11, to end up on about the same level on day 7. Although the absolute titer of the deletions mutants was different to that of *N. magadii* L11, the relative behaviour seemed to be nearly identical to *N. magadii* L11.

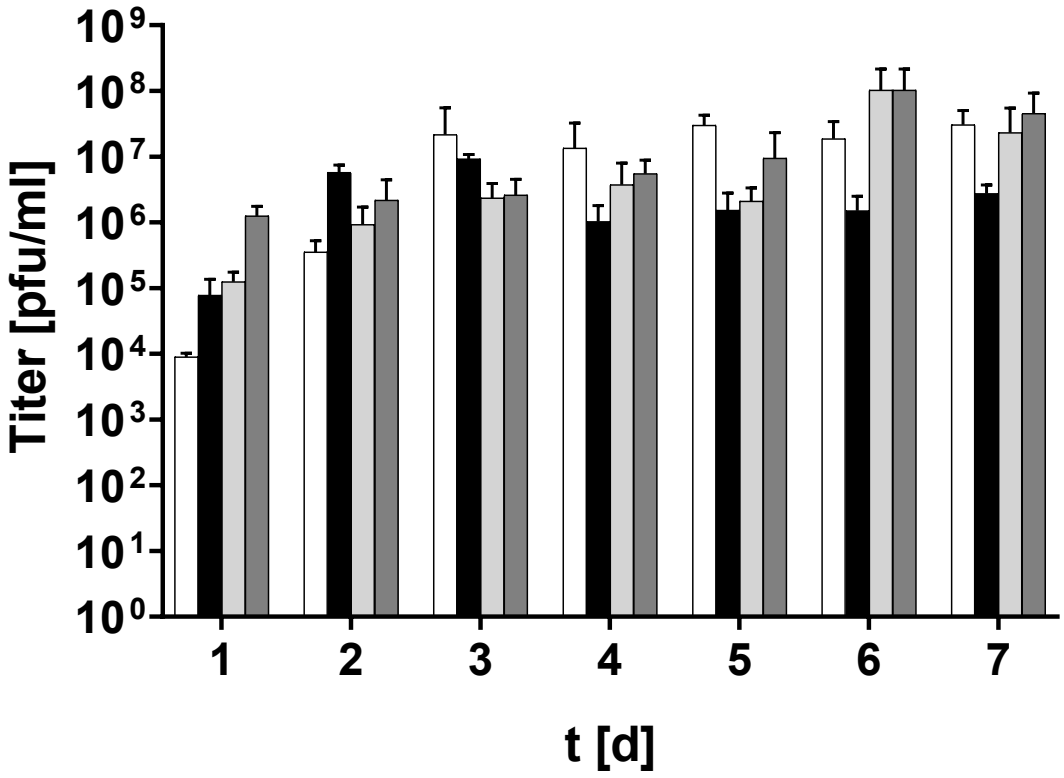

***Figure 24: Virus-Titer of Overexpression experiments**: Virus-Titer measured in supernatant of cultures by infecting the cured N. magadii L13 strain, samples were taken every 24 h starting one day after inoculation; Error bars (±1SD) indicated.*

White: supernatants from culture N. magadii L11.
Black: supernatants from culture N. magadii L11 (pNB102-ORF80).
Light Grey: supernatants from culture N. magadii L11 (pNB102-ORF82).
Grey: supernatants from culture N. magadii L11 (pNB102-ORF80-82).

Virustiter of the overexpression mutants

Since complementation constructs use the pNB102 plasmid to carry deleted open reading frames (ORFs) for complementation, the virus titer and growth behaviour could be influenced by the plasmid itself. To account for this, an *N. magadii* L11 strain containing an empty pNB102 vector was used to compare the complementation constructs. *N. magadii* L11 and the *N. magadii* L11 (pNB102) construct were then compared based on their virus titer. As shown in **Figure 25**, the behaviour of *N. magadii* L11 and the *N. magadii* L11 (pNB102) differs. While *N. magadii* L11 started with relatively low titer rising till day 3 and then stagnating, *N. magadii* L11 (pNB102) started with a high titer of $1.85*10^7$ pfu/ml declining till day 3 to a value of $4.25*10^6$. Afterwards *N. magadii* L11 (pNB102) was rising till day 6 ($8.25*10^8$) only to slightly

decline on day 7 ($3.25*10^8$). This shows a rather clear influence of the plasmid pNB102 on the titer of *N. magadii* L11.

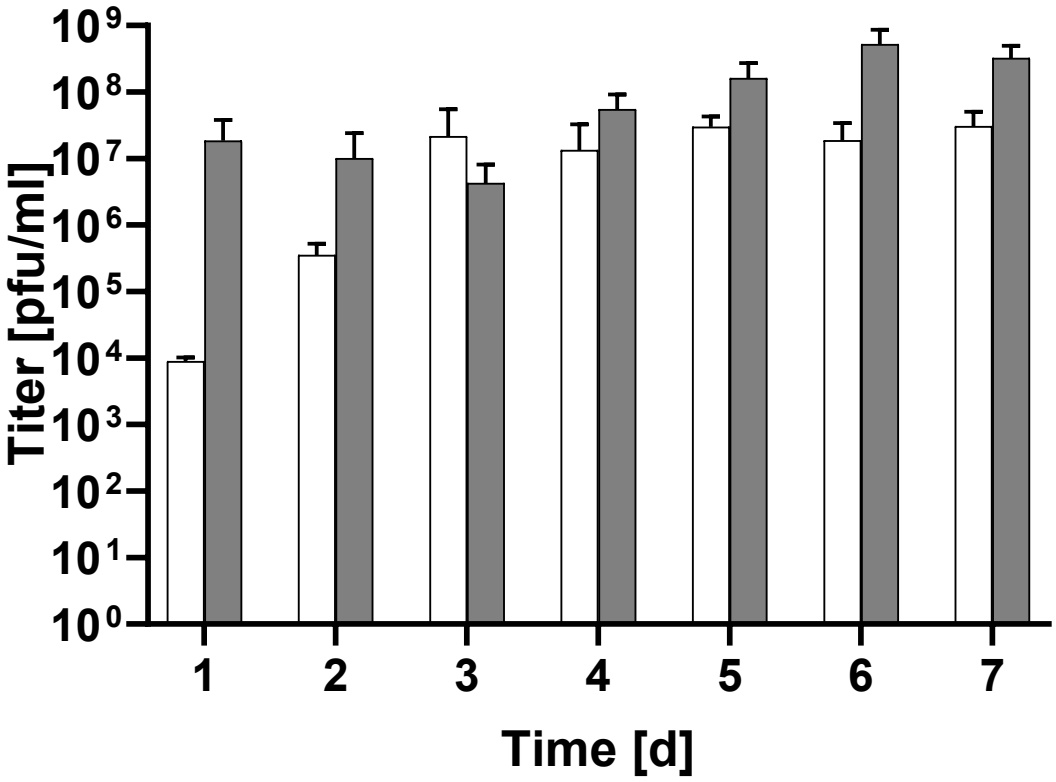

Figure 25: Virus-Titer of L11 and L11 with pNB102*: Virus-titer measured of supernatants of cultures infecting the cured N. magadii L13 strain, samples were taken every 24 h starting one day after inoculation; Error bars (±1SD) indicated. White: supernatants from culture N. magadii L11. Grey: supernatants from culture N. magadii (pNB102).*

Figure 26 depicts the virus titer of the complementation constructs for ORF80 and ORF82, as well as *N. magadii* (pNB102) for comparison.

N. magadii -ΔORF80 (pNB102-ORF80) exhibited dissimilar behavior compared to *N. magadii* (pNB102). It started with a much lower titer ($4.05*10^5$ pfu/ml) and declined further on day 2. However, it surpassed the declining titer of *N. magadii* (pNB102) on day 3 and continued to increase until day 5, reaching a maximum of $4.75*10^8$ pfu/ml. After day 5, the titer declined again until day 7, reaching 8.25×10^7 pfu/ml.

N. magadii-ΔORF82 (pNB102-ORF82) exhibited a similarly high titer on day 1 compared to *N. magadii* (pNB102). Unlike *N. magadii* (pNB102), the titer increased until day 3, reaching the highest titer of all the complementation constructs,

surpassing *N. magadii* (pNB102) on that day with a titer of $3.43*10^8$. From day 4 onward, *N. magadii*-ΔORF82 (pNB102-ORF82) declined slowly until day 6, showing a stronger dip on day 7 to the second-lowest value of $1.3*10^7$.

N. magadii-ΔORF80/82 (pNB102-ORF80-82) exhibited similar behaviour and titers to *N. magadii*-ΔORF82 (pNB102-ORF82) until day 5. On day 6, *N. magadii*-ΔORF80-82 (pNB102-ORF80-82) showed a steeper decline to a titer of $1.2*10^7$, which declined slightly further on day 7 to a value of $3.75*10^6$. On both days, *N. magadii*-ΔORF80-82 (pNB102-ORF80-82) exhibited the lowest titer.

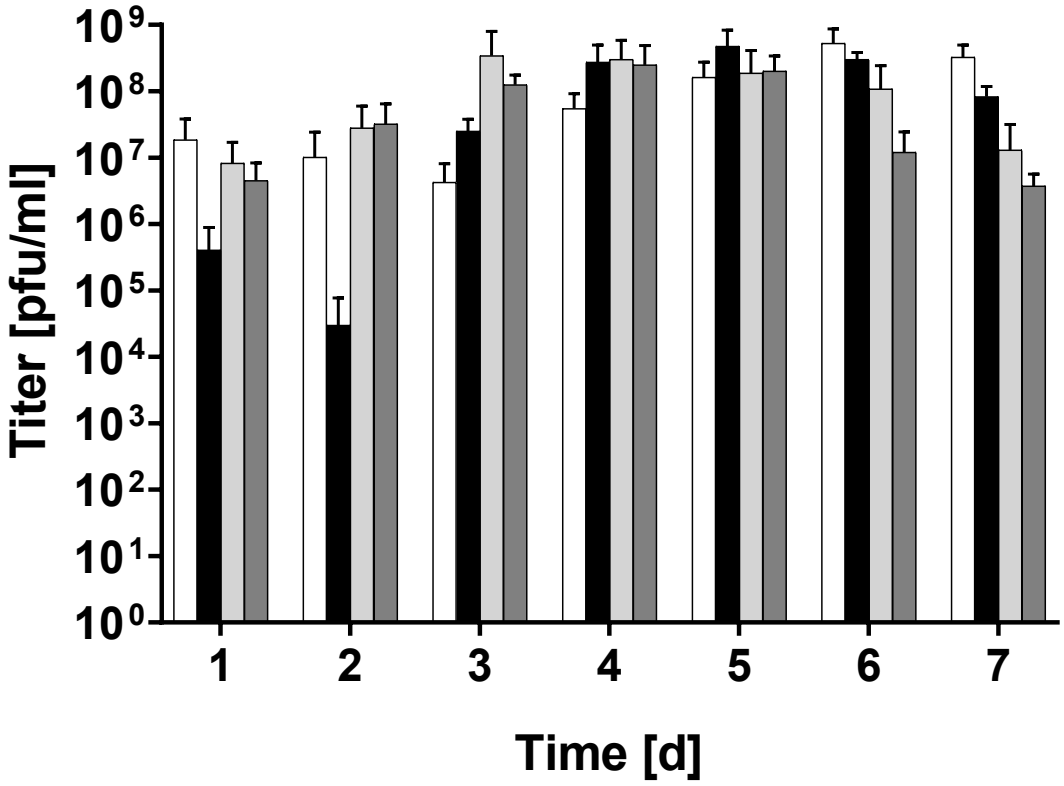

***Figure 26: Virus-Titer of all complemented deletion strains**: Virus-Titer measured in supernatants of culture infecting the cured N. magadii L13 strain, samples were taken every 24 h starting one day after inoculation; Error bars (±1SD) indicated.*

White: supernatants from culture N. magadii L11 (pNB102).
Black: supernatants from culture N. magadii-ΔORF80 (pNB102-ORF80).
Light Grey: supernatants from culture N. magadii-ΔORF82 (pNB102-ORF82).
Dark Grey: supernatants from culture N. magadii-ΔORF80-82 (pNB102-ORF80-82).

To determine if complementation occurred for ORFs 80 and 82, we compared their titers to those of deletion mutants carrying an empty pNB102 plasmid.

For ORF80 (see **Figure 27**), *N. magadii* L11-ΔORF80 (pNB102) behaved differently than *N. magadii* L11-ΔORF80 (pNB102-ORF80). *N. magadii* L11-ΔORF80 (pNB102) began with a higher titer (2.23×10^7 pfu/mL) and followed the same trend, reaching a minimum of 1.65×10^6 pfu/mL on day two. The titer then began to rise again, reaching a maximum of 4.75×10^8 pfu/mL on day 5. Over the remainder of the graph, there was a smaller difference in titer between *N. magadii* L11-ΔORF80 (pNB102) and *N. magadii* L11-ΔORF80 (pNB102-ORF80), showing nearly no difference between them on days 6 and 7.

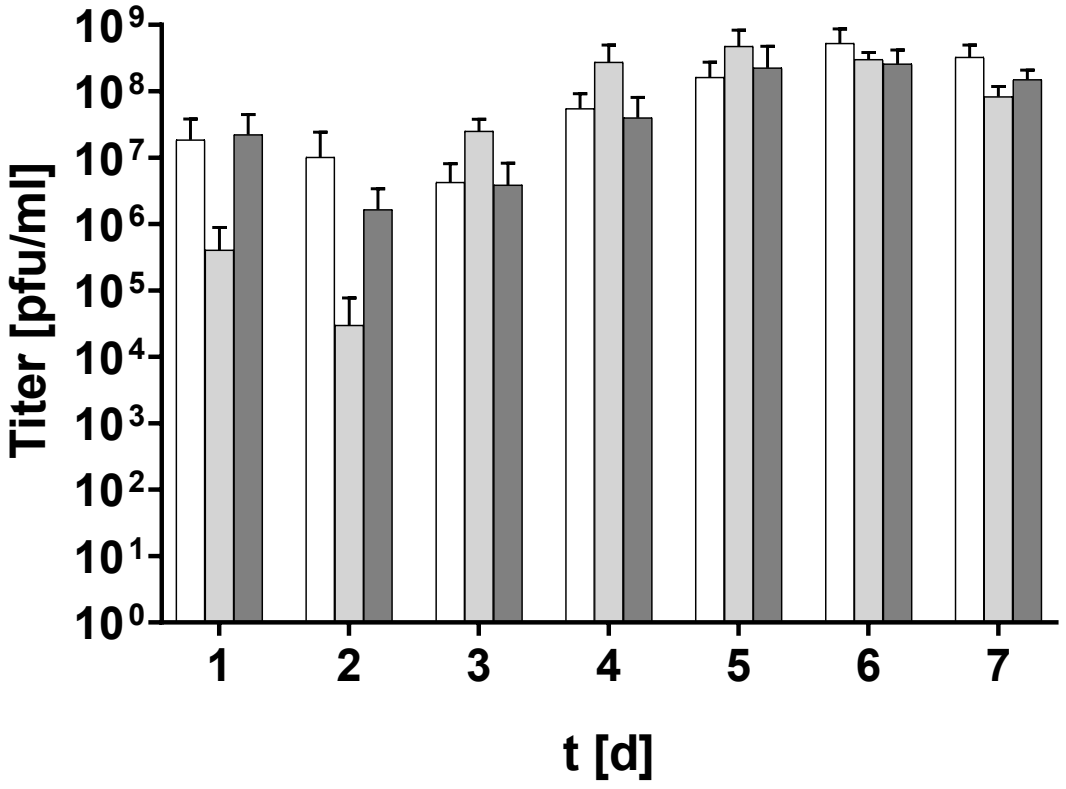

***Figure 27: Virus-Titer of deletion and complementation of ORF80**: The virus titer was measured in the culture supernatant by infecting the cured L13 strain of N. magadii. Samples were taken every 24 hours, starting one day after inoculation. Error bars (±1 SD) are indicated.*

White: supernatants of culture N. magadii L11 (pNB102).
Light gray: supernatants of culture N. magadii L11-ΔORF80 (pNB102-ORF80).
Dark gray: supernatants of culture N. magadii L11-ΔORF80 (pNB102).

N. magadii L11-ΔORF82 (pNB102) exhibited similar behaviour to *N. magadii* L11 (pNB102), with only minor differences in titer (see **Figure 28**). Significant differences were observed between *N. magadii* L11-ΔORF82 (pNB102-ORF82), *N. magadii* L11-ΔORF82 (pNB102), and N. magadii L11 (pNB102) on days 3 and 7. On day 3, *N.*

magadii L11-ΔORF82 (pNB102-ORF82) exhibited the greatest difference in titer, reaching 3.43×10^8 pfu/mL - approximately two orders of magnitude higher than the other two constructs. A second significant difference occurred on day 7, when *N. magadii* L11-ΔORF82 (pNB102-ORF82) exhibited the lowest titer, 1.3×10^7 pfu/mL.

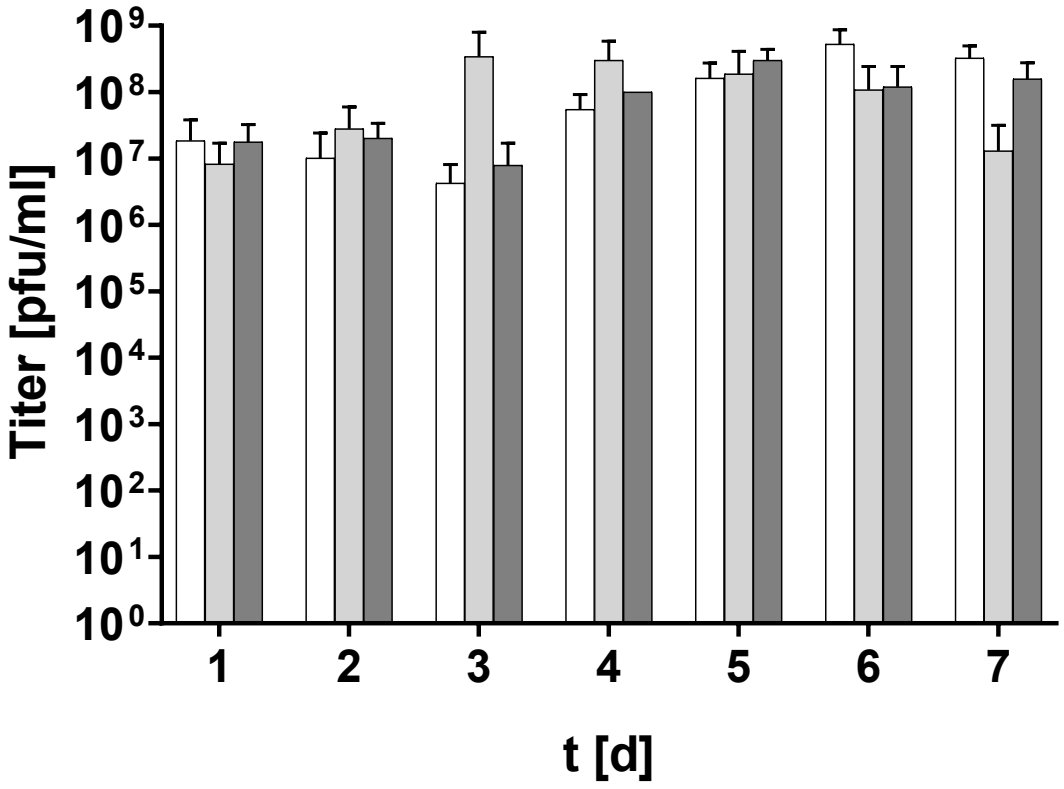

Figure 28: Virus-Titer of deletion and complementation of ORF82*: The virus titer was measured in the culture supernatant by infecting the N. magadii cured L13 strain. Samples were taken every 24 hours, starting one day after inoculation. Error bars (±1 SD) are indicated.*

White: supernatants of culture N. magadii L11 (pNB102).
Light gray: supernatants of culture N. magadii L11-ΔORF82 (pNB102-ORF82).
Dark gray: supernatants of culture N. magadii L11-ΔORF82 (pNB102).

N. magadii L11-ΔORF80/82 (pNB102) (see **Figure 29**) exhibited minimal change in titer until day six, gradually increasing from 3.25×10^7 to 4×10^7 pfu/mL. After day five, the titer increased to a new level between 3×10^8 and 3.5×10^8 pfu/mL. This trend differed from that of *N. magadii* L11-ΔORF80-82 (pNB102-ORF80-82) or *N. magadii* L11 (pNB102). However, the absolute titer was sometimes similar to that of *N. magadii* L11 (pNB102) and/or *N. magadii* L11-ΔORF80-82 (pNB102-ORF80-82).

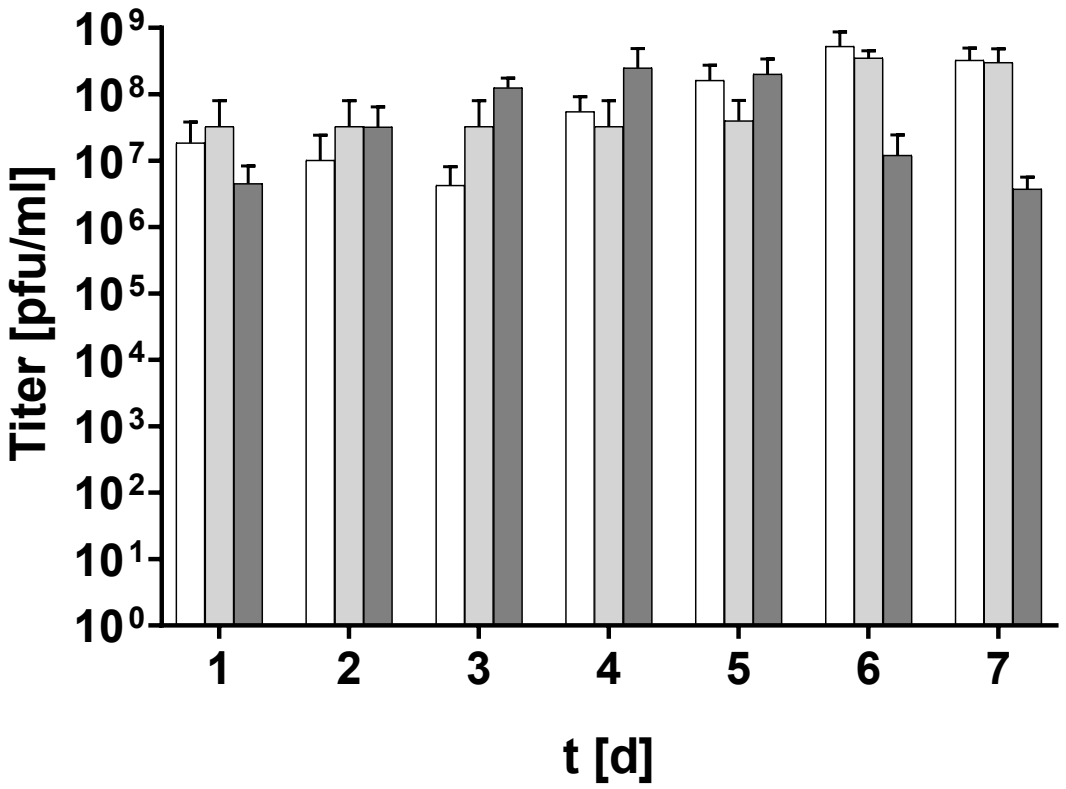

Figure 29: Virus-Titer of deletion and complementation of ORF80 and ORF82*: Virus-Titer measured of supernatant of culture infecting the cured N. magadii L13 strain, samples were taken every 24 h starting one day after inoculation. Error bars (±1SD) indicated.*

White: supernatants of culture (N. magadii L11 (pNB102).
Light Grey: supernatants of culture N. magadii L11-ΔORF80-82 (pNB102).
Dark Grey: supernatants of culture N. magadii L11-ΔORF80-82 (pNB102-ORF80-82)

To analyze the influence of ORF80 and ORF82 on gene expression during a culture's growth stages, samples were taken and analyzed via Western blot during the growth experiment. Three different proteins, which genes are spread over the genome of *N. magadii,* were targeted to ascertain the effect of the ORFs in question. The antibodies targeted the E protein (ORF11), gp34 (ORF34), and Mtase (ORF94). The coding regions of the three targeted proteins are distributed over nearly the entire length of the ϕCh1 genome. To validate the results, *N. magadii* L13 and *N. magadii* L11 samples were chosen as negative and positive controls, respectively, showing the expected results of no signal and a strong signal, respectively.

Gene expression compared via western blot

To analyze the influence of ORF80 and ORF82 on gene expression during a culture's growth stages, samples were collected and examined via Western blot during the growth experiment. Three different proteins spread over the genome of *N. magadii* were targeted to determine the effect of the ORFs in question. The antibodies targeted the E protein (ORF11), gp34 (ORF34), and Mtase (ORF94), the encoding of which is suspected to be by ORF80 and 82. The coding regions of these three proteins span nearly the entire ϕCh1 genome. To validate the results, *N. magadii* L13 and *N. magadii* L11 samples were chosen as negative and positive controls, respectively. The expected results were observed: no signal for the negative control and a strong signal for the positive control.

Expression patterns of the deletion mutants

In this thesis, the deletion mutants were first analyzed in regard to their protein E expression pattern via Western blot (**Figure 33** & **Figure 30**). As can be seen in the graph below, the expression patterns of the different deletion mutants differed substantially. L11 exhibited an exponential increase in the level of protein E until day 4, which held until day 5, after which it plummeted until the end of the measurement period. In contrast, the mutant with a deletion of ORF80 and the double deletion exhibited an exponential increase until day 5. While the level of protein E was lower on day 4, the peak on day 5 was higher than that of *N. magadii* L11 on day 4. After falling, the levels of these two mutants remained relatively high compared to the other tested mutants and *N. magadii* L11; the double mutant's levels were even higher. *N. magadii* L11-ΔORF82 differed most from the other mutants. It reached a much smaller peak on day 3 and showed a minimal amount of protein E on day 5, only to increase exponentially again until the end of the measurement. This value was very similar to that of *N. magadii* L11-ΔORF80. As displayed in **Figure 30** and previously described, showed the double deletion much more similar levels of protein E to *N. magadii* L11-ΔORF80, than to *N. magadii* L11-ΔORF82, which indicates a stronger influence of the deletion of ORF80 of the expression of protein E and similar to the data generated in the growth experiments, showed a dip in between two maxima of

protein E, although at different points in time. Since protein E is a capsid protein of ϕCh1, differences in expression could indicate an influenced virus cycle.

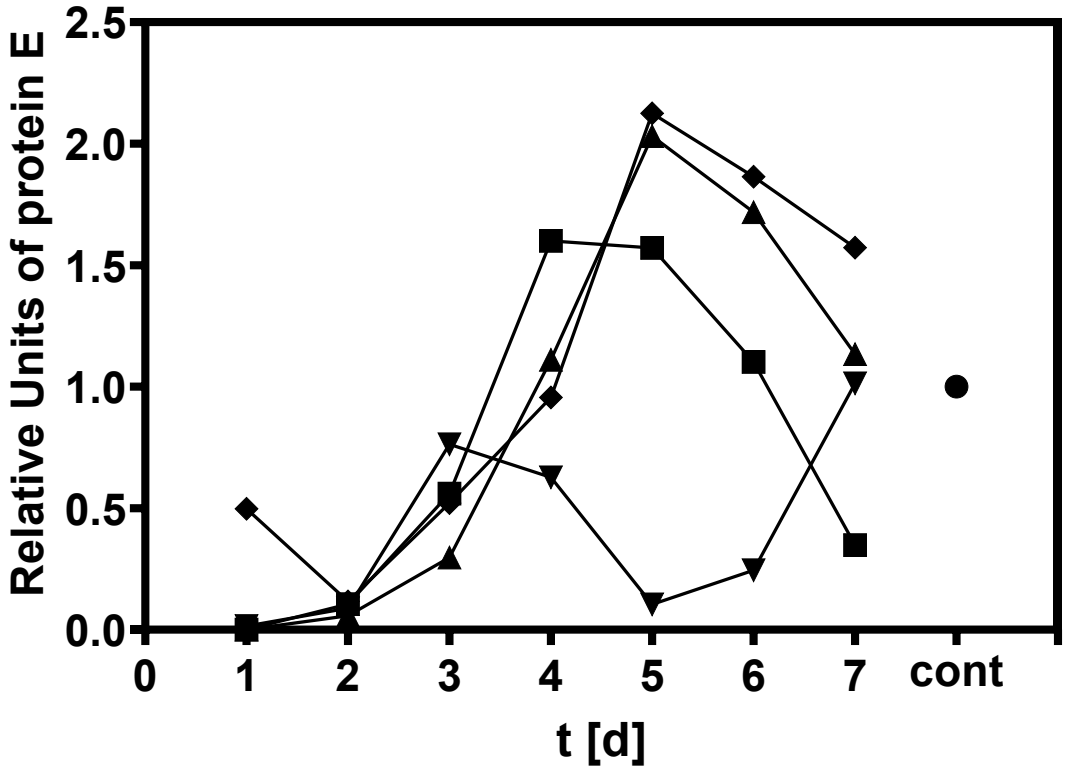

Figure 30: Relative levels of protein E in N. magadii L11 and deletion strains: *The western blot images of the various constructs cultured in NVM CAA were analyzed over 7 days (see **Figure 37**). Samples taken every 24 hours.*
Circle: N. magadii L11 taken after 5 days of growth (used as a control in all blots).
Square: N. magadii L11.
Triangle pointed upwards: N. magadii L11-ΔORF80.
Triangle pointed downwards: N. magadii L11-ΔORF82.
Rhombus: N. magadii L11-ΔORF80-ORF82.

The production of gp34 in *N. magadii* L11-ΔORF82 differed greatly from that in *N. magadii* L11 (see **Figure 31**). While *N. magadii* L11 showed a relatively constant increase until day 5, a plateau from days 5 to 6, and a strong decrease on day 7, *N. magadii* L11-ΔORF82 showed a much stronger increase from the lag phase until day 2 to maximum levels similar to those of L11 on days 3 and 4, with a local minimum on day 6, and then rose to nearly the same level as *N. magadii* L11 on day 7. *N. magadii* L11-ΔORF80 and *N. magadii* L11-ΔORF80-ORF82 showed a different trend again. Gp34 increased steeply in both constructs from the start until reaching a peak on day four, followed by a drastic fall until the next day, after which it reached a plateau. *N. magadii* L11-ΔORF80 exhibited an amplitude like that of *N. magadii* L11 and *N.*

magadii L11-ΔORF82. In contrast, *N. magadii* L11-ΔORF80-ORF82 displayed an amplitude nearly double that of the other constructs investigated. Since *N. magadii* L11-ΔORF80 and *N. magadii* L11-ΔORF80-ORF82 were more similar to each other than to *N. magadii* L11-ΔORF82, the deletion of ORF80 appears to be more influential on the phenotype.

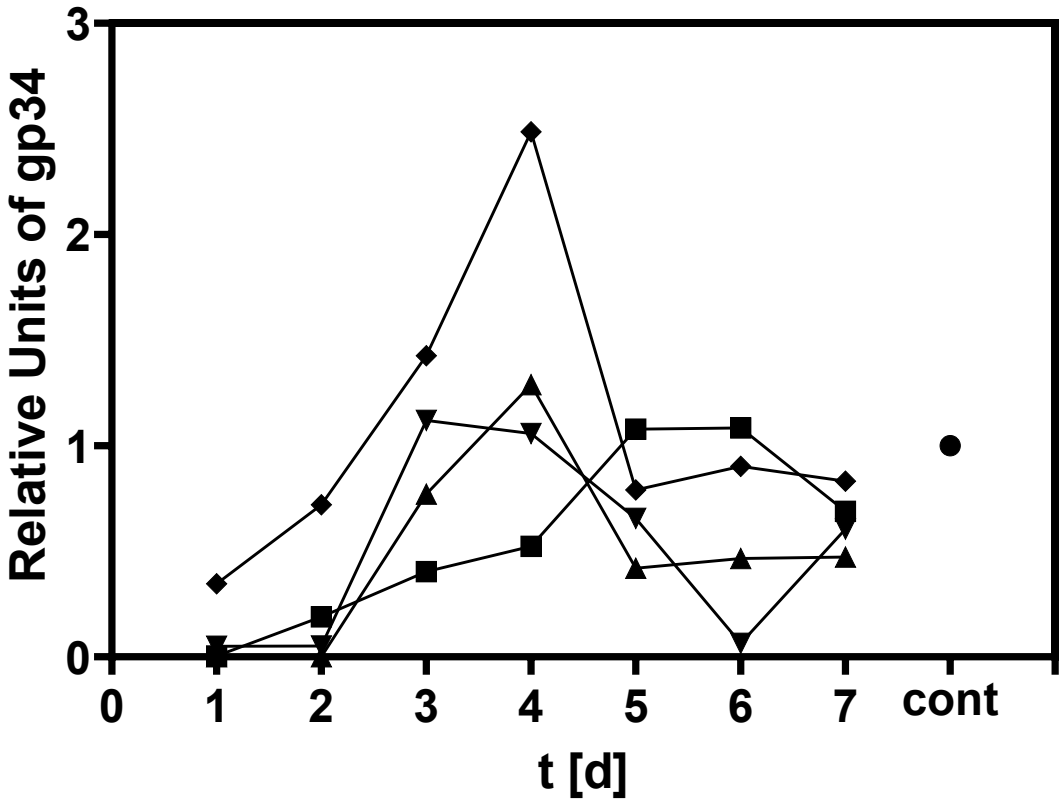

Figure 31: Relative levels of gp34 in N. magadii L11 and deletion mutants: *The western blot images of the different constructs of culture grown in NVM CAA over seven days were analyzed (see* ***Figure 33****). Samples taken every 24 hours.*

Circle: N. magadii L11 taken after 5 days of growth (used as a control in all blots).
Square: N. magadii L11.
Triangle pointed upwards: N. magadii L11-ΔORF80.
Triangle pointed downwards: N. magadii L11-ΔORF82.
Rhombus: N. magadii L11-ΔORF80-ORF82.

As shown in **Figure 32**, comparing the levels of Mtase of *N. magadii* L11 and *N. magadii* L11-ΔORF82 revealed significant differences in expression patterns. While the amount of gp34 in *N. magadii* L11 first increased exponentially until day 3, it then plateaued and decreased slightly until day 7. *N. magadii* L11-ΔORF82 hit a peak higher than the *N. magadii* L11 plateau and then dipped on day 6, reaching a level like

that of *N. magadii* L11 by day 7. As shown in **Figure 31**, *N. magadii* L11-ΔORF80 and *N. magadii* L11-ΔORF80-ORF82 displayed a peak on day four. Unlike before, *N. magadii* L11-ΔORF80 showed a second, smaller peak on day 6. As with the gp34 levels, the peak heights of *N. magadii* L11-ΔORF80 and *N. magadii* L11-ΔORF80-ORF82 were much greater than those of *N. magadii* L11 and *N. magadii* L11-ΔORF82. Additionally, since *N. magadii* L11-ΔORF80 and *N. magadii* L11-ΔORF80-ORF82 exhibited similar trends, the impact of deleting ORF80 appears significant.

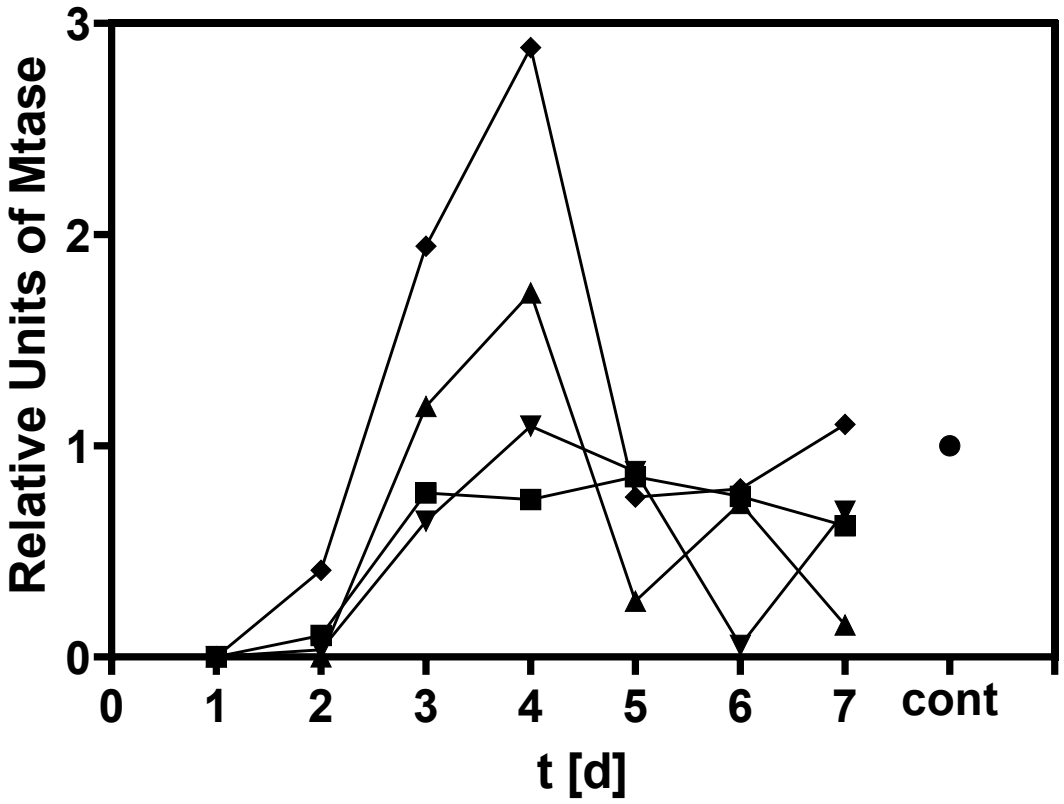

Figure 32: Relative levels of Mtase in N. magadii L11 and deletion mutants: *The western blot images of the different constructs of culture grown in NVM CAA over seven days were analyzed (see **Figure 37**). Samples taken every 24 hours.*

Circle: N. magadii L11 taken after 5 days of growth (used as a control in all blots).
Square: N. magadii L11.
Triangle pointed upwards: N. magadii L11-ΔORF80.
Triangle pointed downwards: N. magadii L11-ΔORF82.
Rhombus: N. magadii L11-ΔORF80-ORF82.

As shown in **Figure 30** as previously described, the double deletion exhibited much higher levels of all proteins like *N. magadii* L11-ΔORF80 than to *N. magadii* L11-ΔORF82. This indicates that the deletion of ORF80 has a stronger influence on protein

expression. Similar to the data generated in the growth experiments, there was a dip in viral protein levels between two maxima at different points in time. This difference depended on the analyzed protein. Since protein E is a ϕCh1 capsid protein, differences in expression could indicate an altered viral life cycle. This is further hinted at since, in **Figure 31** and **Figure 32**, the same major difference from the wild type can be seen in gp34 and Mtase levels.

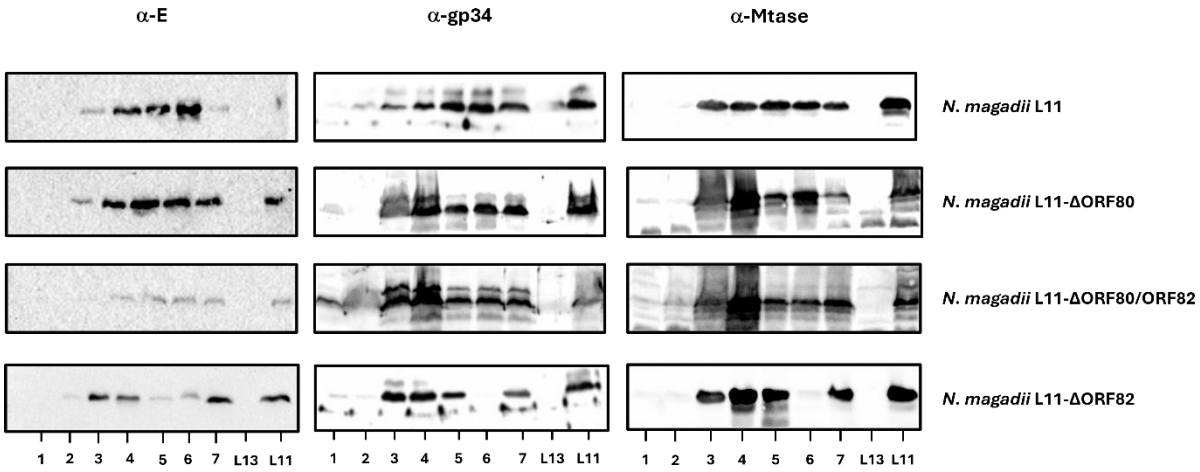

Figure 33: *Western blots of deletion strains. Samples were taken for seven days, and the amount loaded was normalized by OD600. Labeling: 1-7: samples taken every 24 hours after inoculation; L13: sample of uninfected N. magadii; L11: sample of N. magadii infected by ΦCh1; α-E: antibodies against the major capsid protein E of ΦCh1; α-gp34: antibodies against the gene product of ORF34; α-Mtase: antibodies against DNA methyltransferase.*

N. magadii L11: wild type strain used as a control.
N. magadii L11/ϕCh1-ΔORF80: deletion of ORF80.
N. magadii L11/ϕCh1-ΔORF82: deletion of ORF82.
N. magadii L11/ϕCh1-ΔORF80/ORF82: deletion of ORF80 and ORF82.

Expression patterns of the overexpression mutants

Figure 37 depicts the expression patterns of the overexpression constructs and *N. magadii* L11 with the pNB102 plasmid via Western blot. For the production pattern of protein E (analyzed in **Figure 34**), *N. magadii* L11 (pNB102) and *N. magadii* L11 (pNB102-ORF80) exhibited a similar pattern: a weak signal on day 2 that increased until a peak was reached on day 5. This was followed by a decline, though the signal remained present until day 7. However, the intensity of *N. magadii* L11 (pNB102-ORF80) was somewhat higher. *N. magadii* L11 (pNB102-ORF80-ORF82) seems similar to the other two, except the expression starts on day 3 instead of day 2 and is

weaker overall. *N. magadii* L11 (pNB102-ORF80) displays a negligible increase on day 6, followed by a period of stagnation after a brief growth phase from days 2 to 4.

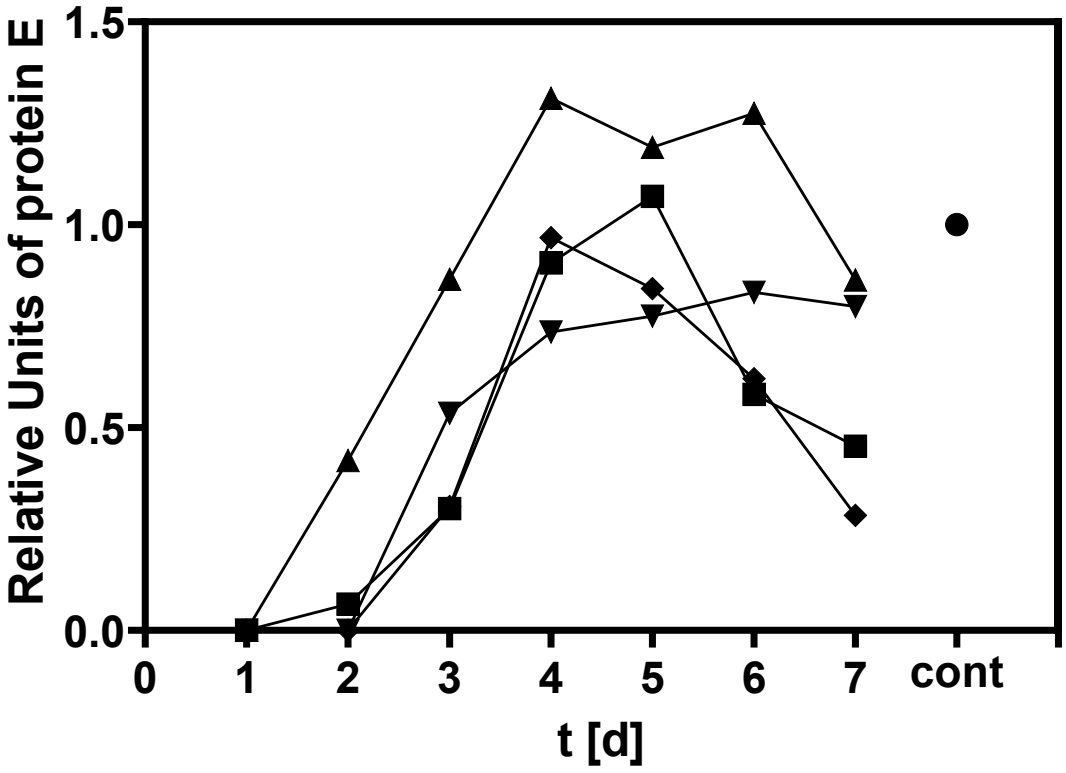

Figure 34: Relative levels of protein E in N. magadii L11 and the overexpression constructs of N. magadii L11*: Analysis of pictures taken of the western blot of the different constructs of culture grown in NVM CAA over 7 days (see* ***Figure 37****). Samples taken every 24 hours.*

Circle: N. magadii L11 taken after 5 days of growth (used as a control in all blots).
Square: N. magadii L11 (pNB102).
Triangle pointed upwards: N. magadii L11 (pNB102-ORF80).
Triangle pointed downwards: N. magadii L11 (pNB102-ORF82).
Rhombus: N. magadii L11 (pNB102-ORF80-82).

As illustrated in **Figure 35** and **Figure 37**, the production patterns of gp34 appear to vary slightly. *N. magadii* L11 (pNB102) started expressing on day 2, with a peak on day 4, declining but still present on day 7. *N. magadii* L11 (pNB102-ORF80) also began expressing on day 2, peaking on day 4; however, the signal decreased much less until day 7. *N. magadii* L11 (pNB102-ORF-82) showed the first weak signal on day 2 and peaked on day 4 with about the same intensity as L11(pNB102) but showed nearly no expression on days 6 and 7. *N. magadii* L11 (pNB102-ORF80-ORF82) began expressing on day three, plateauing from days four to six and declining until day seven.

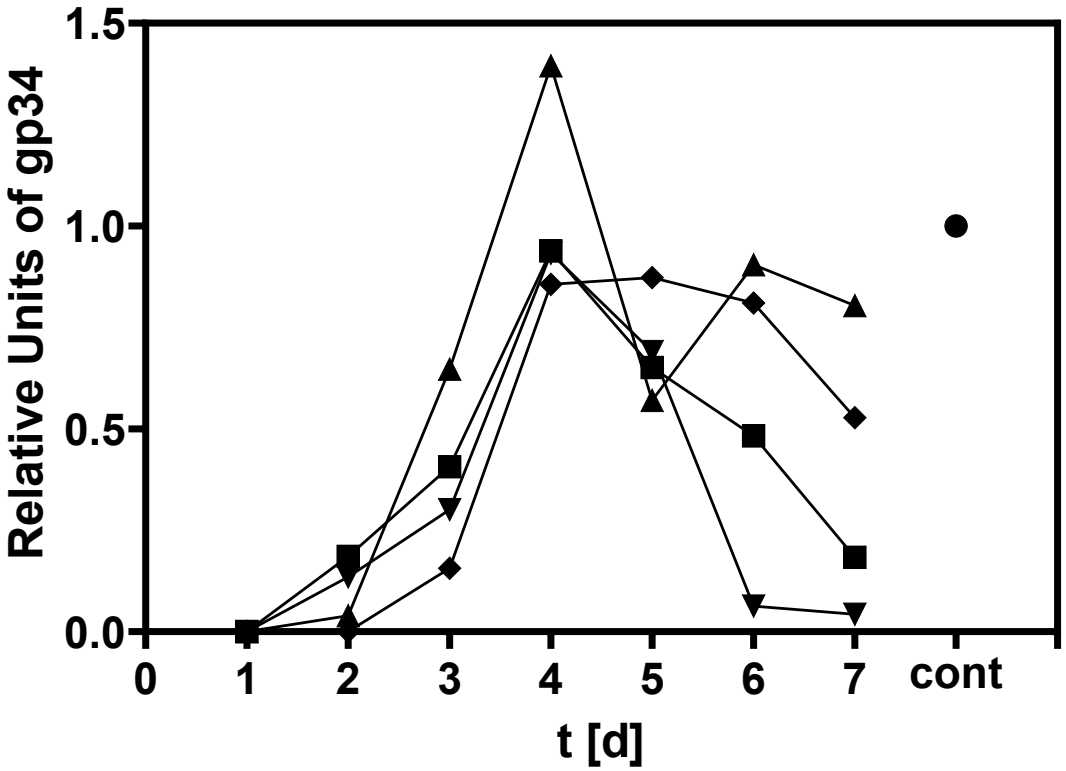

Figure 35: Relative levels of gp34 in N. magadii L11 and the overexpression constructs of N. magadii L11*: Analysis of pictures taken of the western blot of the different constructs of culture grown in NVM CAA over 7 days (see* ***Figure 37****). Samples taken every 24 hours.*

Circle: N. magadii L11 taken after 5 days of growth (used as a control in all blots).
Square: N. magadii L11 (pNB102).
Triangle pointed upwards: N. magadii L11 (pNB102-ORF80).
Triangle pointed downwards: N. magadii L11 (pNB102-ORF82).
Rhombus: N. magadii L11 (pNB102-ORF80-82).

The expression of the Mtase gene (see **Figure 36** and **Figure 37**) started in *N. magadii* L11 (pNB102) on day 2, peaked on day 4, and decreased until day 7. This is also true for *N. magadii* L11 (pNB102-80), except it started on day 3 and dipped on day 5. *N. magadii* L11 (pNB102-ORF82) exhibited a comparable pattern to L11(pNB102), but with a reduced overall amount. *N. magadii* L11 (pNB102-ORF80-ORF-82) already showed a signal on day 1 and behaved similarly to *N. magadii* L11 (pNB102), although the intensity from days 4 to 6 was much higher.

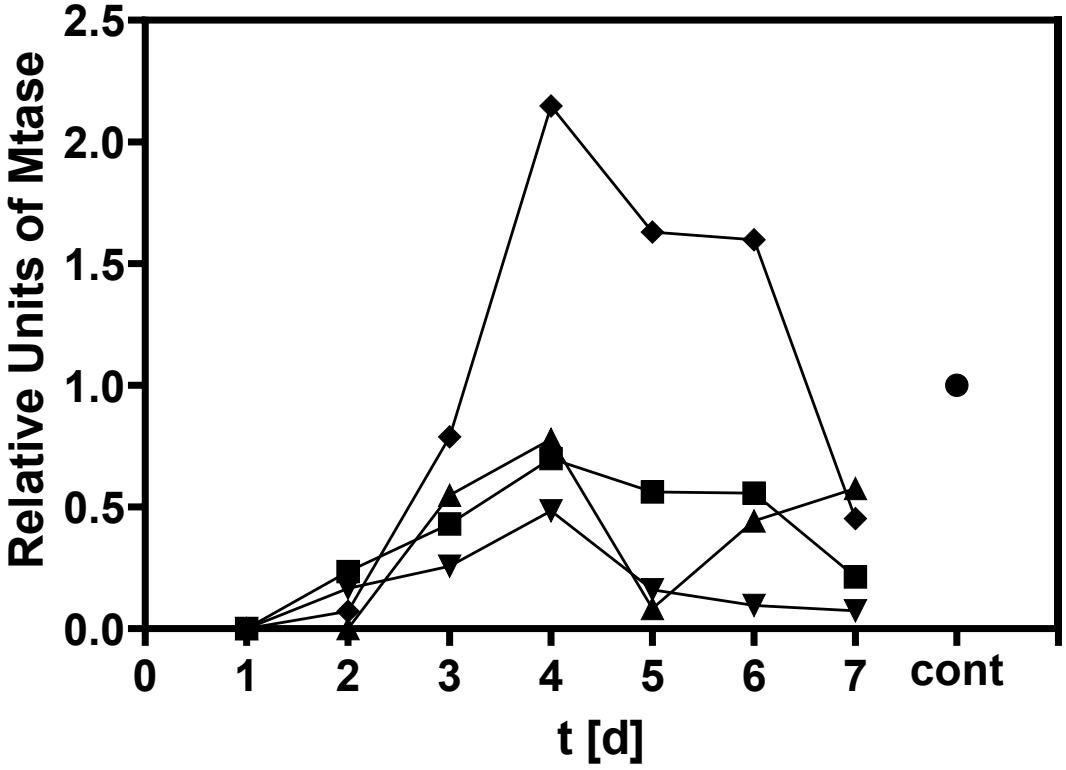

Figure 36: Relative levels of Mtase in N. magadii L11 and the overexpression constructs of N. magadii L11*: Analysis of pictures taken of the western blot of the different constructs of culture grown in NVM CAA over 7 days (see* ***Figure 37****). Samples taken every 24 hours.*

Circle: N. magadii L11 taken after 5 days of growth (used as a control in all blots).
Square: N. magadii L11 (pNB102).
Triangle pointed upwards: N. magadii L11 (pNB102-ORF80).
Triangle pointed downwards: N. magadii L11 (pNB102-ORF82).
Rhombus: N. magadii L11 (pNB102-ORF80-82).

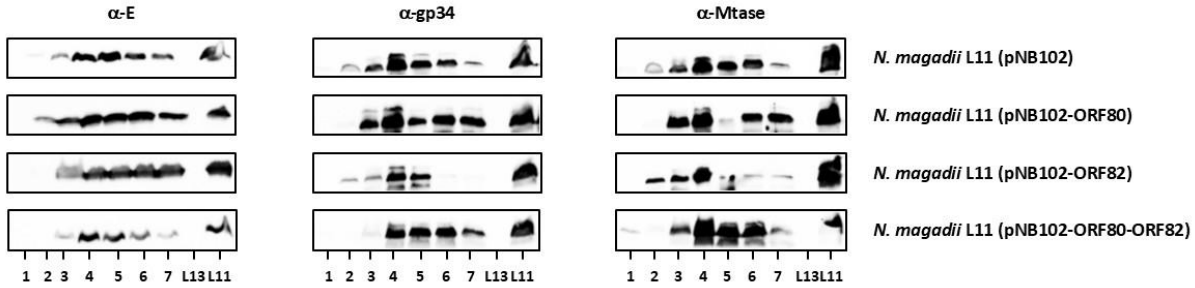

Figure 37: Western blots of overexpressing strains*. Samples were taken for seven days, and the amount loaded was normalized by OD600. Labeling: 1-7: samples taken every 24 hours after inoculation; L13: sample of uninfected N. magadii; L11: sample of N. magadii infected by ΦCh1; α-E: antibodies against the major capsid protein E of ΦCh1; α-gp34: antibodies against the gene product of ORF34; α-Mtase: antibodies against DNA methyltransferase.*

N. magadii L11: wild type strain used as a control.
N. magadii L11-ΔORF80: deletion of ORF80.
N. magadii L11-ΔORF82: deletion of ORF82.
N. magadii L11-ΔORF80-82: deletion of ORF80 and ORF82.

Expression patterns of the complementation mutants

To verify the successful complementation of the deletion mutants, we determined the protein levels of protein E, Gp34, and Mtase for the complementation constructs (see **Figure 41**).

The synthesis pattern of protein E (see **Figure 38**) is the same for *N. magadii* L11 (pNB102) and *N. magadii* L11 ΔORF80 (pNB102-ORF80), showing the presence of the protein starting on day 4. However, in the case of *N. magadii* L11 ΔORF80 (pNB102-ORF80), the amount is the lowest of all complementation mutants. *N. magadii* L11 ΔORF82 (pNB102-ORF82) and *N. magadii* L11 ΔORF80-ORF82 (pNB102-ORF80-ORF82) have a similar pattern, starting low on day 3 and peaking on day 4 or 5, respectively, then declining until day 7. Although the patterns are similar, the relative amount between the constructs differs, with *N. magadii* L11-ΔORF82 (pNB102-ORF82) showing the highest amount, followed by *N. magadii* L11-ΔORF80-82 (pNB102-ORF80-82), *N. magadii* L11 (pNB102), and *N. magadii* L11-ΔORF80 (pNB102-ORF80) with the lowest amount.

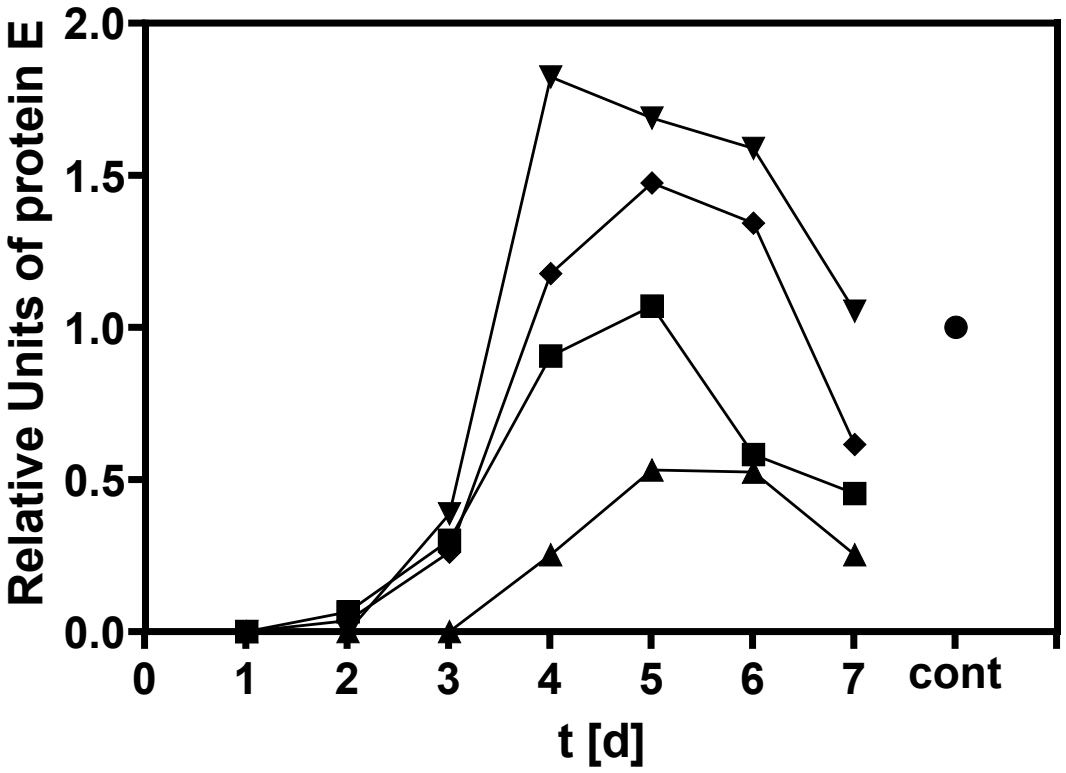

Figure 38: Relative levels of protein E in N. magadii L11 and complementation constructs: *The western blot images of the different constructs of culture grown in NVM CAA over seven days were analyzed (see* ***Figure 37****). Samples taken every 24 hours.*

Circle: N. magadii L11 taken after 5 days of growth (used as a control in all blots).
Square: N. magadii L11 (pNB102).
Triangle pointed upwards: N. magadii L11-ΔORF80 (pNB102-ORF80).
Triangle pointed downwards: N. magadii L11-ΔORF82 (pNB102-ORF82).
Rhombus: N. magadii L11-ΔORF80-ORF82 (pNB102-ORF80_ORF82.

In the case of gp34 (see **Figure 39** and **Figure 41**), *N. magadii* L11 (pNB102) showed quick growth from day 2 to day 4 and continuously decline afterwards, a pattern shared with *N. magadii* L11-ΔORF80-ORF82 (pNB102-ORF80-ORF82). *N. magadii* L11-ΔORF80 (pNB102-ORF80) and *N. magadii* L11-ΔORF82 (pNB102-ORF82) share a similar pattern with little growth on day 3 peaking on day 5 and declining till day 7. Although *N. magadii* L11-ΔORF80 (pNB102-ORF80/) shows much less decline from day 5 to 6, showing otherwise a nearly identical pattern. In case of gp34 relative levels of the double mutants showed the highest peak above *N. magadii* L11 and the single mutants, which was different from protein E.

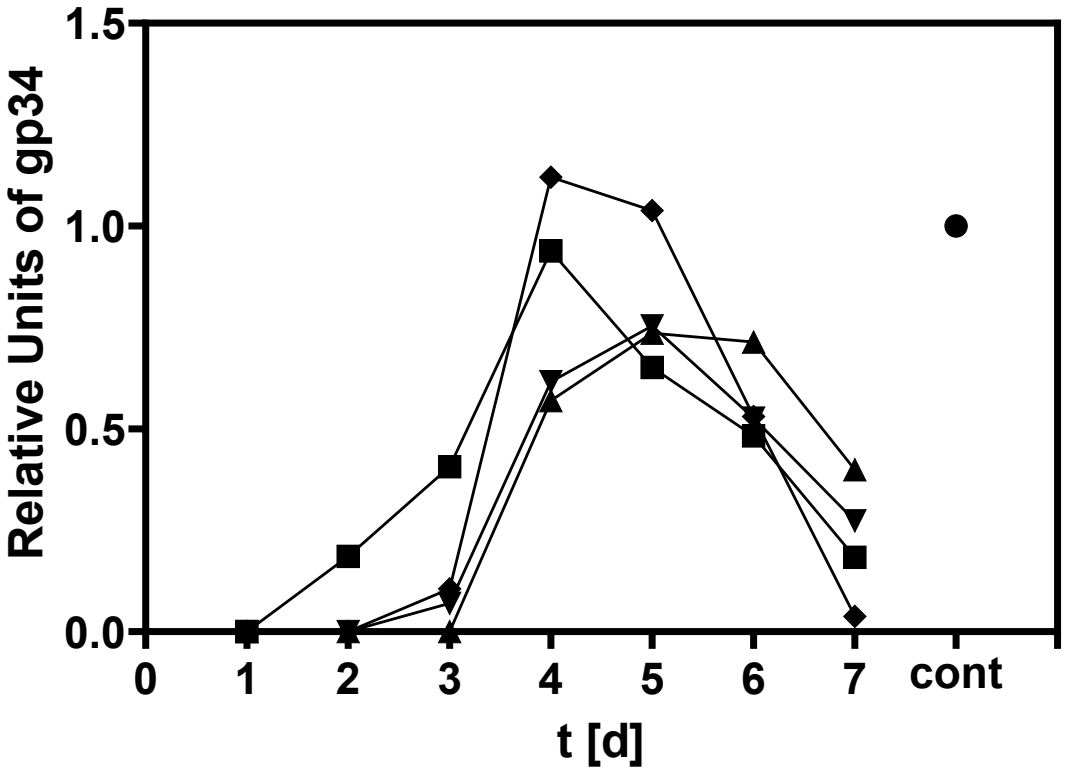

Figure 39: Relative levels of gp34 in N. magadii L11 and complementation constructs: *The western blot images of the different constructs of culture grown in NVM CAA over seven days were analyzed (see* ***Figure 37****). Samples taken every 24 hours.*

Circle: N. magadii L11 taken after 5 days of growth (used as a control in all blots).
Square: N. magadii L11 (pNB102).
Triangle pointed upwards: N. magadii L11-ΔORF80 (pNB102-ORF80).
Triangle pointed downwards: N. magadii L11-ΔORF82 (pNB102-ORF82).
Rhombus: N. magadii L11-ΔORF80-ORF82 (pNB102-ORF80-ORF82).

For Mtase (see **Figure 40** and **Figure 41**), *N. magadii* L11 (pNB102) exhibited the earliest growth on day 2, peaking on day 4. It then plateaued on days 5 and 6 before declining on day 7. *N. magadii* L11(pNB102-ORF82/ΔORF82) showed a somewhat similar behaviour, although it only began to grow on day 3 and reached a much higher peak than *N. magadii* L11 (pNB102), while still declining to the same low on day 7. *N. magadii* L11 (pNB102-ORF80/ΔORF80) and *N. magadii* L11 (pNB102-ORF80-ORF82/ΔORF80-ORF82) exhibited a similar pattern: they began on day 3, peaked on day 5, and declined to the same low on day 7 as L11(pNB102). In this instance, *N. magadii* L11 exhibited the least significant amount, the double deletion exhibited the second least significant amount, and the two single deletions exhibited the most significant amount.

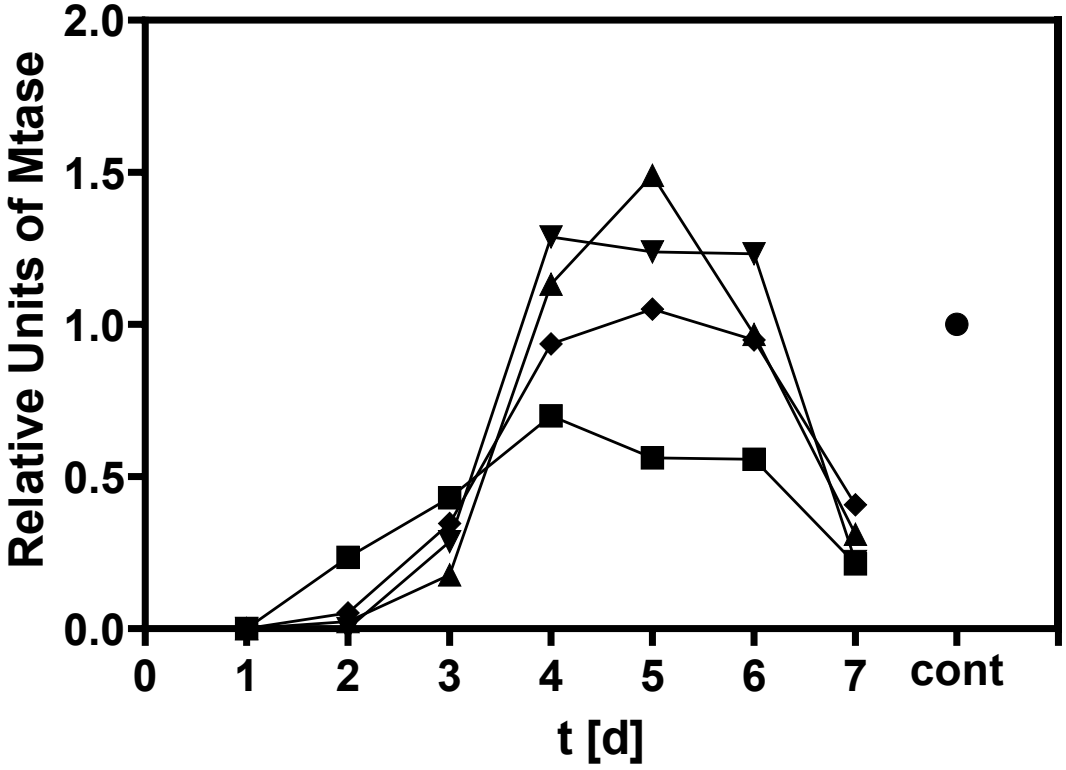

Figure 40: Relative levels of Mtase in N. magadii L11 and complementation constructs: *The western blot images of the different constructs of culture grown in NVM CAA over seven days were analyzed (see* ***Figure 37****). Samples taken every 24 hours.*

Circle: N. magadii L11 taken after 5 days of growth (used as a control in all blots).
Square: N. magadii L11 (pNB102).
Triangle pointed upwards: N. magadii L11-ΔORF80 (pNB102-ORF80).
Triangle pointed downwards: N. magadii L11-ΔORF82 (pNB102-ORF82).
Rhombus: N. magadii L11-ΔORF80-ORF82 (pNB102-ORF80-ORF82).

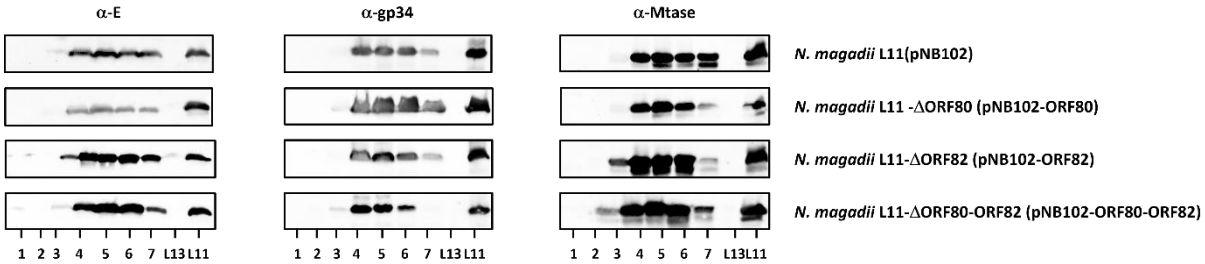

Figure 41: Western Blots of complementation growth experiments*; Samples taken for 7 days and amount loaded normalized by* OD_{600}*; Labelling: 1-7:Multiples of 24 h after inoculation at which samples were taken, L13: Sample of uninfected N. magadii, L11 Sample of N. magadii infected by φCh1; α-E: Antibodies against Major capsid protein E of ΦCh1; α-gp34: Antibodies against the gene product of ORF34; α-Mtase: Antibodies against DNA-Methyltransferase; N. magadii L11(pNB102): Unmodified L11 with vector-plasmid used as control; N. magadii L11-ΔORF80 (pNB102-ORF80): Strain of N. magadii-L11 with a deletion of ORF80 complemented with pNB102 plasmid carrying ORF80; N. magadii L11-ΔORF82 (pNB102-ORF82): Strain of N. magadii-L11 with a deletion of ORF82 complemented with pNB102 plasmid carrying ORF82; N. magadii L11-ΔORF80/ORF82 (pNB102-ORF80-ORF82): Strain of N. magadii-L11 with a deletion of ORF80 and ORF82 complemented with pNB102 plasmid carrying ORF80 and ORF82;*

All complementation constructs exhibited different levels of the investigated proteins compared to *N. magadii* (pNB102), but a similar pattern was observed. Additionally, the decrease in protein levels seen in the *N. magadii* L11-ΔORF82 and *N. magadii* (pNB102-ORF80) samples was no longer evident in the complemented constructs, suggesting successful complementation.

Discussion

Success of complementation of the deletion mutants

Regarding the complementation constructs, it was demonstrated that complementation was successful. First, the OD measurements in "Growth Behaviour of *N. magadii* L11 Strains Over Time" showed that the complemented strains exhibited behaviour similar to that of *N. magadii* L11. Notably, they lacked the dip observed in *N. magadii* L11-ΔORF80 and exhibited a consistent plateau, behaviour dissimilar to the deletion strains to be complemented and similar to L11. Similarly, the expression pattern, as measured by Western blot, showed a similar result (see "Protein expression compared via Western blot"). While all proteins showed a dip in *N. magadii* L11-ΔORF82, as well as in *N. magadii* L11 (pNB102-ORF80) and the Mtase curve of *N. magadii* L11 (pNB102-ORF80-82), the complemented strains showed no dip. However, they still showed different peak heights compared to *N. magadii* L11. Since both the OD measurements and the western blots showed evidence of successful complementation, the complementation can be considered successful.

Inference on possible functions of ORF80 and ORF82

The most notable difference in the growth behaviour of the deletion mutants was the dip observed in the optical density (OD) of *N. magadii* L11-ΔORF80 and *N. magadii* L11-ΔORF80-82. Since the decrease in OD occurred only with the single deletion of ORF80, this ORF appears to be involved in regulating the cell cycle/lysis by preventing it from happening too early. ORF82 also appears to be involved, as the decrease in OD was significantly reduced in the growth curve of the double deletion.

A similar decrease was observed in the protein expression patterns of *N. magadii* L11-ΔORF82 instead of *N. magadii* L11-ΔORF80. For protein E, the minimum occurred on

day 5; for gp34 and Mtase, it occurred on day 6, compared to the dip in OD on day 4. In the overexpression experiments, the decrease occurred in *N. magadii* L11 (pNB102-ORF80) for all three proteins. *N. magadii* L11 (pNB102-ORF80-82) also showed a dip for Mtase, though it was weaker than in L11 for the same protein. The very similar OD of the overexpression mutants confirms that these differences stemmed from different expression levels. Since the deletion of ORF82 and the overexpression of ORF80 led to similar results for all the tested proteins distributed across the ϕCh1 genome, the ratio of ORF80 and ORF82 gene products may be relevant to the regulation of viral genome gene expression in general.

Previous studies (Klein et al., 2002) have shown that the sequences of ORF80 and ORF82 are like different DNA methyltransferases and that they regulate lysis and protein expression. However, the status of ORF80 and ORF82 as methyltransferase encoding genes has to be further confirmed.

Sources

Baranyi, U., Klein, R., Lubitz, W., Krüger, D. H., & Witte, A. (2000). The archaeal halophilic virus-encoded Dam-like methyltransferase M.ϕCh1-I methylates adenine residues and complements dam mutants in the low salt environment of Escherichia coli. Molecular Microbiology, 35(5), 1168–1179. https://doi.org/10.1046/j.1365-2958.2000.01786.x

Woese, C. R., & Fox, G. E. (1977). Phylogenetic structure of the prokaryotic domain: The primary kingdoms. Proceedings of the National Academy of Sciences, 74(11), 5088–5090. https://doi.org/10.1073/pnas.74.11.5088

Rothschild, L. J., & Mancinelli, R. L. (2001). Life in extreme environments. Nature, 409(6823), 1092–1101. https://doi.org/10.1038/35059215

Pikuta, E. V., Hoover, R. B., & Tang, J. (2007). Microbial Extremophiles at the Limits of Life. Critical Reviews in Microbiology, 33(3), 183–209. https://doi.org/10.1080/10408410701451948

Lloyd, K. G., May, M. K., Kevorkian, R. T., & Steen, A. D. (2013). Meta-Analysis of Quantification Methods Shows that Archaea and Bacteria Have Similar Abundances in the Subseafloor. Applied and Environmental Microbiology, 79(24), 7790–7799. https://doi.org/10.1128/aem.02090-13

DeLong, E. F. (1998). Everything in moderation: Archaea as 'non-extremophiles.' Current Opinion in Genetics & Development, 8(6), 649–654. https://doi.org/10.1016/s0959-437x(98)80032-4

Karner, M. B., DeLong, E. F., & Karl, D. M. (2001). Archaeal dominance in the mesopelagic zone of the Pacific Ocean. Nature, 409(6819), 507–510. https://doi.org/10.1038/35054051

Soliman, G. S. H., & Trüper, H. G. (1982). Halobacterium pharaonis sp. nov., a New, Extremely Haloalkaliphilic Archaebacterium with Low Magnesium Requirement. Zentralblatt Für Bakteriologie Mikrobiologie Und Hygiene: I. Abt. Originale C: Allgemeine, Angewandte Und Ökologische Mikrobiologie, 3(2), 318–329. https://doi.org/10.1016/s0721-9571(82)80045-8

Tindall, B. J., Ross, H. N. M., & Grant, W. D. (1984). Natronobacterium gen. nov. and Natronococcus gen. nov., Two New Genera of Haloalkaliphilic Archaebacteria. Systematic and Applied Microbiology, 5(1), 41–57. https://doi.org/10.1016/s0723-2020(84)80050-8

Kamekura, M., Dyall-Smith, M. L., Upasani, V., Ventosa, A., & Kates, M. (1997). Diversity of Alkaliphilic Halobacteria: Proposals for Transfer of Natronobacterium vacuolatum, Natronobacterium magadii, and Natronobacterium pharaonis to Halorubrum, Natrialba, and Natronomonas gen. nov., Respectively, as Halorubrum vacuolatum comb. nov., Natrialba magadii comb. nov., and Natronomonas pharaonis comb. nov., Respectively. International Journal of Systematic Bacteriology, 47(3), 853–857. https://doi.org/10.1099/00207713-47-3-853

Breuert, S., Allers, T., Spohn, G., & Soppa, J. (2006). Regulated Polyploidy in Halophilic Archaea. PLoS ONE, 1(1), e92. https://doi.org/10.1371/journal.pone.0000092

Witte, A., Baranyi, U., Klein, R., Sulzner, M., Luo, C., Wanner, G., Kru¨ger, D. H., & Lubitz, W. (1997). Characterization of Natronobacterium magadii phage ΦCh1, a unique archaeal phage containing DNA and RNA. Molecular Microbiology, 23(3), 603–616. https://doi.org/10.1046/j.1365-2958.1997.d01-1879.x

Klein, R., Baranyi, U., Rössler, N., Greineder, B., Scholz, H., & Witte, A. (2002). Natrialba magadii virus ϕCh1: first complete nucleotide sequence and functional organization of a virus infecting a haloalkaliphilic archaeon. Molecular Microbiology, 45(3), 851–863. https://doi.org/10.1046/j.1365-2958.2002.03064.x

Klein, Reinhard, Greineder, Barbara, Baranyi, Ulrike, & Witte, Angela. (2000). The Structural Protein E of the Archaeal Virus ϕCh1: Evidence for Processing in Natrialba magadii during Virus Maturation. Virology, 276(2), 376–387. https://doi.org/10.1006/viro.2000.0565

Witte, Angela, Baranyi, Ulrike, Klein, Reinhard, Sulzner, M., Luo, C., Wanner, G., Kru¨ger, D. H., & Lubitz, W. (1997). Characterization of Natronobacterium magadii phage ΦCh1, a unique archaeal phage containing DNA and RNA. Molecular Microbiology, 23(3), 603–616. https://doi.org/10.1046/j.1365-2958.1997.d01-1879.x

Haan, C., & Behrmann, I. (2007). A cost effective non-commercial ECL-solution for Western blot detections yielding strong signals and low background. Journal of Immunological Methods, 318(1–2), 11–19. https://doi.org/10.1016/j.jim.2006.07.027

Soliman, G. S. H., & Trüper, H. G. (1982). Halobacterium pharaonis sp. nov., a New, Extremely Haloalkaliphilic Archaebacterium with Low Magnesium Requirement. Zentralblatt Für Bakteriologie Mikrobiologie Und Hygiene: I. Abt. Originale C: Allgemeine, Angewandte Und Ökologische Mikrobiologie, 3(2), 318–329. https://doi.org/10.1016/s0721-9571(82)80045-8

Wilson, G. G. (1991). Organization of restriction-modification systems. Nucleic Acids Research, 19(10), 2539–2566. https://doi.org/10.1093/nar/19.10.2539

Lurie-Weinberger, M. N., & Gophna, U. (2015). Archaea in and on the Human Body: Health Implications and Future Directions. PLOS Pathogens, 11(6), e1004833. https://doi.org/10.1371/journal.ppat.1004833

Reuter, M., Schneider-Mergener, J., Kupper, D., Meisel, A., Mackeldanz, P., Krüger, D. H., & Schroeder, C. (1999). Regions of Endonuclease EcoRII Involved in DNA Target Recognition Identified by Membrane-bound Peptide Repertoires. Journal of Biological Chemistry, 274(8), 5213–5221. https://doi.org/10.1074/jbc.274.8.5213

Lanyi, J. K. (1979). Salt Tolerance in Microorganisms. In The Biosaline Concept (pp. 217–233). Springer US. https://doi.org/10.1007/978-1-4613-3021-9_10

Madern, D., Ebel, C., & Zaccai, G. (2000). Halophilic adaptation of enzymes. Extremophiles, 4(2), 91–98. https://doi.org/10.1007/s007920050142

Guffanti, A. A., & Hicks, D. B. (1991). Molar growth yields and bioenergetic parameters of extremely alkaliphilic Bacillus species in batch cultures, and growth in a chemostat at pH 10.5. Journal of General Microbiology, 137(10), 2375–2379. https://doi.org/10.1099/00221287-137-10-2375

Sturr, M. G., Guffanti, A. A., & Krulwich, T. A. (1994). Growth and bioenergetics of alkaliphilic Bacillus firmus OF4 in continuous culture at high pH. Journal of Bacteriology, 176(11), 3111–3116. https://doi.org/10.1128/jb.176.11.3111-3116.1994

Hunte, C., Screpanti, E., Venturi, M., Rimon, A., Padan, E., & Michel, H. (2005). Structure of a Na+/H+ antiporter and insights into mechanism of action and regulation by pH. Nature, 435(7046), 1197–1202. https://doi.org/10.1038/nature03692

Oren, A. (1999). Bioenergetic Aspects of Halophilism. Microbiology and Molecular Biology Reviews, 63(2), 334–348. https://doi.org/10.1128/mmbr.63.2.334-348.1999

Tenchov, B., Vescio, E. M., Sprott, G. D., Zeidel, M. L., & Mathai, J. C. (2006). Salt Tolerance of Archaeal Extremely Halophilic Lipid Membranes. Journal of Biological Chemistry, 281(15), 10016–10023. https://doi.org/10.1074/jbc.m600369200

Oren, A. (2002). Diversity of halophilic microorganisms: Environments, phylogeny, physiology, and applications. Journal of Industrial Microbiology & Biotechnology, 28(1), 56–63. https://doi.org/10.1038/sj/jim/7000176

Mevarech, M., Frolow, F., & Gloss, L. M. (2000). Halophilic enzymes: proteins with a grain of salt. Biophysical Chemistry, 86(2–3), 155–164. https://doi.org/10.1016/s0301-4622(00)00126-5

Comai, L. (2005). The advantages and disadvantages of being polyploid. Nature Reviews Genetics, 6(11), 836–846. https://doi.org/10.1038/nrg1711

Mayrhofer-Iro, M., Ladurner, A., Meissner, C., Derntl, C., Reiter, M., Haider, F., Dimmel, K., Rössler, N., Klein, R., Baranyi, U., Scholz, H., & Witte, A. (2013). Utilization of Virus ϕCh1 Elements To Establish a Shuttle Vector System for Halo(alkali)philic Archaea via Transformation of Natrialba magadii. Applied and Environmental Microbiology, 79(8), 2741–2748. https://doi.org/10.1128/aem.03287-12

Zhou, M., Xiang, H., Sun, C., & Tan, H. (2004). Construction of a novel shuttle vector based on an RCR-plasmid from a haloalkaliphilic archaeon and transformation into other haloarchaea. Biotechnology Letters, 26(14), 1107–1113. https://doi.org/10.1023/b:bile.0000035493.21986.20

Gregor Sommerkamp. Characterization of mutant ϕCh1-ΔORF94 and investigation of ORF75 of ϕCh1: does it encode an activator?. (2022)

Helene Eliaçık. The characterization of the mutant ΦCh1-ΔORF94 and complementation and investigation of ΦCh1-ΔORF75, (2024)

Harlow, E. D., & Lane, D. (1988). A laboratory manual. *New York: Cold Spring Harbor Laboratory*, *579*, 44.

Weier, H. U., & Gray, J. W. (1988). A programmable system to perform the polymerase chain reaction. *DNA*, *7*(6), 441–447. https://doi.org/10.1089/dna.1.1988.7.441

Abbreviations

- Units
    - g: Grams
    - mg: Milligrams
    - ng: Nanograms
    - hr: Hours
    - min: Minutes
    - s: seconds
    - kDa: Kilodalton
    - L: Litre
    - mL: Millilitres
    - µl: Microliters
    - M: Molar
    - mM: Millimolar
    - OD: Optical Density
    - pH: Power of Hydrogen or potential of Hydrogen
    - PFU: Plaque Forming Units
    -
- Media

- Mev: Mevinolin
- Nov: Novobiocin
- NVM: Natrialba Rich Media
- CAA: Casamino Acids
- CH: Casamino hydrolysate

- Vocabulary
  - bp: Base pairs
  - DNA: Desoxyribonucleic Acid
  - MTase: Methyltransferase
  - ORF: Open Reading Frame
  - PCR: Polymerised Chain Reaction
  - RNA: Ribonucleic acid
  - rRNA: Ribosomal RNA
  - mRNA: Messenger RNA
  - SDS-PAGE: Sodium Dodecyl Sulphate-Polyacrylamide Gel Electrophoresis
  - TBS: Tris-Buffered Saline
  - ECL: Enhanced Chemiluminescence
  - SEM: Standard Error of Mean
  - OD: optical density